Characterizing Heme Pockets

Patrick Finnerty

Biosciences

Universtat Autonoma de Barcelona

A thesis submitted for the degree of

Master of Science

Fall 2021

Acknowledgements

In case anyone reads this in the future, some context may be appreciated: I attended and completed this Master's during the COVID-19 global pandemic from September 2020 to September 2021.

Thanks professors

Thanks lab

Thanks UAB

Thanks Spain, and Catalonia, allowing me in and then also having public health measures unlike Donny's America

Thanks classmates

Thanks fam, friends

Thanks to the media and the creators of media that facilitated the survival of my sanity through the pandemic.

Finally, I'd like to quote a well-known artist from California. He was referencing his own work, but I wholly identify with his appreciation for the subject of his esteem:

"Last but not least, I wanna thank me. I wanna thank me for believing in me. I wanna thank me for doing all this hard work. I wanna thank me for having no days off. I wanna thank me for, for never quitting. I wanna thank me for always being a giver, and trying to give more than I receive. I wanna thank me for trying to do more right than wrong. I wanna thank me for just being me at all times." – Calvin Cordozar Broadus Jr.

Abstract

TO BE COMPLETED UPON AGREEMENT OF DISCUSSION/CONCLUSION

Metalloproteins compose approximately 40 percent (look up how to do percents in latex) of all known proteins, and use some metallic group to accomplish their chemistry. One such metallic group is heme. Heme is a member of the porphyrin family, which are able to catalyze a broad range of reactions. Heme in particular catalyzes many different reactions and is present in many proteins. However, the underlying structural requirements to host heme in a protein are not well studied.

In this study, all heme or heme-c containing proteins as of xx were downloaded and processed in order to determine underlying structural characteristics these proteins may have in common. Parameters that were examined include: xx. Overall, we found: xx. These results may have implications for protein engineering; or if I fucked up this illustrates the difficulty of the field and demonstrate the wide range of acceptable environments of heme; it may therefore be more appropriate to take a more hands-on approach until perhaps other computational methods evolve to better examine structure-function relationships.

Contents

List of Figures

List of Tables

List of Abbreviations

1-D, 2-D . . . One- or two-dimensional, referring **in this thesis** to spatial dimensions in an image.

Otter . . . . . One of the finest of water mammals.

Hedgehog . . . Quite a nice prickly friend.

Lay Summary

I investigated how heme, a molecule involved in many biological processes, binds to proteins. I did this by...

Introduction

Proteins that contain metal ion cofactor(s) are known as metalloproteins, and they compose approximately 40% of all proteins. The metal ion can be free, or bound within a ligand. One such ligand is heme, a complex of iron and a porphyrin ring. Heme is employed by many metalloproteins to catalyze a broad range of reactions.

Proteins containing heme are known as hemoproteins - hemoglobin and myoglboin are well-known examples, using heme to store and transport oxygen. Other examples hemoproteins are peroxidases, catalases (a type of peroxidase), nitric oxide synthases, heme oxygenases, and cytochrome p450s. Peroxidases and catalases catalyze oxidation-reduction reactions using a histidine-bound heme, with catalases in particular specializing in the decomposition of hydrogen peroxide. Nitric oxide synthases catalyze the reaction of L-arginine into nitric oxide, which is vitally important to cellular signaling (Poulos [1]). Free heme molecules may be released upon degradation of hemoproteins (especially hemoglobin), however, heme is prooxidative and therefore toxic to cells and must be cleared. Heme oxygenases assist in the degradation of heme, and are regarded as potential therapeutics, due to anti-inflammatory effects[2].

The enzymes with arguably the most potential applications, cytochrome P450s function as powerful monooxygenases. They participate in many reactions: capable oxidizing a wide range of substrates, serving to oxidize carbohydrates, steroids, fatty acids; catalyzing hormone degradation and synthesis; and degrading the majority of drugs(Poulos [1]). Due to their extraordinary utility and range of reactions, cytochrome p450s are of great interest in the protein engineering field. Cytochrome P450s have the potential to be used in industrial biocatalysis, e.g. in pharmaceutical production, bioremediation of environmental pollutants[3, 4]. The limiting factor

preventing its deployment has been the struggle to increase enzymatic efficiency and therefore yield of processes employing the enzyme[5, 6].

Echoing the many applications of its host enzymes, the heme molecule itself has its own variety. Thus far, only heme-b has been discussed (although it is the most abundant and most employed). There are several types of heme, structurally and chemically different, that are used to achieve different chemical reactions: in this study, we examined heme-b, heme-c, siroheme, and verdoheme. Their structures are shown in Figures 1-5.

All types of heme are a coordination complex composed of an iron atom coordinated and bound to a porphyrin ring. Porphyins are composed of four pyrrole subunits (pentagonal structures of four carbons and a nitrogen) that are bound together via methine (i.e. carbon) bridges (FIXME get a citation for this stuff). Porphyrins are considered macrocycles, molecules with large ring structures. The ring within porphyrins is heterocyclic, and considered aromatic, and therefore acts as a large resonant structure capable of transferring electrons. Coupled with an iron atom to enable reduction-oxidation reactions and the macrocycle of the porphyrin ring, the overall heme complex is therefore highly suited for reactions involving electron transfer.

Aware I need to scale some of the figures and make this nice and uniform

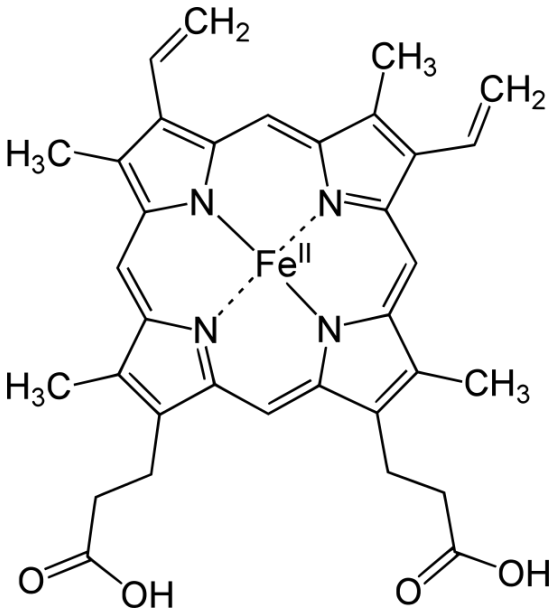

Figure 1: Heme-b (HEM)

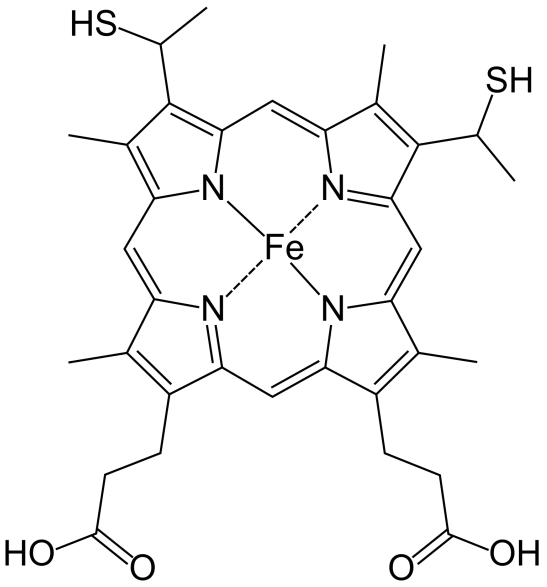

Figure 2: Heme-c (HEC)

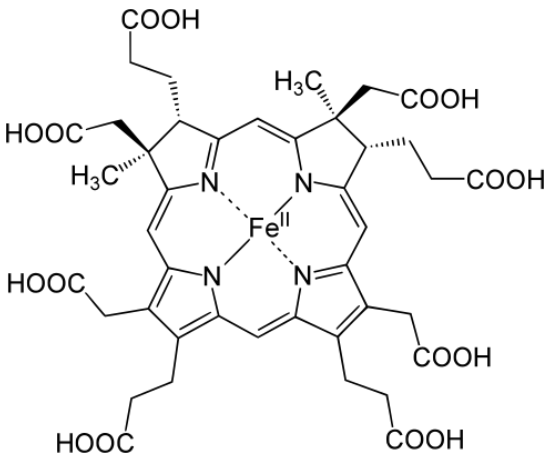

Figure 3: Siroheme (SRM)

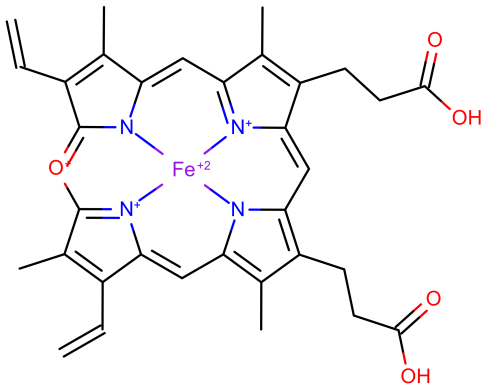

Figure 4: Verdoheme, VEA

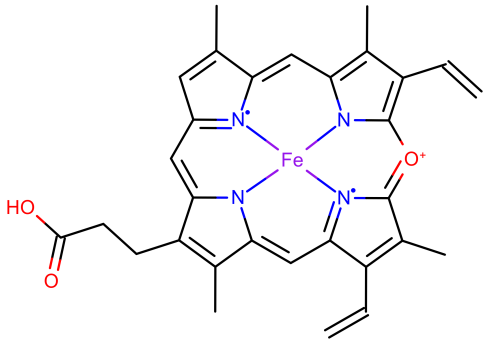

Figure 5: Verdoheme, VER

##Types of Heme

The most common heme is heme-b. It is employed by the vast majority of hemoproteins. It is composed of an iron and porphyrin ring complex, with the addition of two propionate groups. These two propionate groups interact with polar amino acids in the binding pocket. The iron atom is usually coordinated to a histidine or cysteine, depending on the enzyme.

Heme-c is derived from heme-b. It is fairly similar to heme, with two notable excetions: the iron atom binds, with few exceptions, covalently to cysteine residues in the binding pocket; and its two vinyl groups form thioester bonds with amino acids in the protein binding pocket. Its function is much more specific than heme-b, mostly serving as an electron carrier rather than catalyzing a plethora of reactions. The reason for this is not abundantly clear, but several studies suggest that because of its covalent bonding, heme-c has an electronic potential that is can be far lower and in general more broad, and more specifiable, than heme-b. [7, 8]

Siroheme is even more limted in its applications, but highly specialized for its role. It is still an iron atom-porphyrin coordination complex, but it contains far more carboxyl and propionate groups than the other types of heme, making it highly polar. It is used exclusively in sulfite and nitrite reductases, which catalyze

the reduction of the sulfates and nitrates plants uptake from the ground, providing the sources of nitrogen and sulfur used to produce nitrogen and sulfur-containing amino acids(Tripathy et al. [9]). The reason for the use of siroheme in this reaction rather than heme-b is not completely understood. But one study suggests that the bridge that siroheme forms between its catalyic iron atom, and the protein matrix envrionment (which also necessarily involves another cofactor, a cluster of cubane for electron transfer and provision) is more efficient at channeling electrons than the bridge that could be formed by heme.[10]

Lastly, verdoheme is an intermediate product in the degradation of heme-b by heme oxygenase. When heme oxygenase degrades heme-b, biliverdin, carbon monoxide, and iron are produced; verdoheme is the precusor to bilverdin[11, 12]. While a product of prior reactions wthin heme oxygenase, verdoheme appears to be oriented and bound differently [13]. The two structures used in the study, VEA and VER, are either partially oxidized or partially oxidized and contain one less propionate group.

In summary, heme molecules are varied, and used in a diverse set of reactions. Several enzymes have the potential to be of great value either in biocatalysis or pharmaceutical applications. There are multiple methods employed to design molecules, but rational design in particular (basically, the mutation of certain residues based on an understanding of the structure-function relationships) is at least partially hampered by an incomplete understanding of the binding environment for heme. The importance of the binding environment was noted in a study seeking to design *de novo* heme-c based enzymes, and found the binding environment likely to be of importance in modulating redox potential [14].

A fairly recent study conducted a structural analysis of 125 hemoprotein chains(Li et al. [15]). The study suggested hemoproteins undergo small conformational changes during binding; and that apo-form (ligand-containing) proteins may therefore be suitable for bioinformatics-based prediction and protein design. Additionally, the heme binding environment of the protein dataset used in the study was found to be rich in aromatic and nonpolar residues.

The aforementioned study was published in 2011 - since then the PDB has been populated with far more hemoproteins. The 125 protein chains used in the study were sourced from a small dataset of proteins (FIXME: Double check but their Table 2 is like 20 proteins), compared to the amount of hemoproteins now available in the PDB. The focus of the study was on conformational differences induced by heme-binding. And as for the binding environment, the focus was largely on interactions with the coordinating iron atom rather than interactions that occur with the porphyrin ring. **could add the distances arbitrary definition thing but I hesitate to write anything that could be construed as uh, negative**

The interactions heme forms with its binding environment have been well documented. And many studies have demonstrated the importance of these interactions and have either demonstrated or at least furnished theoretical mechanisms by which the heme molecule functions in reactions involving hemoproteins. However, there has not been significant work dedicated to examining the heme-binding environment itself.

In this study, we present research focused on elucidating the binding environment of multiple heme molecules: heme-b (HEM), heme-c (HEC), siroheme (SER), and verdoheme (VEA/VER). UCSF Chimera was used to both extract and predict properties of a diverse set of hemoproteins. R was used to analyze the results. A robust and high-throughput framework was constructed to process the datasets for each heme molecule, requiring only inputs of which ligand is to be examined per dataset.

The properties extracted and predicted of the heme molecules were (I need to figure out how to do a bullet list in this format): +Amino acid frequencies within binding pockets +Volumes +Solvent accessible and excluded surface areas of heme and binding pockets +Distances of amino acids from the Fe atom of heme +Planar angles of amino acids in binding pocket v. heme +CA-CB-Fe angles of amino acids in binding pocket v. heme

These results may be of use in rational design of hemoproteins in future studies, or at least improve the understanding of the heme binding environment.

WILL INSERT PARAGRAPH ABOUT THE MEANING OF THESE RESULTS IN THE DESIGN ARTIFICAL METALLOPROTEINS, AND BRIEFLY INTRODUCE THEM EARLIER. 'AS MENTIONED PREVIOUSLY, THERE ARE MANY OPPORTUNITIES TO EMPLOY IMPROVED HEMOPROTEINS, AND A MORE THOROUGH UNDERSTANDING OF THE HEME BINDING ENVIRONMENT WOULD AID IN THEIR DESIGN. . . '

1 Methods

1.1 Datasets

A list of PDBs was assembled that represented either a representative sample of a variety of proteins, with a resolution better than 3A, (HEM and HEC) or, all proteins containing these ligands were downloaded from the PDB (in the case of SRM, VER, VEA). Not all downloaded PDBs were appropriate for this study (e.g. contained "wobble" structures) and therefore the amount of PDBs was culled. The datasets are current as of 16 August 2021.

The size of the datasets actually used in the study were as follows: HEM (n=58), HEC(n=14), SRM (n=9), VER (n=2) and VEA (n=2) for a combined n=4 for VERDOHEME.

The name of all proteins used in the study and their source organism are provided tables within Appendix B.1.

1.2 Preprocessing

Many of the PDBs downloaded were multimeric structures. While many of the scripts employed in the study may function with multimeric structures, the number of subunits per protein (FIXME! better way to say this?) would skew results in

favor of multimeric proteins with more subunits. The information gleaned from similar subunits would also not be of utility in this study.

Therefore all downloaded PDBs were converted to monomeric structures. This was achieved by saving a single chain (chain A) of each PDB and eliminating all other chains. The single chain was then saved as a PDB and used in all subsequent scripts.

1.3 Processing Monomers

UCSF-Chimera was used to generate all data in this study. Multiple scripts were employed to achieve a high-throughput process where all monomeric PDBs could be processed in the same session.

Chimera was used to predict the following qualities: Volume of the ligand binding pocket, accessible and excluded surface area of the ligand, and accessible and excluded surface area of the binding pocket. These calculations require a population of atoms to be selected for the calculation.

Atoms were selected within a distance cutoff, to be considered as "interacting" with the ligand or forming the binding pocket. Distance cutoffs from the ligand of 5A and 7A were chosen; for the predicted qualities, the algorithms were run twice to get values at 5A and 7A. For the distance and angle calculations, only the 7A distance cutoff was used, as the cutoff does not factor into any calculations and may be set during analysis.

as these are selected arbitrarily, data from the 5A and 7A runs are overlaid in the figures reported in Appendix **??**. Data tables are also provided in Appendix **??**.

1.3.1 Amino Acid Frequency

Amino acids within the bounds of the lower and upper distance cutoff were selected and recorded. These were then counted for frequency per residue.

1.3.2 Volume Calculations

Volume of the binding pocket was predicted via Surfnet, run with default parameters of Grid Interval = 1.0 and Distance Cutoff = 10.0 (the latter option does not relate to the distance cutoff from the ligand(FIXME! find source for this, appears 100% to be true?)).

1.3.3 Surface Area Calculations

Excluded and accessible surface areas of both the ligand and the binding pocket were calcualted using Chimera's "surf" algorithm, available as "Measure Volume and Area" via the GUI.

1.3.4 Distance Calculations

Distances of amino acids from the ligand could not be calculated accurately nor precisely in a direct way. Instead, distances for each atom composing a residue were calculated. The distances of all atoms within a residue were averaged, and this value was taken as the mean distance of the entire residue and used in subsequent steps.

The data produced in this step therefore include the mean distance of each amino acid. This is traceable, and the angular data below are cross-referenced with this list of distances. All data shown in figures (FIME! Also for tables?) are multidimensional and may be filtered for distance.

1.3.5 Planar Angle Calculations

Individual residues and the ligand were defined as axes The angle between each residue's axis and the axis of the ligand were calculated. Each axis functions essentially as a separate plane. (FIXME! Include a picture of what this looks like?) This employed the "define axis", and "angle" functions of Chimera; the Axes/Planes/Centroids Structural Analysis function of Chimera via GUI.

1.3.6 CA-CB-Fe Calculations

Residues within the distance cutoff were examined one by one. The angle of between each residue's carbon alpha (CA) and carbon beta (CB) and the Fe of the ligand was calculated, using the "angle" function of Chimera. The ligand nor the Fe atom were compared with themselves.

1.4 Import to R

All data were imported to R and processed from text files into organized data formats. R was used to cross-reference angle and distance data. All plots and tables were constructed using R and imported directly to this document using Rmarkdown.

2

Results and Discussion

Contents

–>

2.1 Analysis of Nearby Residues of Natural Porphyrins

The first part of the study aimed at providing statistics on the amino acid propensity to interact with hemes in natural proteins. We studied heme-b, heme-c, siroheme and verdoheme. Because we are not looking only at the iron environment, but instead at the environment of the entire microcycle, we did the analysis for any

amino acid with potential contact with the heme. This was defined as any AA having at least one atom within the cutoff distances of 5 and 7 Angtroms (A).

Amino acid frequencies were obtained for distance cutoffs of 5A and 7A - these figures and data are shown in **FIXME ADD APPENDICES LATER** The trends in these data are very similar and therefore only the data pertaining to the 7A distance cutoff are discussed below.

2.2 AA Frequency

2.2.1 Heme-b

Amino Acid Frequencies in Binding Pocket

Figure 2.1 plots the frequency of each residue within 7A of heme-b. Immediately below is Figure 2.2, which plots the frequency of each residue within the entire monomer. **I'm thinking put tables in back they dont add much value here** Data tables are available in Appendix...

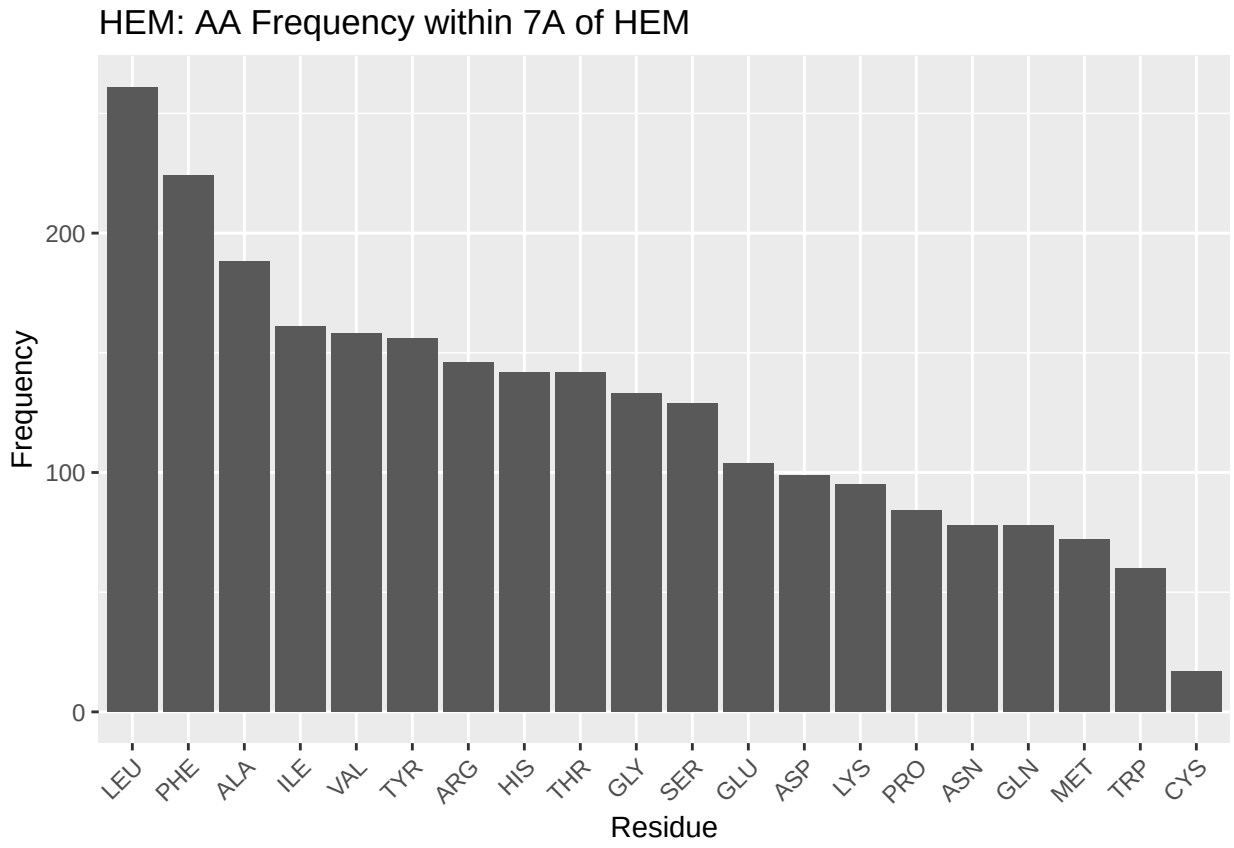

Figure 2.1: HEM: AA Frequency within 7A

Table 2.1: HEM AA Freq

Residue	Freq
LEU	261
PHE	224
ALA	188
ILE	161
VAL	158
TYR	156
ARG	146
HIS	142
THR	142
GLY	133
SER	129
GLU	104
ASP	99
LYS	95
PRO	84
ASN	78

Table 2.1: HEM AA Freq *(continued)*

Residue	Freq
GLN	78
MET	72
TRP	60
CYS	17

I use 'surprising, striking' a lot in this discussion. I'll reword this to have some variety later. The results are at least interesting!

Beginning at the left of the figure and moving right, large, nonpolar amino acids appear most frequently within 7A: LEU and PHE; ILE appears less frequently than these two amino acids but nonetheless is in high frequency. Small, nonpolar amino acids ALA and VAL also appear very frequently. As the majority of the heme-b molecule is made up of the nonpolar porphyrin ring, these amino acids are therefore likely in such high frequency to provide the nonpolar interactions/environment with the pyrole groups and methyl and vinyl groups.

Tyrosine, arginine, histidine appear next most frequently. The two propionate groups on heme are used to coordinate the heme in the binding pocket. These polar residues are therefore likely interact with the propionate groups, providing the polar interactions necessary, in addition to the nonpolar interactions above, to provide as hospitable of a binding environment as possible to coordinate the heme. In additon, the arginine and histidine groups are positively charged (at pH 7),further facilitating interaction with the electronegative proprionate groups of heme-b. It should be noted histidine is one of the residues that coordinates the iron atom, and this may therefore inflate its frequency in the binding pocket.

Glycine is a small residue and cannot form significant interactions within its environment; however, its frequency, or lack thereof (compared to background frequency, discused later), suggests the binding pocket may not require as much flexibility or... spatial considerations as in the rest of the protein. This would logically follow from the need for conserved binding sites.

Next appear serine, glutamate (glutamic acid) and aspartate (aspartic acid) and lysine. These are polar residues, and glutamate and aspartate are negatively charged; lysine is polarpositively charged. The negative charge is unlikely of importance in interaction with heme-b, however these polar amino acids likely again interact with the propionate groups on heme; only, infrequently. What is most interesting is why lysine is in such low abundance relative to the other polar, positively charged residues, arginine and histidine. Perhaps lysine's fairly linear structure prevents it from fitting into the binding pocket; however, arginine is also somewhat linear and features prominently. The exact reason for why this could be is beyond the scope of this study.

Proline is a small nonpolar amino acid in low frequency; the trend for heme-b, at least, appears to be to favor large nonpolar amino acids in the binding pocket. This may suggest that a large amount of nonpolar interactions, per residue, is favored in the binding pocket, perhaps because of the limited space available to position residues to interact with heme.

Asparagine and glutamine are both medium-sized polar amino acids; given the trends already discussed it is surprising these are not in greater abundance. But as with proline, it may simply be a matter of maximizing the benefit of the interactions that may be formed with the heme; while asparagine and glutamine are polar, amino acids like arginine and histidine are both polar and positively charged, capable of stronger interactions with the electronegative propionate groups.

Methionine and tryptophan appear very infrequently in the binding pocket. All nonpolar amino acids already mentioned do not possess a sulfur (thio something?) bond in their structure; perhaps it is less favorable for the sulfur atom to interact with the porphyrin ring than another carbon **HELP I'M AT A LOSS ON EXPLAINING THIS ONE**. Tryptophan is very surprising to find as second-to-least frequent. It is a large nonpolar amino acid - but perhaps its single, potential hydrogen bond, although weak, is enough to prefer completely nonpolar residues. Or, with its size, it is preferable to have more numerous, smaller nonpolar residues

that can favorably interact with the porphyrin while reducing steric hindrance of other residues in the environment (taking up less space).

Cystine appears most infrequently of all the amino acids in the binding pocket. This is quite surprising - cystine is highly evolutionarily conserved to coordinate the iron in the binding pocket. Perhaps the sample of PDBs used in this study mostly use histidine to coordinate the iron - but this would only account for one residue in the binding pocket per pdb. Therefore these results suggest that while cystidine may be well suited to coordinate the iron in heme, it is poorly suited to form any nonpolar interactions with the porphyrin ring, leaving the task up to other, more suitably/intensely nonpolar amino acids.

Moving away from discussing individual amino acid populations, what is especially notable of the data for heme-b is that nonpolar residues appear in much greater frequency than polar residues. Nonpolar interactions with heme are therefore more numerous than polar interactions; quite logical, given there are only two polar propionate groups on a large porphyrin ring that is otherwise nonpolar. Their multiplicity may also suggest that they are potentially of greater importance than previously thought. At the very least, these results suggest that polar interactions and coordination of the iron atom, while necessary for heme binding, are insufficient, and that nonpolar intercations and the population of nopolar residues in the binding pocket should be considered when examining the binding environment of heme.

Comparison with Background Amino Acid Frequencies

While the frequencies of amino acids in the binding pocket have been discussed, it may also be of interest to compare against the background amino acid frequency, the general frequency of amino acids within the entire monomer. The degree to which this may affect the significance of the frequencies of the amino acids in the binding pocket is unclear - those amino acids are still employed and placed such as to bind the heme, rather than being a random assortment of residues. However, a in depth examination of simlarities and differences may reveal that some amino

acids may simply be extremely highly conserved by chance and by virtue of their numerous population, rather than some chemical benefit.

Figure **??** documents the frequencies of amino acids overall within the monomer.

Leucine and alanine as in the binding pocket frequencies are highly frequent in the overall monomer. This may suggest their prevalence in the binding pocket may simply be due to a high pulation of leucine and alanine in hemoproteins.

However, after these two amino acids the tendencies in frequency for the binding pocket and the monomer at large diverge.

Glycine is in high frequency - likely due to more complex geometry e.g. helices outside the binding pocket. In interest of brevity, the remaining frequencies are summed up thus: the same trends that appear to exist in the binding pocket do not appear to exist in the monomer at large. While the order of frequencies in conserved binding pockets can be rationalized, justifying the overall frequencies in monomers invites significant speculation.

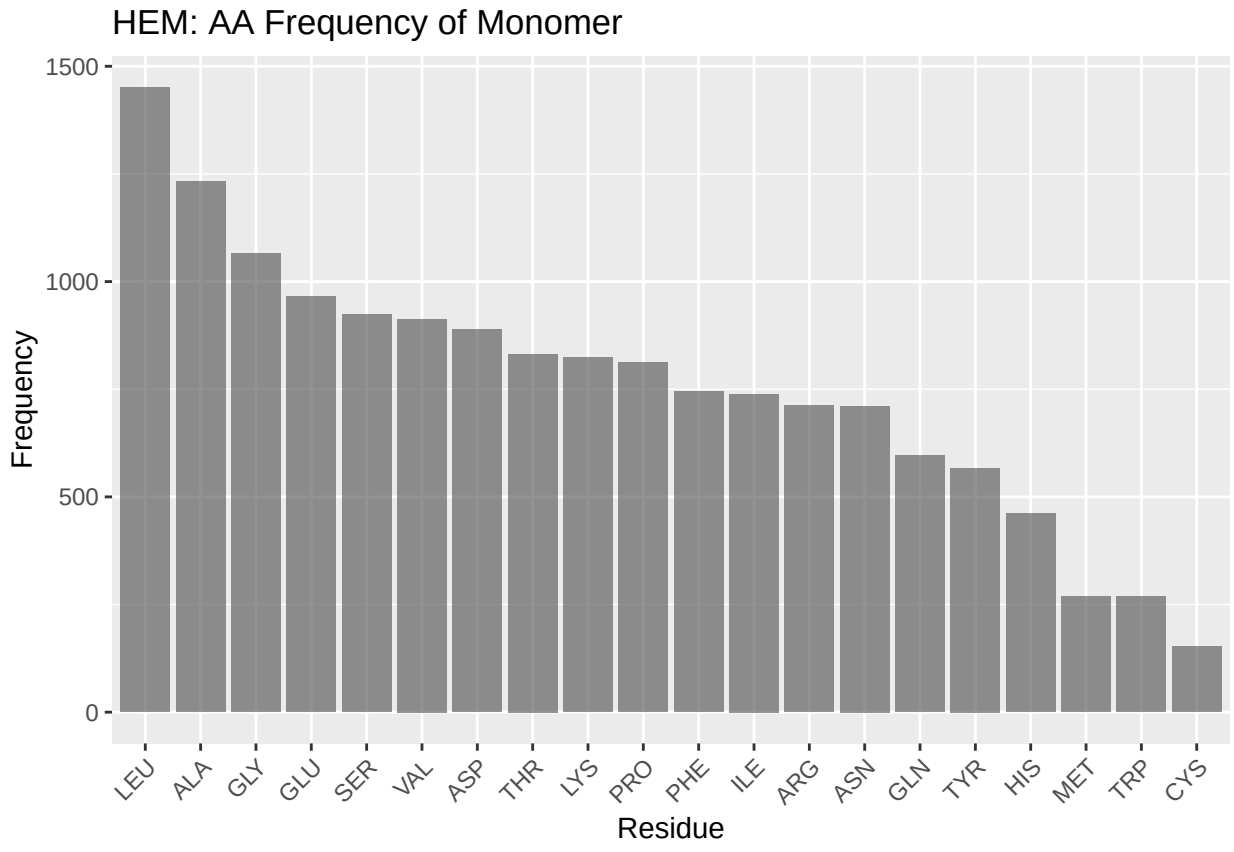

Figure 2.2: HEM: AA Frequency of Monomer

Distributon of Amino Acids over Distance

After an exhaustive exploration of the relative frequencies of amino acids in the binding pocket, the figure below is fairly straightfoward. Figure 2.3 plots the distribution of amino acids in the binding pocket against their distance from the iron of the heme.

We find that only a few residues come in close contact (<4A) of the heme: Cys, His, Tyr. Most residues center their distribution at around 6A, although Lys seems more biased than the remaining residues to be a bit closer. Cystidine and histidine may be at least in part explained to be close due to their use as coordnating residues; histidine, being in greater frequency, may also be this close due to favorable interactions with the porphyrin ring.

The proximity of tyrosine however, is lkely more notable. It cannot form coordination bonds with the heme iron, but tyrosine residues do interact with the propionate groups; and these results suggest that of all potentially interacting polar/positively charged residues, tyrosine is the most likely at least to be in close proximity to the heme molecule. Whether this illustrates an extreme imortance of tyrosine to interact with propionate groups, or instead the need for tyrosine to be in close proximity in order to form such interactions, is beyond the scope of this study.

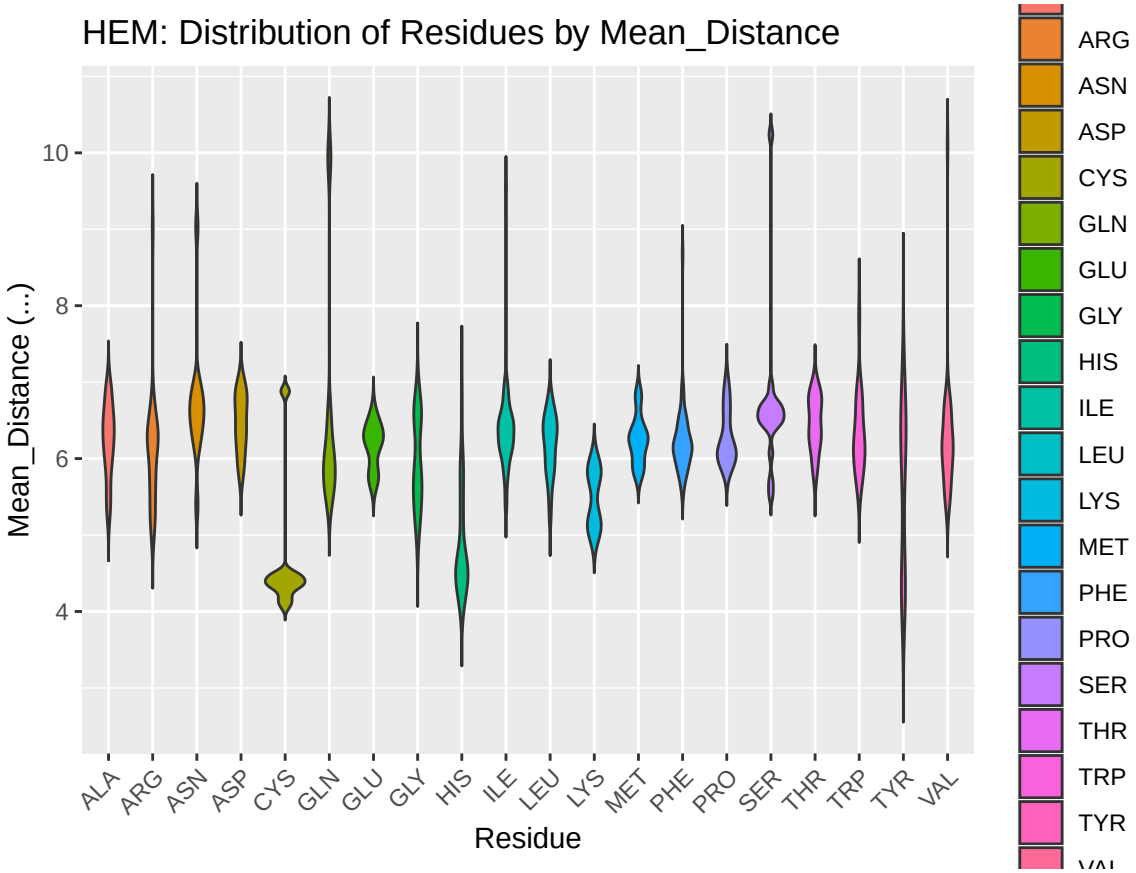

Figure 2.3: HEM: AA Distances

2.2.2 Heme-c

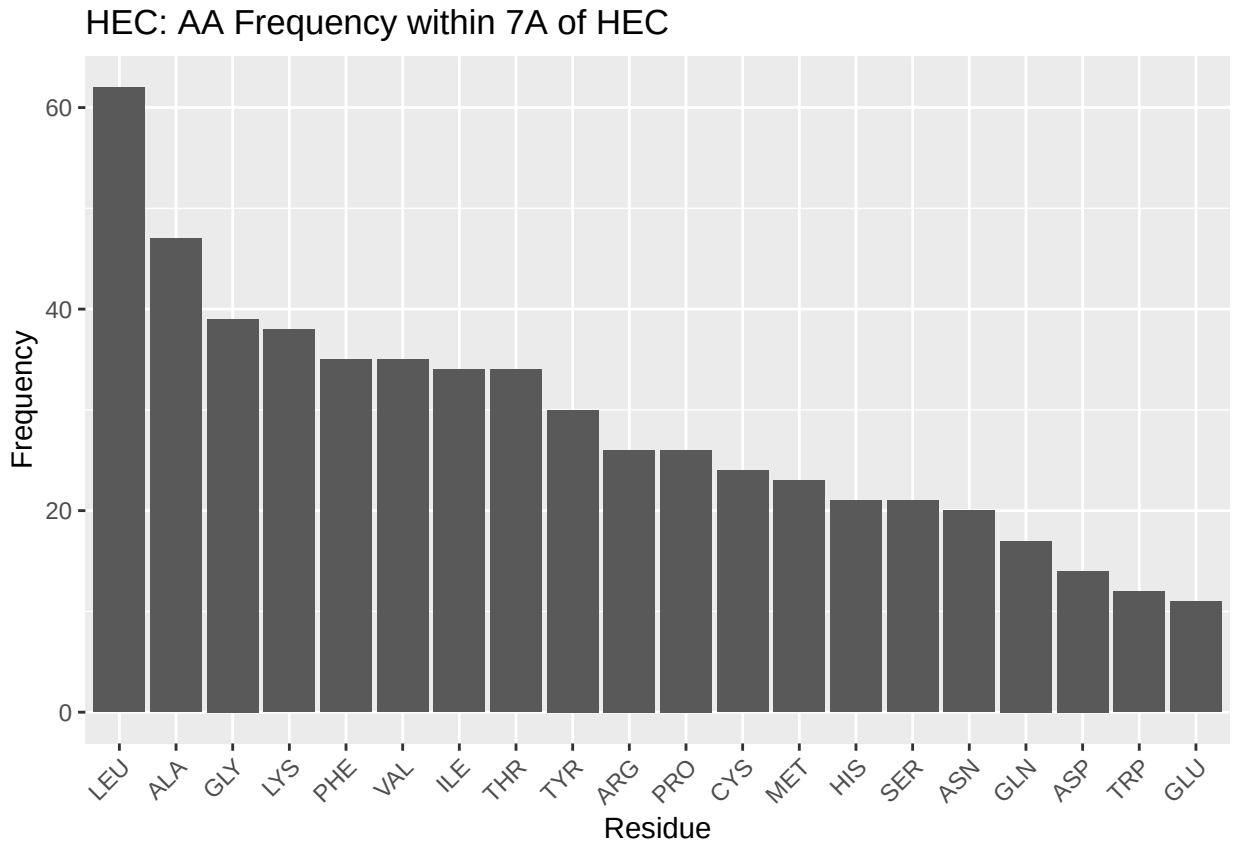

Figure 2.4: HEC: AA Frequency

Table 2.2: HEC AA Freq

Residue	Freq
LEU	62
ALA	47
GLY	39
LYS	38
PHE	35
VAL	35
ILE	34
THR	34
TYR	30
ARG	26
PRO	26
CYS	24
MET	23
HIS	21

Table 2.2: HEC AA Freq *(continued)*

Residue	Freq
SER	21
ASN	20
GLN	17
ASP	14
TRP	12
GLU	11

Leucine and alanine again are highly frequent for HEC, followed by quite similar trends and therfore HEC will not be as thoroughly discussed as HEM. The most notable differences may be that GLY and CYS are in far higher frequency than in heme. Heme-c almost always covalently binds to CYS, and this may explain that frequency: but as for the high frequency of glycine, perhaps the covalent binding of CYS is sufficient for other interactions to be of 'lower priority', and the flexibility and shape of the binding pocket to be prioritized, therefore leading to more glycines being included in order to shape the pocket favorably. A note on this last part: **I feel like this is grasping at straws without much support, add more qualifiers or remove**

Comparison to background frequency

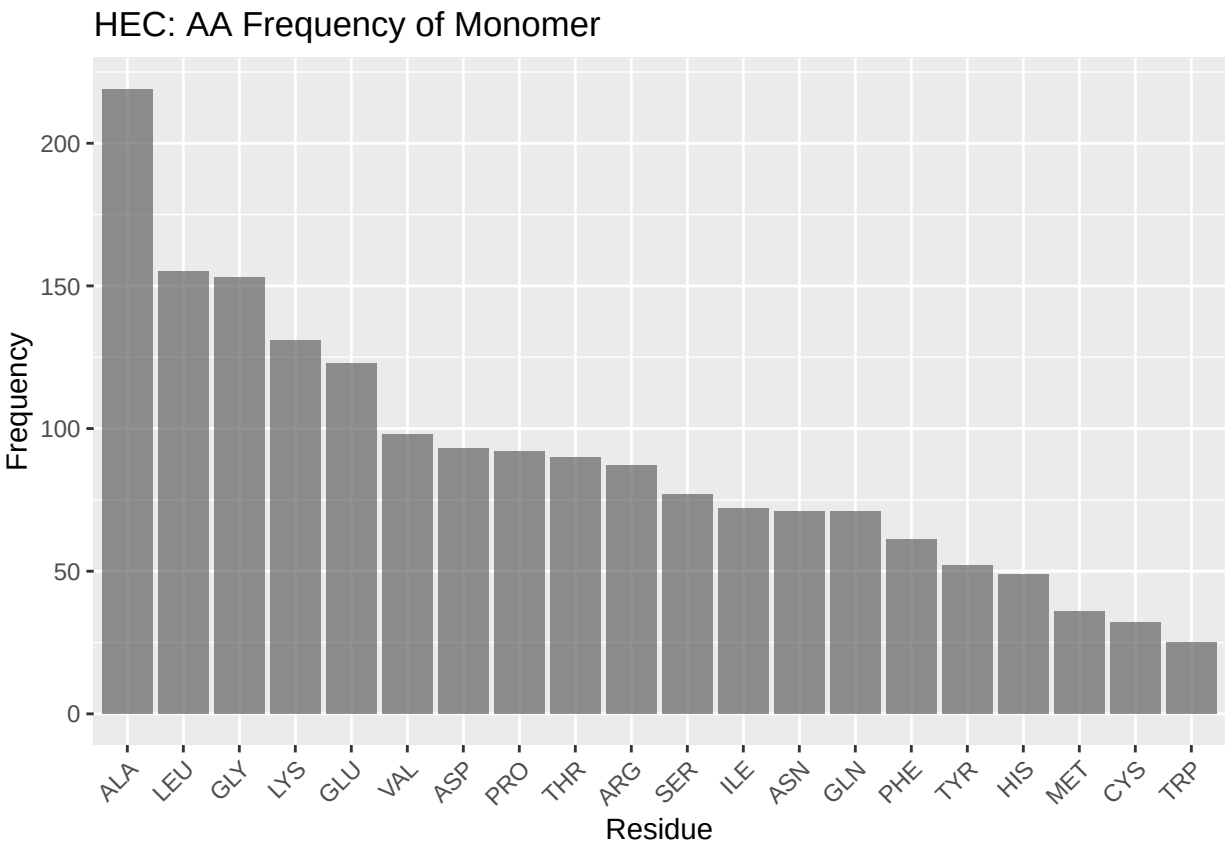

Figure 2.5: HEC: AA Frequency of Monomer

Generally, the heme-c monomer is similar to the heme-b monomer, with a high frequency of alanine and leucine, followed by a divergence in the frequency of amino acids and therefore a struggle to form any meaningful discussion when it comes to comparing the binding pocket frequencies against background frequencies.

AA Distribution v. Distance

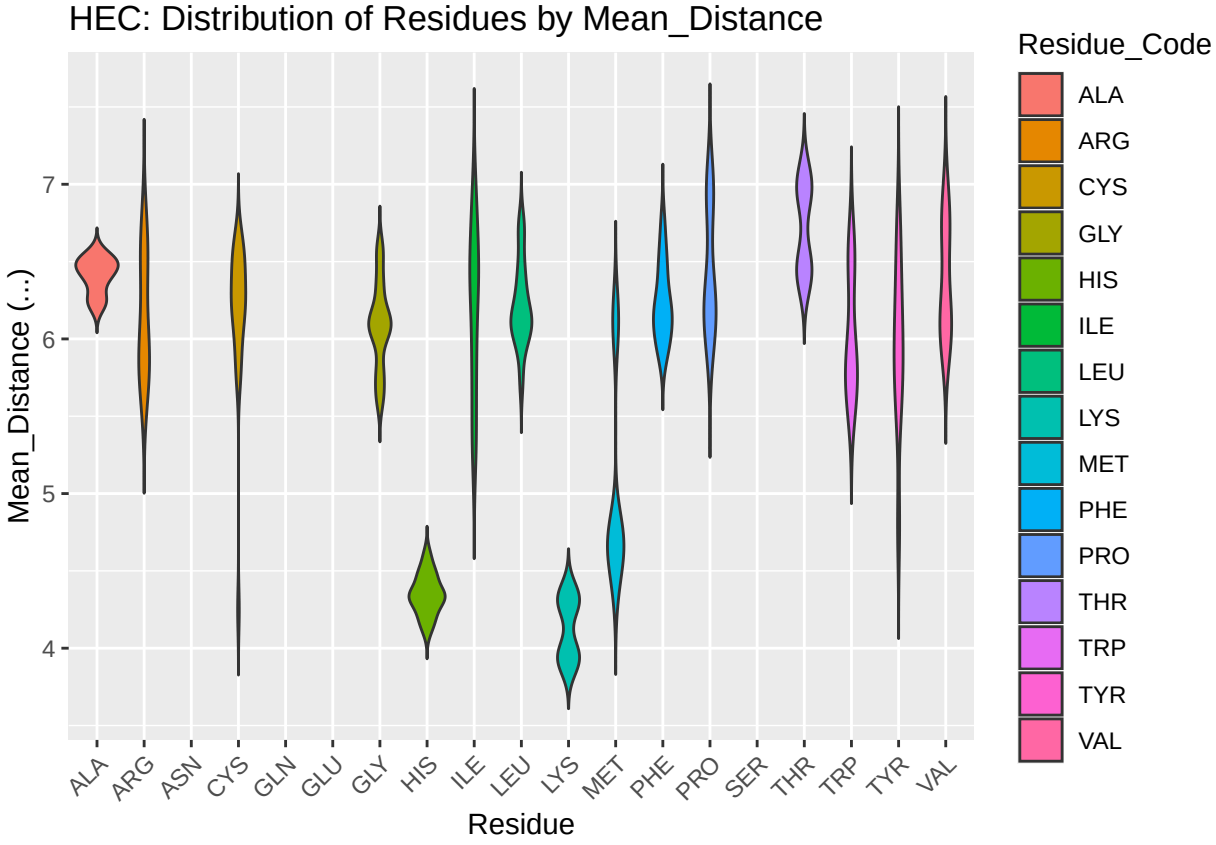

Figure 2.6: HEC: AA Distances

The distribution of amino acids over distance from the heme iron for HEC is similar to HEM, with some exceptions. Cys, His, Tyr again are amongst the closest residues to HEC, likely for the same reasons of very strong polar interactions or coordination. Additionally, cysteine forms covalent, thioester bonds with heme-c, providing further justification for its proximity. However, for heme-c, lysine and methionine also are very proximal. The methionine residues are nonpolar and **HELP, NOT SO SURE WHY THEY'D BE SO CLOSE** Lysine is polar and positively charged, and therefore in the case of HEC being covalently bonded, and therefore reliably, specifically, positioned, the environment may be such that a lengthy, polar, charged residue may also be positioned well enough to be consistently nearby and forming interactions with the propionate groups. **GRASPING AT STRAWS AGAIN** .... Maybe just leave it that for heme-c

in particular, lysine and methionine appear favored. For good reason, they're nonpolar. But it's unclear why for heme-c these residues are employed but others aren't. I've left other sections like that.

2.2.3 Verdoheme

Got some conflicting stuff here

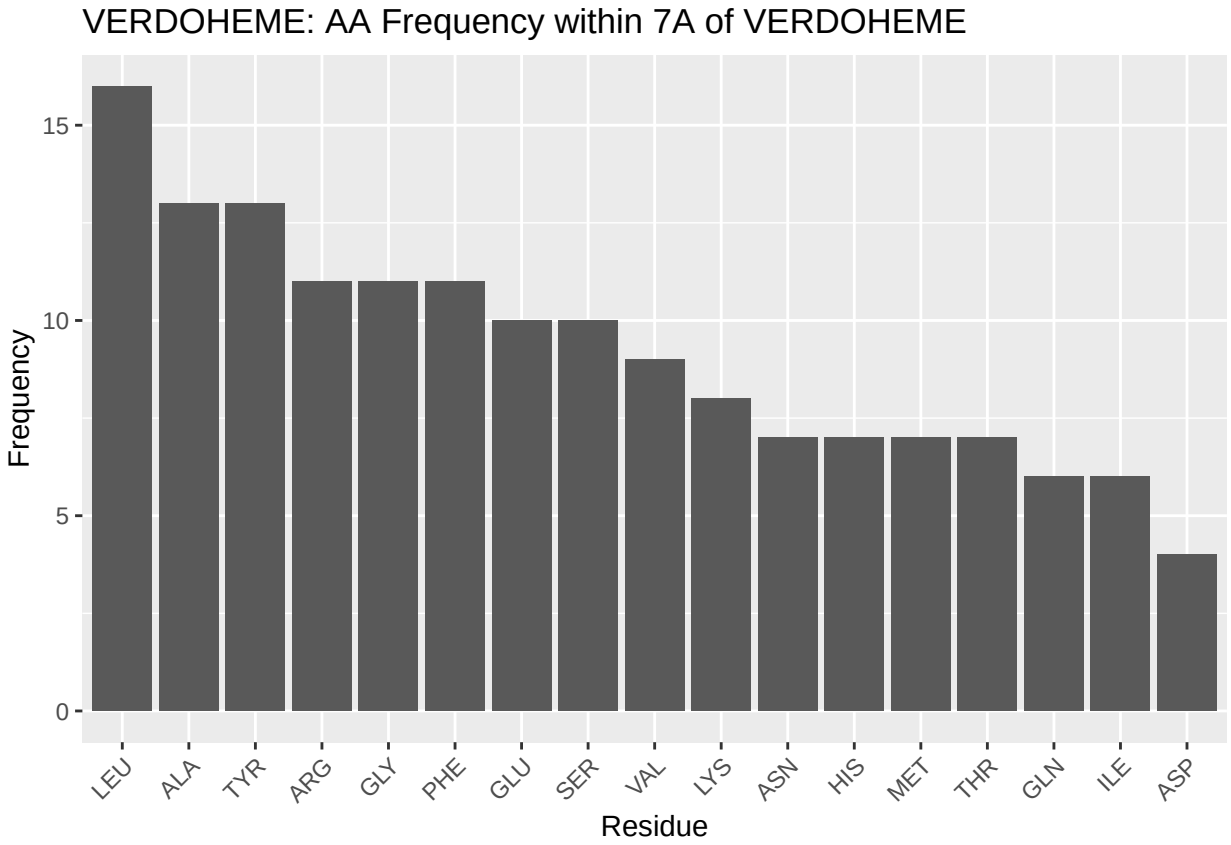

Figure 2.7: VERDOHEME: AA Frequency

Table 2.3: VERDOHEME AA Freq

Residue	Freq
LEU	16
ALA	13
TYR	13
ARG	11
GLY	11
PHE	11
GLU	10

Table 2.3: VERDOHEME AA Freq *(continued)*

Residue	Freq
SER	10
VAL	9
LYS	8
ASN	7
HIS	7
MET	7
THR	7
GLN	6
ILE	6
ASP	4

Verdoheme is dissimilar from HEM and HEC above. This is fairly surprising, given that verdoheme is an intermediate in the binding pocket for heme within heme oxygenases. The results discussed below may be attributable to the small sample size of verdoheme PDBs (n=4, combining VEA and VER), and should be appreciated with some skepticism. Nonetheless, the results will be discussed.

Leucine and alanine are again most frequent, but after this results diverge. Tyrosine and arginine are next most frequent - surprising, given that this is still the same pocket that bound heme. The data for heme-b indicate more frequent nonpolar residues before tyrosine. It is possible that heme's reorientation during its degradation moves it closer to another region of the binding pocket. Chemically, it may be that as heme is oxidized, there is greater need for polar interactions; this would help to explain the high frequency of polar residues.

Glycine is the next most frequent - it is in lower frequency, relatively, for heme-b.... **I'm gonna hold off on discussing this further until I double check the paper that described heme's reorientation.**

Comparison to background freq

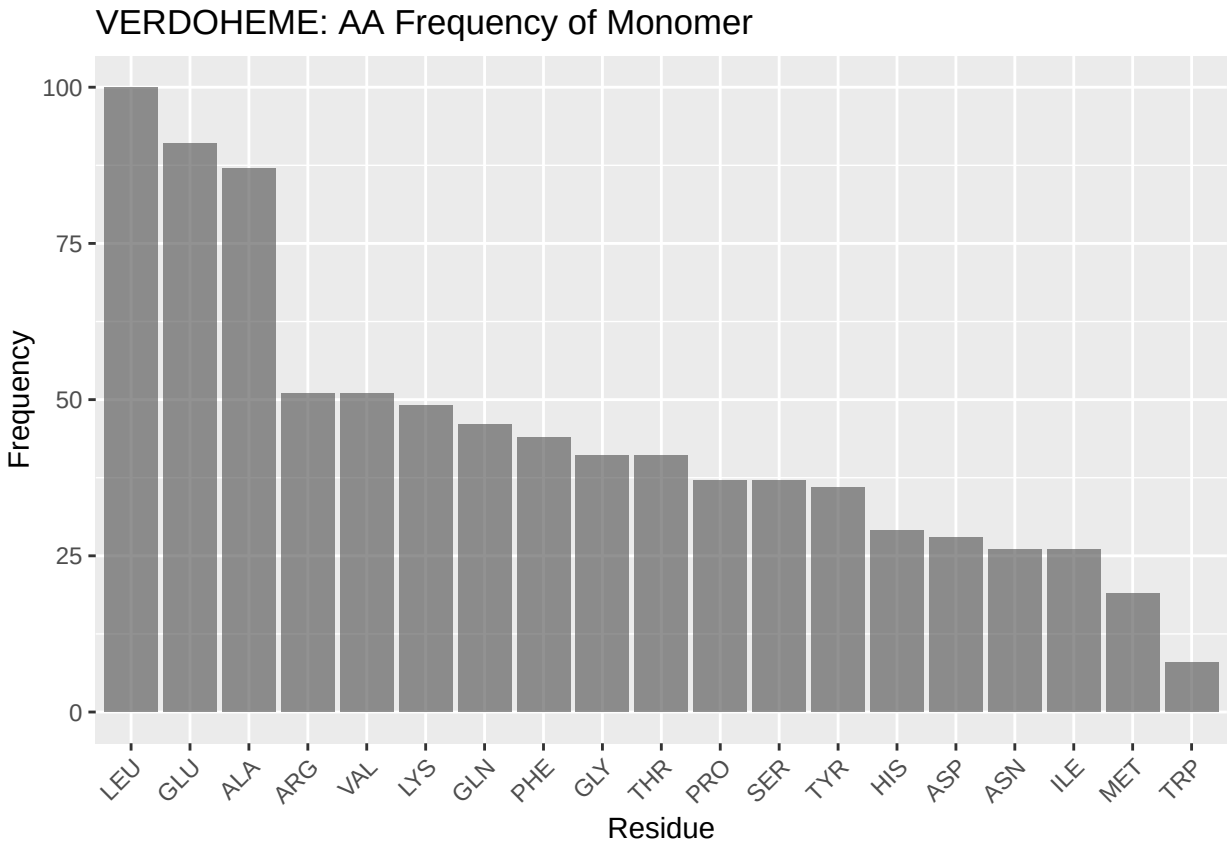

Figure 2.8: VERDOHEME: AA Frequency of Monomer

AA Distribution over distance

I'll double check why so few data appear here. I suspect it may be simply that there is not enough data/atoms to pull and form a decent enough graph. The highly conserved histidine for hemoproteins is exclusively within 5A for verdoheme. This result again suggests that at least some of the data for verdoheme may be highly biased because of the small sample size - heme-b data included a greater range for histidine. Nonetheless, this data suggests that verdoheme may be of different orientation during heme-b degradation, but is not spatially displaced far from the conserved binding site.

Glycine's proximity to verdoheme is just weird WTF.

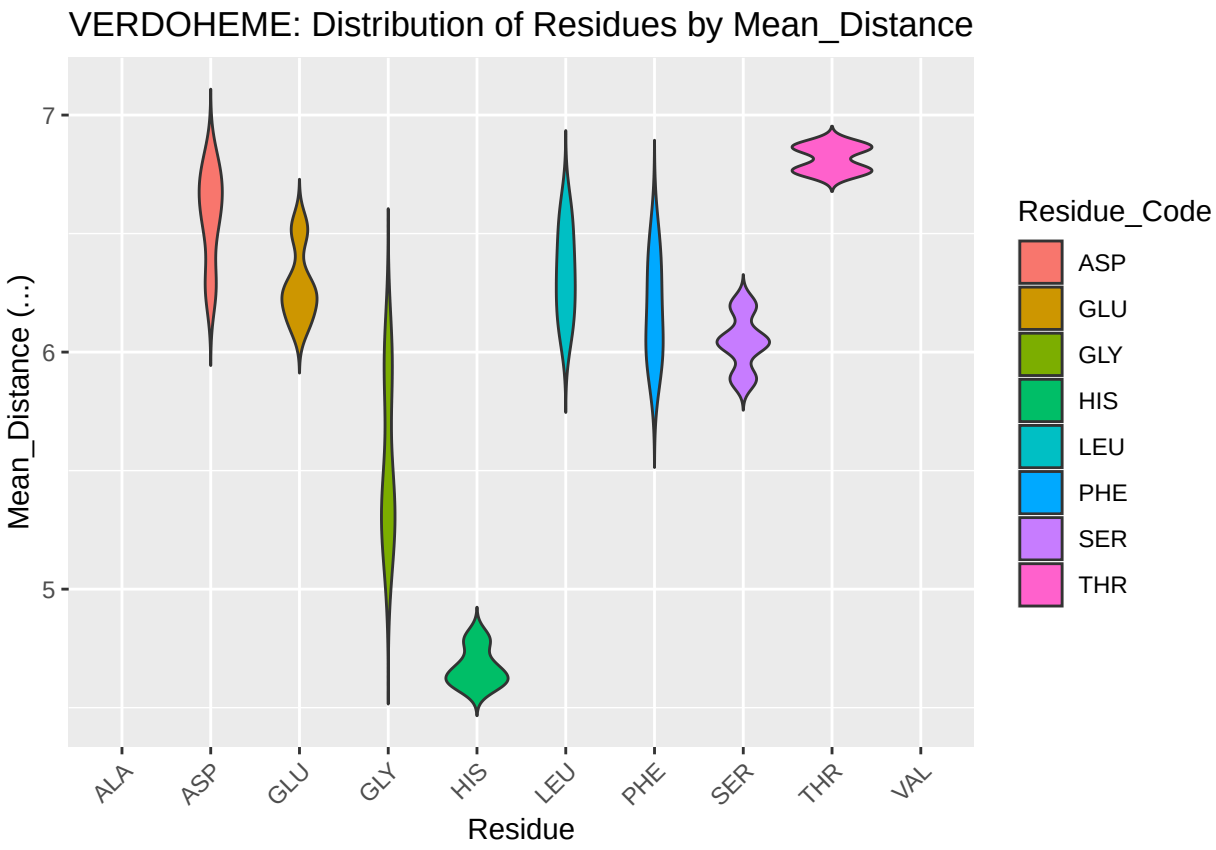

Figure 2.9: VERDOHEME: AA Distances

2.2.4 Siroheme

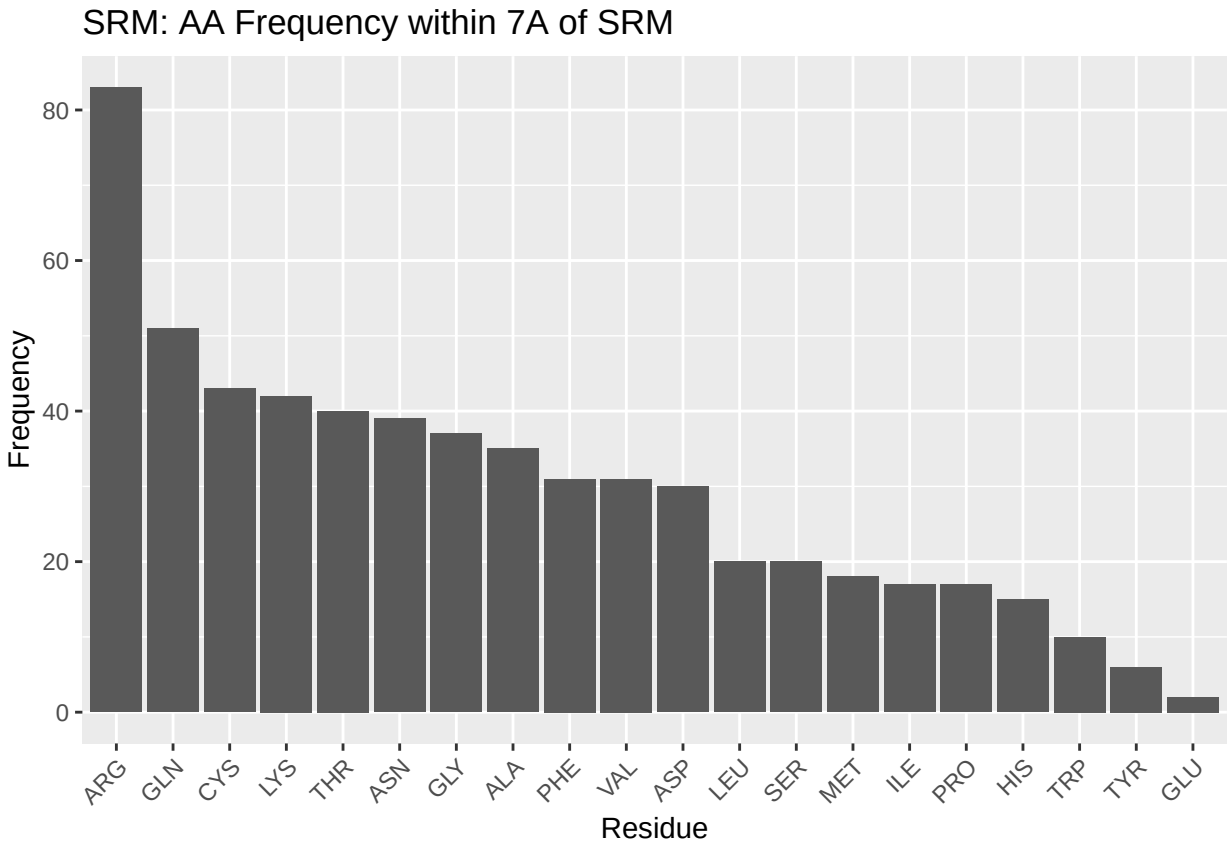

Figure 2.10: SRM: AA Frequency

Table 2.4: SRM AA Freq

Residue	Freq
ARG	83
GLN	51
CYS	43
LYS	42
THR	40
ASN	39
GLY	37
ALA	35
PHE	31
VAL	31
ASP	30
LEU	20
SER	20
MET	18

Table 2.4: SRM AA Freq *(continued)*

Residue	Freq
ILE	17
PRO	17
HIS	15
TRP	10
TYR	6
GLU	2

Siroheme, with a structure highly dissimilar to the other heme molecules examined, should be expected to have a different amino acid frequency profile - and indeed we confirm this in our results.

Nonpolar residues are not the most abundant in the siroheme binding pocket. In fact, disproportionately frequent to the rest of the residues in the binding pocket is arginine. Siroheme is saturated with carboxyl and propionate groups; the entire porphyrin ring surrounded by polar, electronegative groups. And therefore a polar, positively charged amino acid such as arginine is reasonable to expect in the binding pocket - what is striking, however is the extreme preference for arginine; such a profile does not exist for the other hemes.

Arginine is followed by other polar amino acids: glutamine, cystine, lysine (positively charged), threonine, and asparagine; a more homogenous trend than seen for the other heme molecules, in that there are no nonpolar residues at all in this first... group of frequencies. **reword**. Though these results could be expected, they demonstrate the extent to which siroheme's binding pocket is dominated by polar residues. The preference for arginine out of all polar amino acids may be attributed to its positive charge, and very low pKa; lysine also has a positive charge and a low pKa (~10.5), but arginine's is much, much lower (~13.8) **fixme add citation** and it is able to form an additional hydrogen bond, and therefore reasonably dominates amongst the polar amino acids. Cysteine is used to coordinate the iron of siroheme, and while this did not significantly affect the frequency for other heme molecules, it is still possible this inflates the value for cysteine for siroheme.

After this group of polar amino acids, glycine is the next most frequent. Glycine has been situated at about a median frequency for other heme molecules, so perhaps its frequency here, slightly above the median, is of note. Only speculation is possible; perhaps ensuring the dominance of polar amino acids in the binding pocket requires extenive folding in the protein, therefore favoring glycine residues.

Finally we come to several nonpolar amino acids: alanine, phenylalanine, and valine. These amino acids define roughly the median of the frequency data. With all the polar groups on siroheme, it might be expected that only polar interactions would be desirable. However, the not miniscule frequency of these residues suggests nonpolar interactions still occur in the binding pocket; the porphyrin ring remains, as well as methyl groups and the small nonpolar portion of the carboxyl and propionate groups. It is perhaps in these areas that the nonpolar residues interact.

After these nonpolar residues the remaining frequencies do not follow a clear trend but regardless are discussed. After aspartate the remaining frequencies are considerably lower. This may be an artefact of a small sample size, or may suggest the remaining residues form, if any, less favorable interactions with the heme.

Aspartate appears next most frequently; it is a polar, negatively charged amino acid (at pH 7). Siroheme is saturated with other electronegative groups, and the repulsion of htese charges perhaps explains while aspartate, despite being a polar residue, appears not very frequently in the binding pocket.

Leucine is the first of the residues of diminished frequency. It is nonpolar. It, and, skipping a frequency, methionine, isoleucine, and proline, appear less frequently, and therefore are likely disfavored from forming the relatively few nonpolar interactions that do occur. Why is not clear - other small, nonpolar residues, and other lengthy nonpolar residues appear in the pocket in greater frequency. **double check pKa?**

Serine appears just less frequently than leucine, and in this context may likely be considered a polar residue that is not as strongly polar or positively charged and therefore less preferred to include in the binding pocket to form polar interactions with siroheme as other residues.

2. Results and Discussion

Histidine appears quite infrequently. As with siroheme, other, more strongly polar and perhaps less bulky residues are likely preferred.

Tryptophan is the least frequent nonpolar residue. The presence of a weak hydrogen bond and its size may preclude its inclusion in the binding pocket in lieu of more uniformly nonpolar residues that take up less space.

Tyrosine and glutamate are the least frequent polar residues. This is in stark opposition to the other heme molecules - tyrosine seemed to be favored for other heme molecules to form interactions with the propionate groups. Glutamate is also extremely infrequent, even in spite of its similarity to aspartate. Both are electronegative at pH 7 - glutamate's extra carbon may provide sufficient steric hindrance to render it less favored. In either case, the infrequency of these residues and the tendencies of other, more intensely polar or nonpolar amino acids to be more populous, suggests tyrosine and glutamate, in the siroheme binding environment, do not interact strongly enough to be favored over other polar residues. **I'm gonna need to get the pka table maybe**

Comparing to SRM AA Background Freq

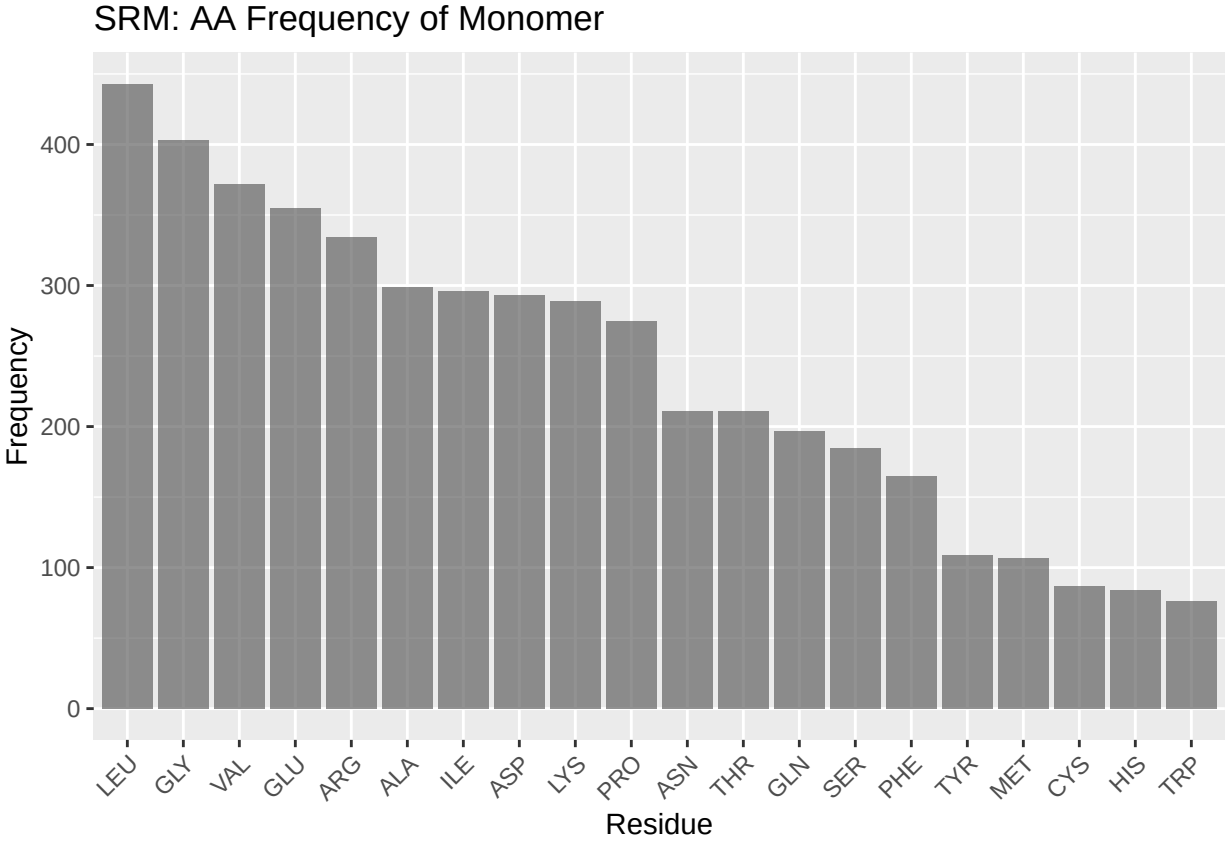

Figure 2.11: SRM: AA Frequency of Monomer

Compared to the other heme molecules, siroheme's binding pocket amino acid frequencies are even more different than the background frequencies. Arginine is far and away the most frequent amino acid in the binding pocket - leucine is the most populous amino acid in the monomer overall, seeming to follow a trend amongst the hemoproteins examined so far. Again discussing the remainder of the frequencies of the monomer would be pure conjecture, but it is worthwhile to note that the pocket frequencies certainly appear unique against the background.

Distance stuff

Residues appear less uniformly distributed over distance for siroheme binding pockets when compared against the distribution for other heme molecules. Cysteine is the only residue that comes within 5A of siroheme; it is used to coordinate

the iron in siroheme, so this result is expected. The lack of other residues being within 5A, differing from other heme molecules, suggests the many carboxyl and propionate groups on siroheme prevent, or preclude the need for closer interaction except for coordinating residues.

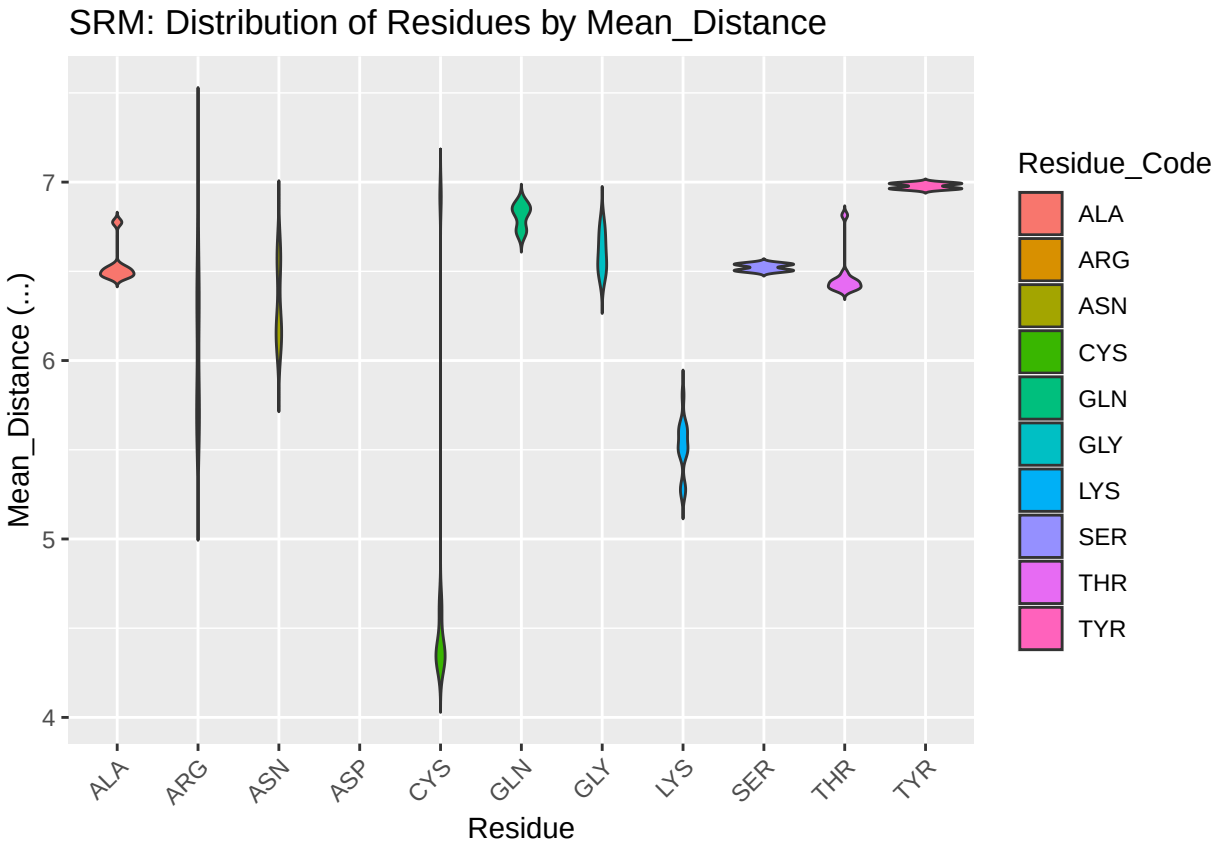

Figure 2.12: SRM: AA Distances

2.3 Volume Discussion

Figures can be found in Appendix A.2.

worthwhile to add SD measures? 'x% values fall within... The utility of this result is somewhat dubious, at least within the context of this study. Volume results were rather spread out, with close agreement only found for heme-b. In general, volume for all heme molecules regardless of distance cutoff averaged about 1200 A^3. This is somewhat contrived, and the result is not useful for elucidating the binding environment further; perhaps for other studies this result, or its lack of precision, may be informative.

2.4 Surface Areas

2.4.1 Surface Area of Heme Molecules

Just going off solvent accessible, since that's really all that's of chemical importance. Can mention the excluded data is in the appendix

Both solvent accessible and solvent excluded surface areas were calculated for heme molecules and binding pockets. The results are extremely similar and only solvent accesible surface area, a measure more practically interpreted into chemical phenonema, is discussed; figures and data for solvent excluded surface areas are available in Appendix (FIXME: insert reference)

worth it to add SD etc? I think maybe, if time. Would leave raw data in appendix and add summary statistics in this section

The solvent accessible surface area for all heme molecules themselves centers around values of 1000 A^2. This result is reasonable, given the similarity in size and structure of all heme molecules, in spite of the attached groups. Figures are shown below; extreme outliers have been removed from these figures but full data tables are available in (FIXME add appendix number). The outliers are likely artefacts of the method used to calculate surface area and potential conflicts with the method used to convert multimeric proteins to monomers. **worth to include this last statement?**

2.5 Surface Area of Binding Pockets

The surface area of binding pockets is more varied than the heme surface areas.

Heme-b and verdoheme, being highly similar molecules, with the same propionate groups, and one the derivative of the other, have quite similar surface areas, centering around 10,000-11,000 A^2. This is useful as a baseline to discuss the surface area of the binding pockets of the other two heme molecules below.

The surface area of the binding pocket of heme-c is considerably lower than that of heme-b and verdoheme. Its values center around 7500 A^2. Heme-c is bound

covalently to the hemoprotein, forming thioether bonds with cysteine residues at two sites, excluding these sites from interacting with water molecules. **is this all that explains the reduction in SA? forgive my ignorance!**

The surface area of siroheme's binding pocket is far greater than that for other heme molecules - values center around 21000 A^2. Siroheme's extra groups do not appear to affect its own surface area, per above. However, it is effectively a very polar molecule and appropriately the binding pocket is highly saturated with very polar amino acids, as seen in the amino acid frequency analysis. The binding pocket is therefore completely different from the other heme molecules, and these populous, polar amino acids favorably interact with aqueous solvent, negating the need to bury any hydrophobic residues and reduce surface area.

2.6 Angular Data

**I think I'll just stick all of this in the appendix, including highlighting the clusters of data. Nothing can be discussed from it - it is interesting to note and perhaps I'll include some examples below very briefly, but otherwise, I don't know what value would be added to the report of "verdoheme always has his interact with a planar angle of 116 degrees"

Figures can be found in A.7

These data, for all ligands, except potentially for heme-c, largely serve to compare as noise for the next section. The planar angles of all residues, falling within the upper distance cutoff of 7A, are plotted.

In the notable exception of heme-c, Figure **FIXME: insert figure name** seems to suggest that GLU, MET and LYS have fairly specific planar angles with the ligand. Lysine is effectively the median of amino acid frequency for heme-c, methionine is even less frequent and glutamine is the least frequent amino acid. For the latter two amino acids their tight range of planar angles is therefore likely an artefact of a small sample size of amino acids. However, for lysine the tight range of angles may be significant; this is dicussed further below.

2.7 Planar Angles of Closest Residues

Figures can be found in A.8

Here, the three closest residues to the ligand in each PDDB and their planar angle to the ligand are plotted. Data are summarized below, and discussed below.

HEM has a fairly inconclusive set of data for this measure. GLU and GLN nearby HEM do appear to fall within a tight range, though, of approximately 75 degrees and 80 degrees respectively.

The data for residues nearby HEC diverge from what is found for all residues around HEC. The most agreement is found for ILE and LYS, with angles concentrated about 50 degrees and 75 degrees, respectively.

2.8 All CA-CB-Fe Angles

Figures can be found in A.9

2.9 CA-CB-Fe Angles of Closest Residues

Figures can be found in A.10

2.10 Limitations of the Study

Limited sample size

Limited experimental data to reference to verify

NO experimental data in this study to verify, all theoretical

Only one software package/few algorithms used to calculate all these properties. Others were evaluated but none are compared w.

Algorithms may introduce bias based on how they work e.g. all the bubbles

Arbitrary selection of parameters; some based on rule of thumb or visual evaluation but all or almost all arbitrary

Unknown if the qualities measured are truly the most critical for the heme binding. Some papers suggest other properties may also be important but cannot be calculated, at least right now, e.g. ionic bonding strength etc.

Visual examination itself to OK the parameters/algorithms can introduce bias

3
Conclusion

A knowledge gap in the binding environment for heme exists in the present literature. A high-throughput framework employing UCSF Chimera was constructed to process diverse sets of hemoproteins and output information about their binding pockets: amino acid frequencies and distances from heme, volume, surface area, angles. Data was gathered and predicted from representative and varied datasets for heme-b, heme-c, verdoheme, and siroheme, and their respective hemoproteins. R was used to analyze all data.

The results of this study are limited by the small sample size, but suggest that binding pockets for hemoproteins have some requirements for binding that may be overlooked, e.g. a high population of nonpolar amino acids for heme-b, heme-c, and verdoheme which may provide much of the interactions necessary to bind heme; in the case of siroheme there is a preponderance of polar amino acids. In either case both polar and nonpolar amino acids appear in force, suggesting both types of interactions are important to bind heme. Volumes are within reason. Surface area results reinforce, demonstrate the significance of the amino acid frequency results and show pockets have lesser or greater surface area depending on the involvemnt of covalent bonds or preferences for polar amino acids. Angular data, while not able to be interpreted into useful results, is produced and a framework provided for future study.

These results may be useful in the rational design of hemoproteins in the future, with the importance of nonpolar interactions in particular likely of great interest. The framework constructed can be applied to any list of PDBs and their respective ligands, thereby facilitating similar research for other proteins.

Appendices

A
Figures

A.1 AA Frequency

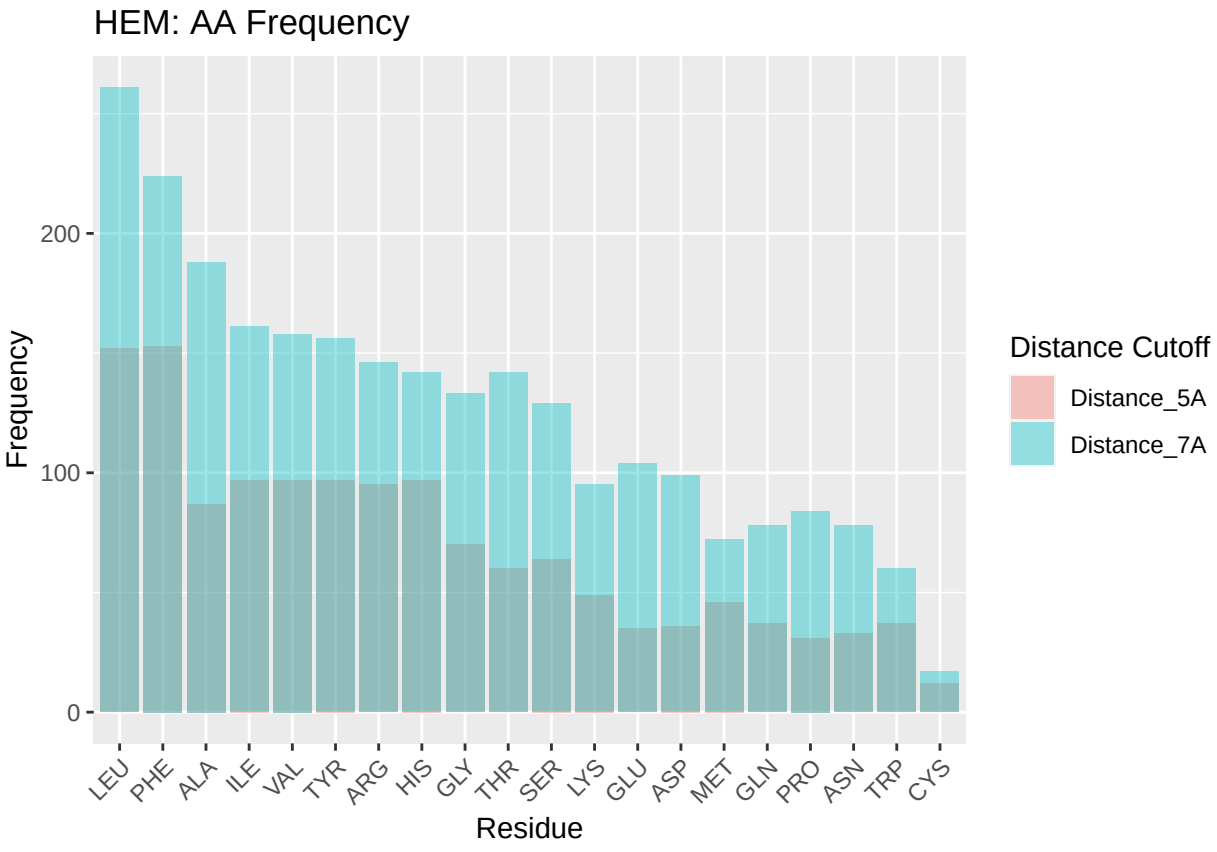

Figure A.1: HEM: AA Frequency

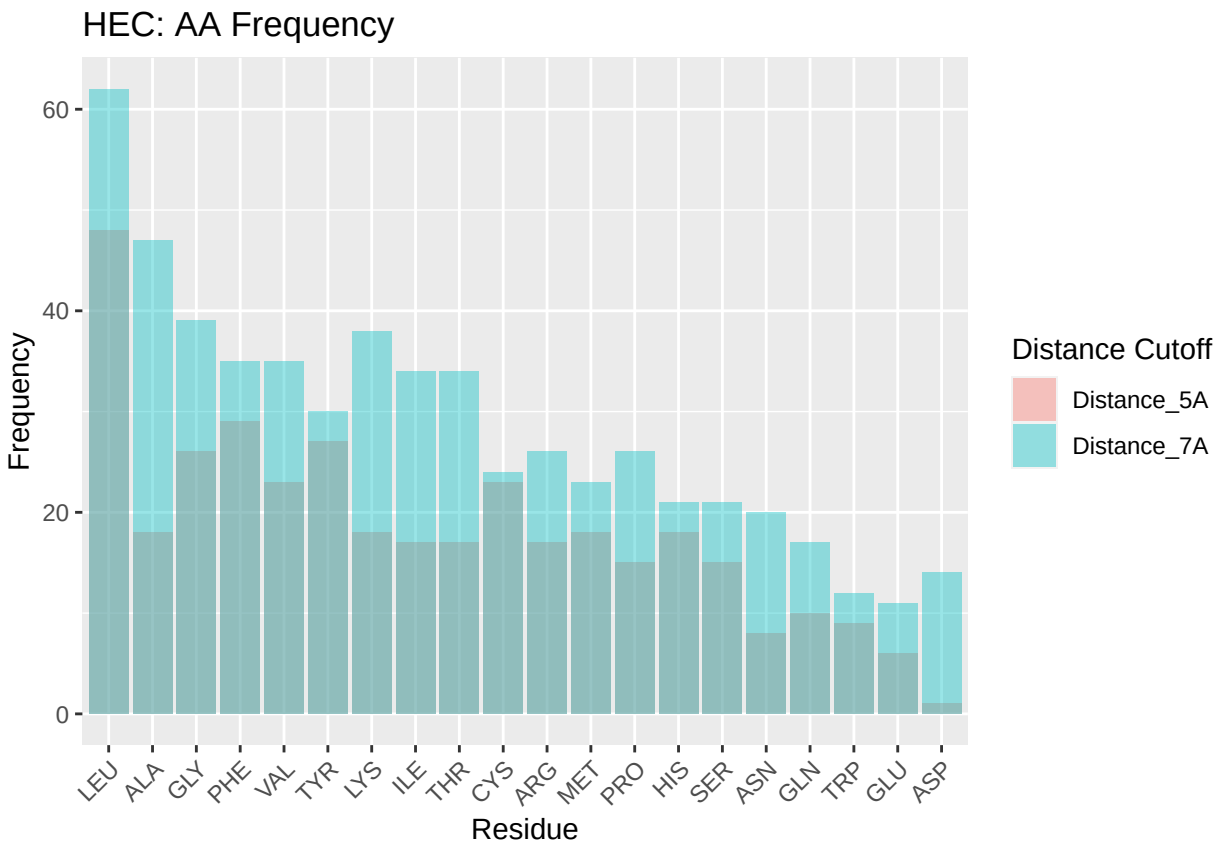

Figure A.2: HEC: AA Frequency

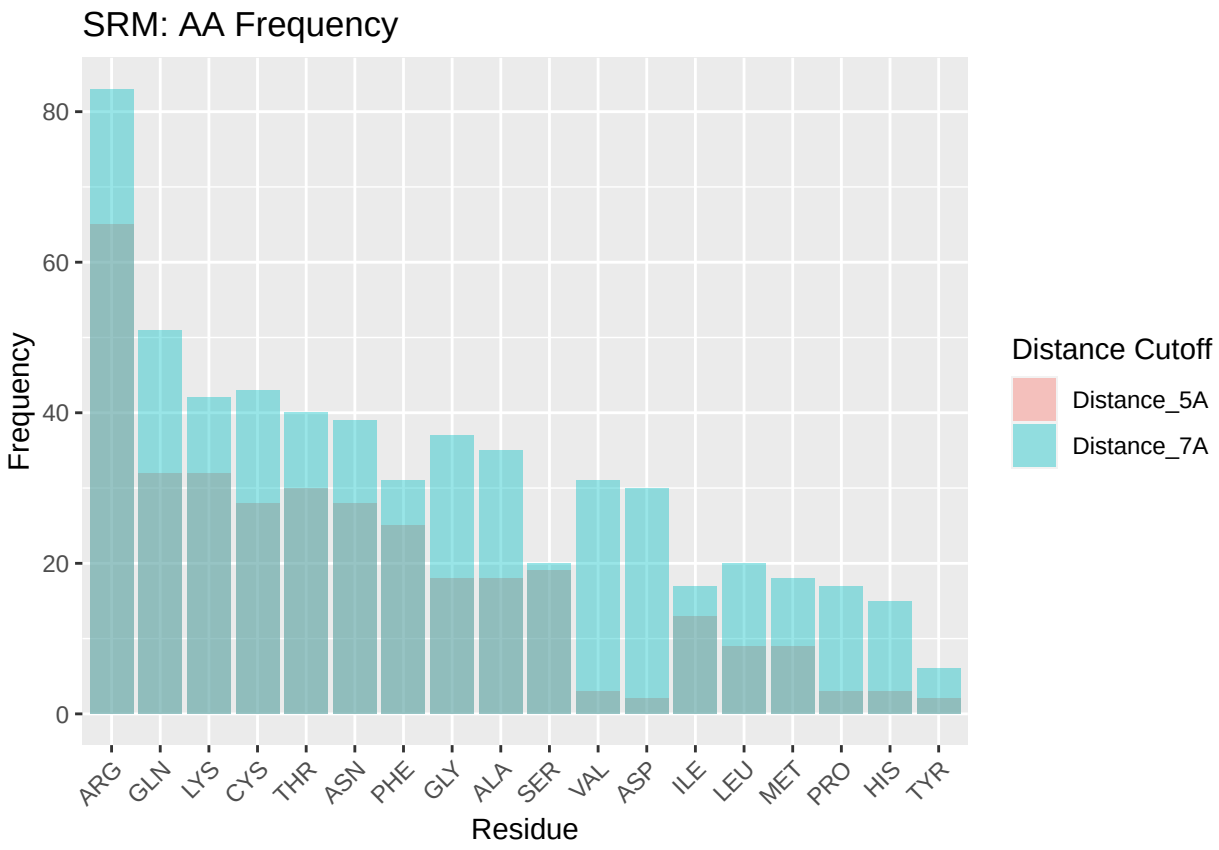

Figure A.3: SRM: AA Frequency

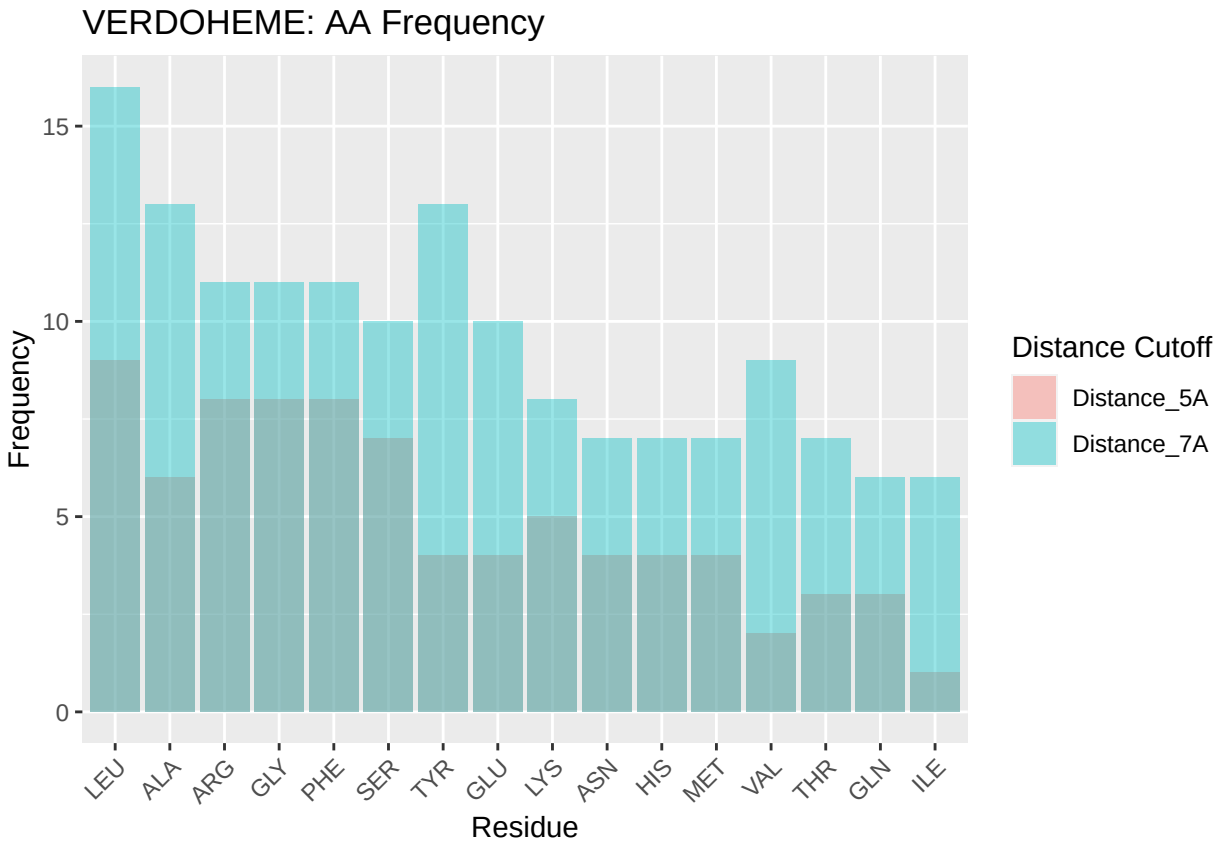

Figure A.4: VERDOHEME: AA Frequency

A.2 Volume

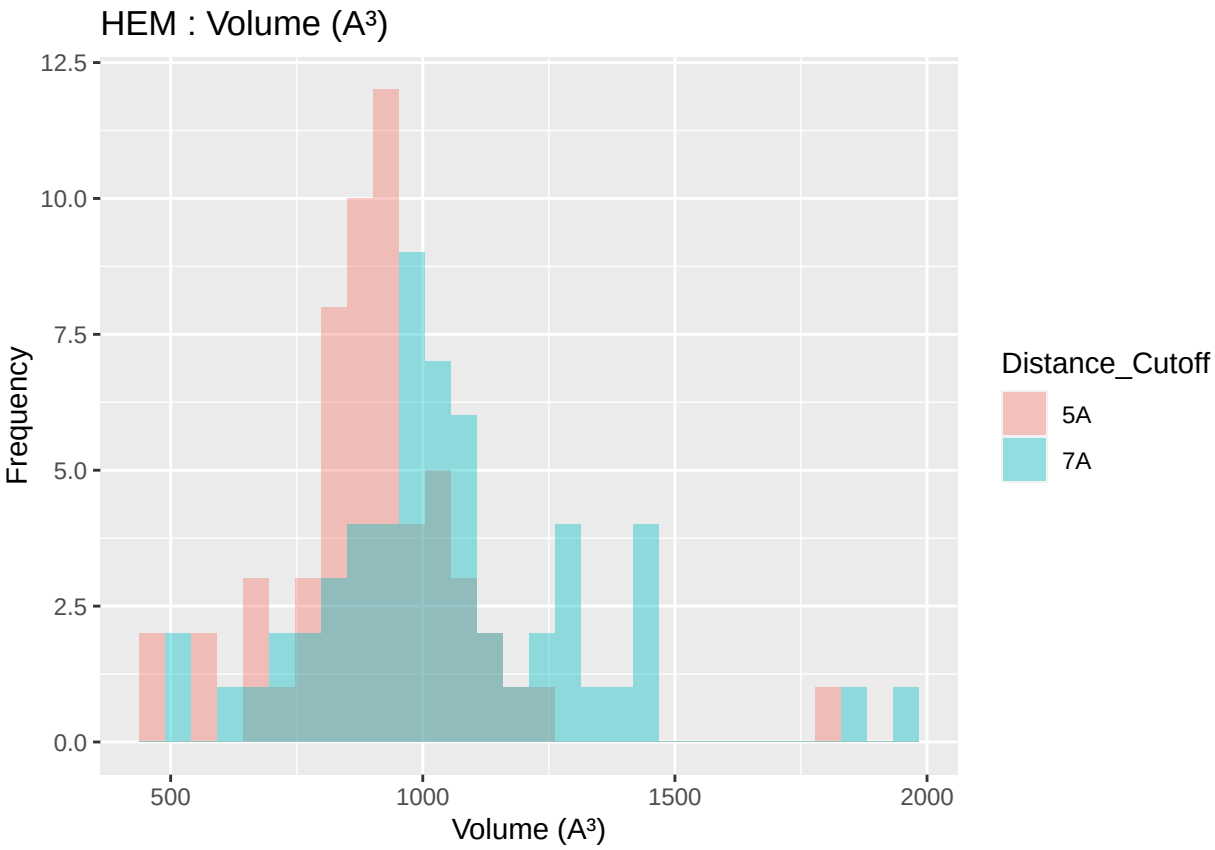

Figure A.5: HEM: Volume

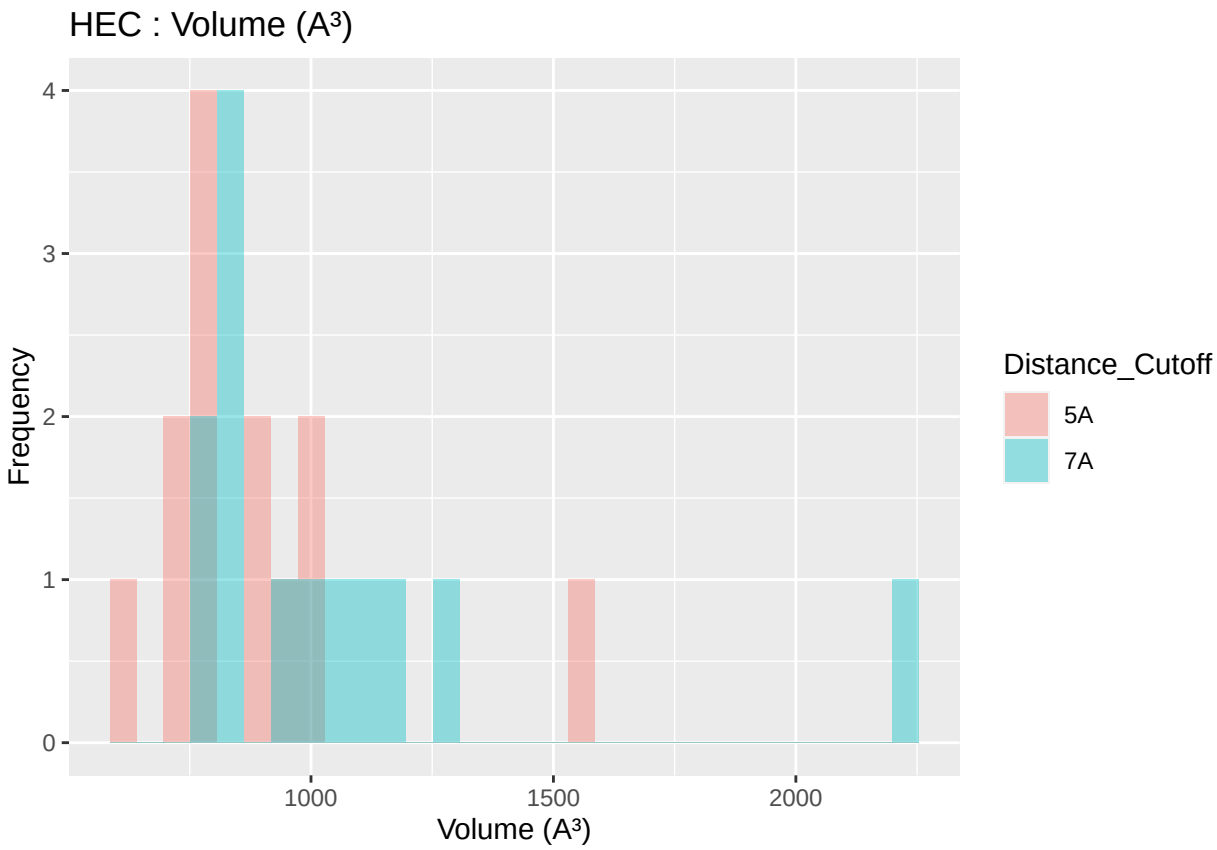

Figure A.6: HEC: Volume

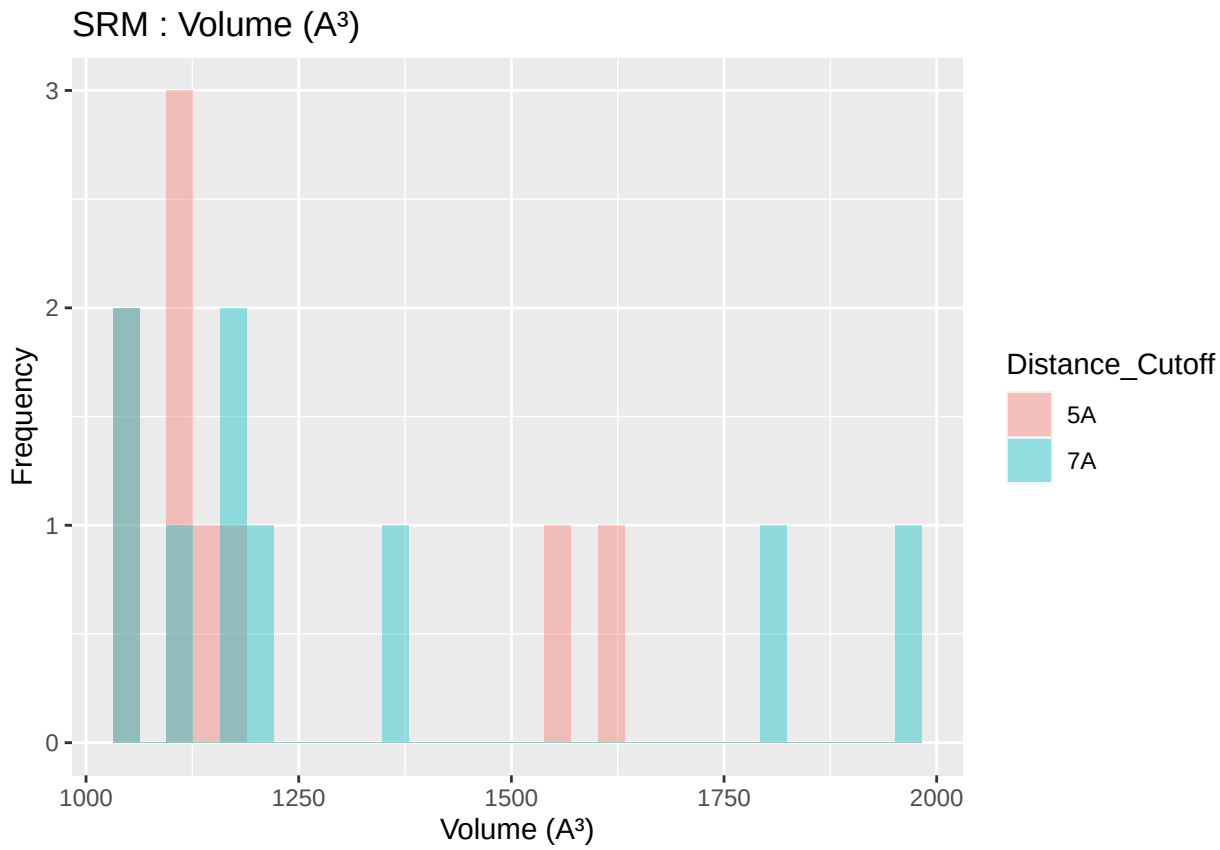

Figure A.7: SRM: Volume

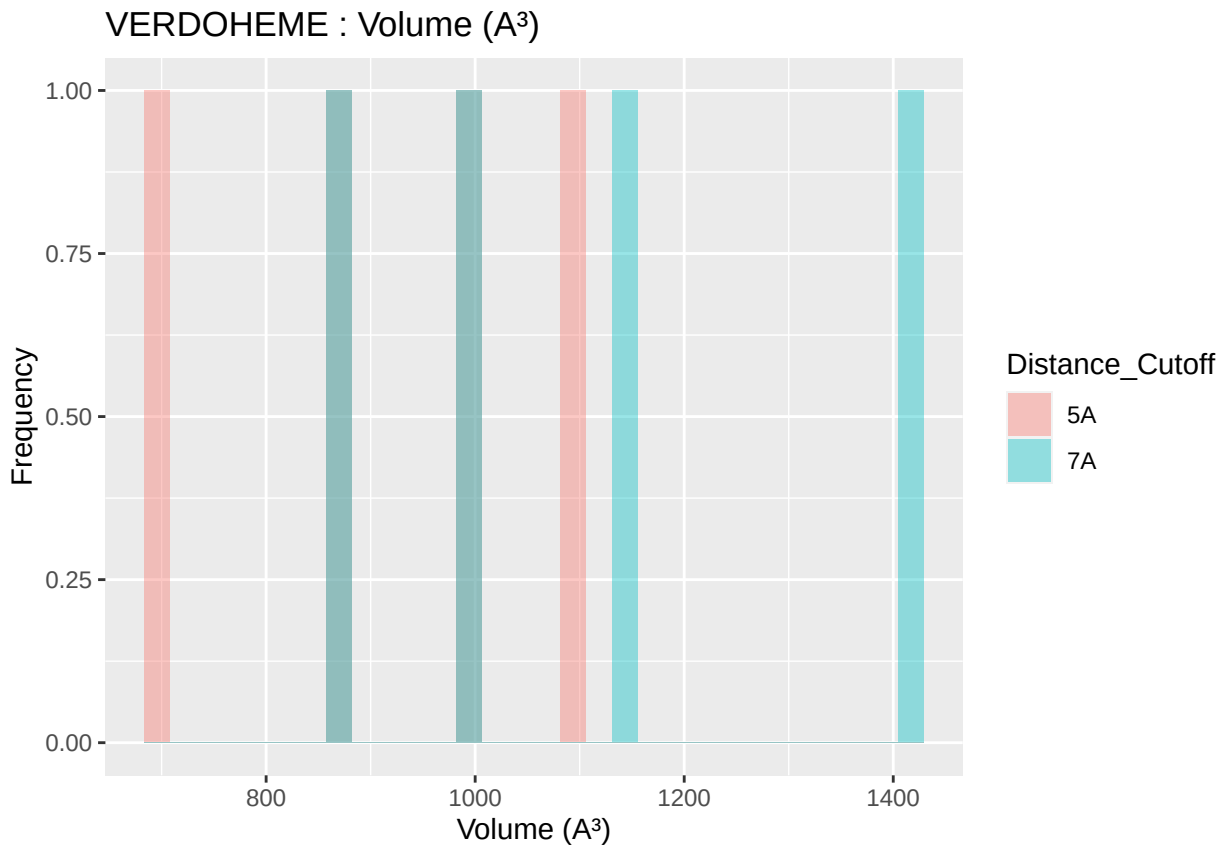

Figure A.8: VERDOHEME: Volume

A.3 Ligand Excluded Surface Area

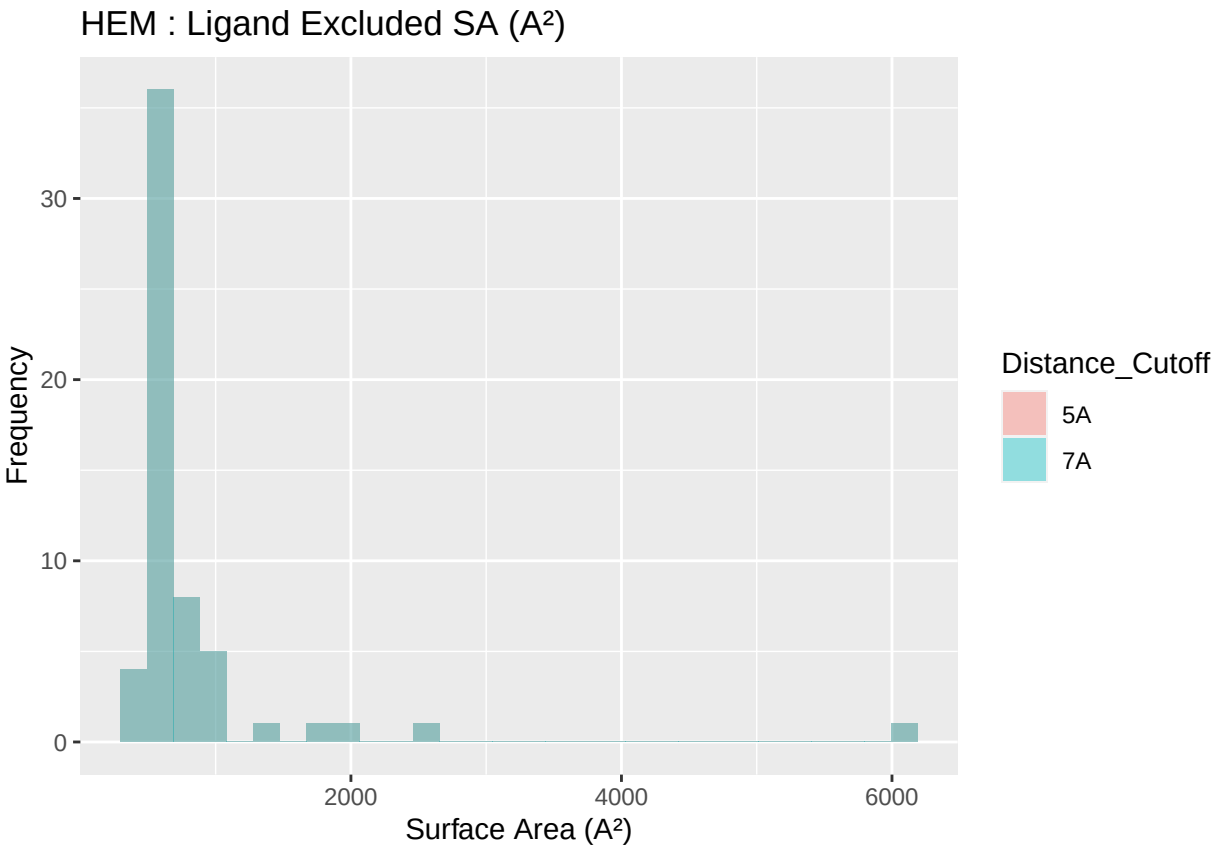

Figure A.9: HEM: Ligand Excluded Suface Area

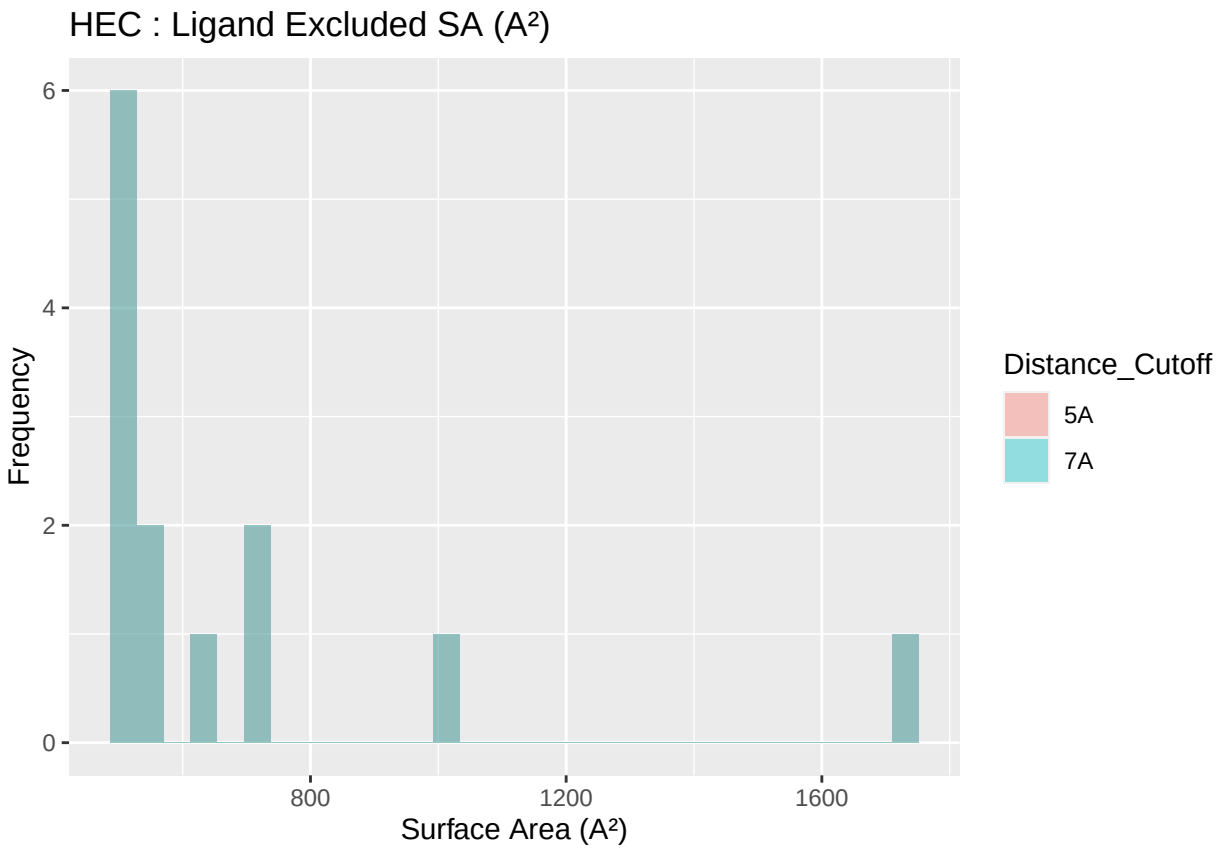

Figure A.10: HEC: Ligand Excluded Suface Area

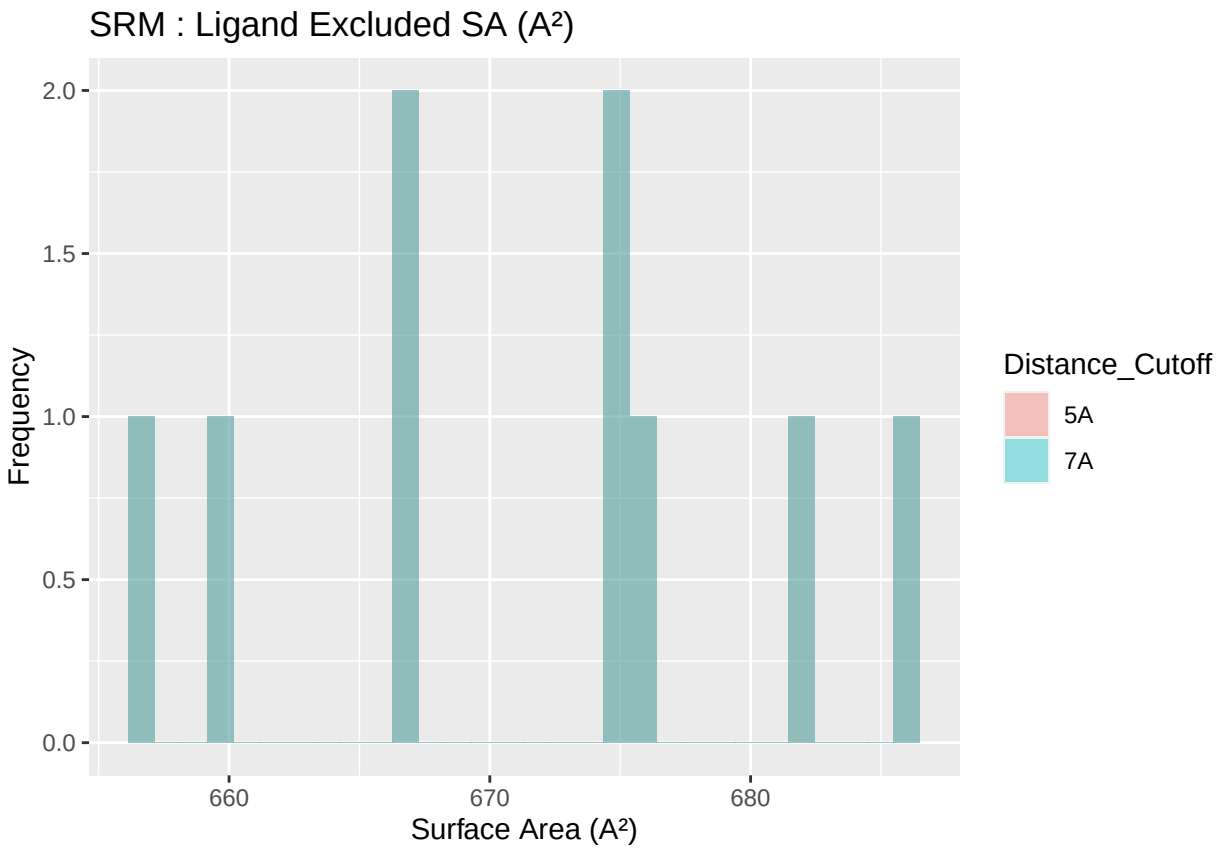

Figure A.11: SRM: Ligand Excluded Suface Area

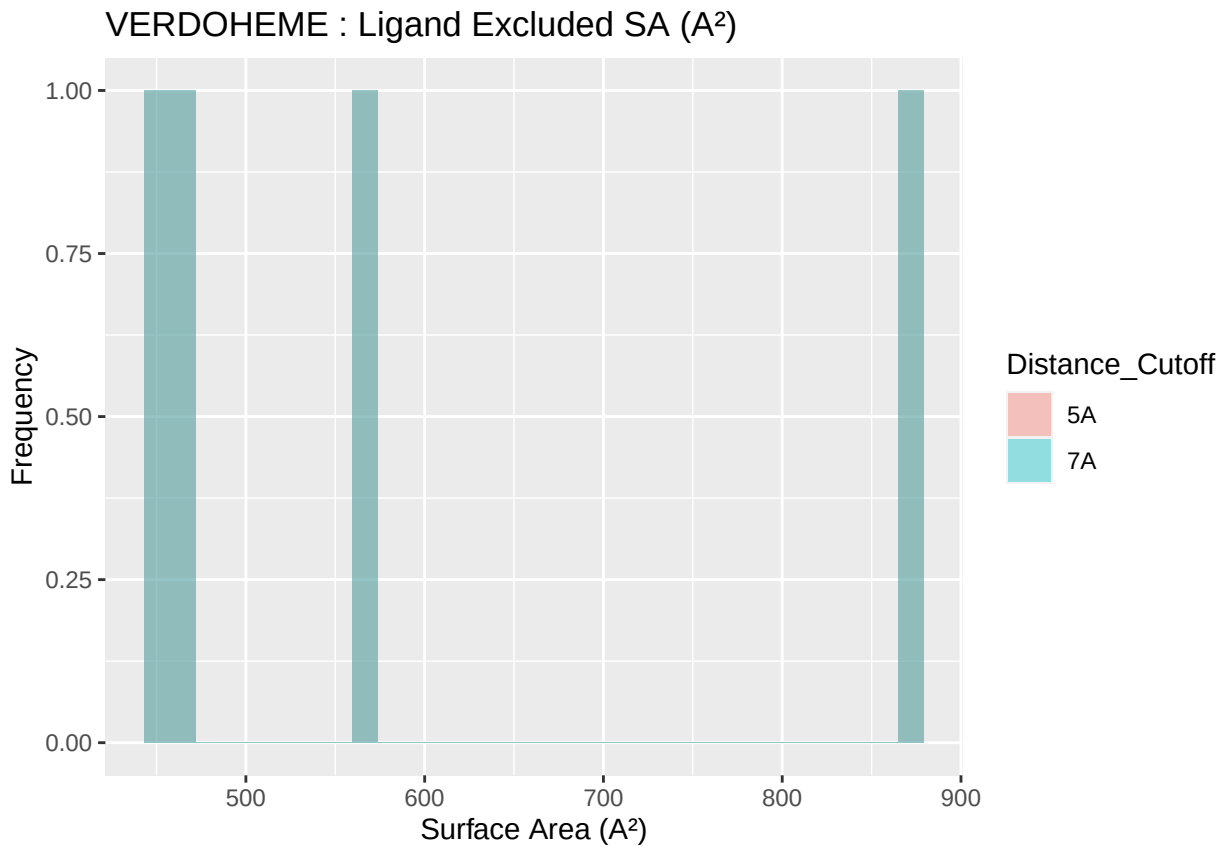

Figure A.12: VERDOHEME: Ligand Excluded Suface Area

A.4 Ligand Accessible Surface Area

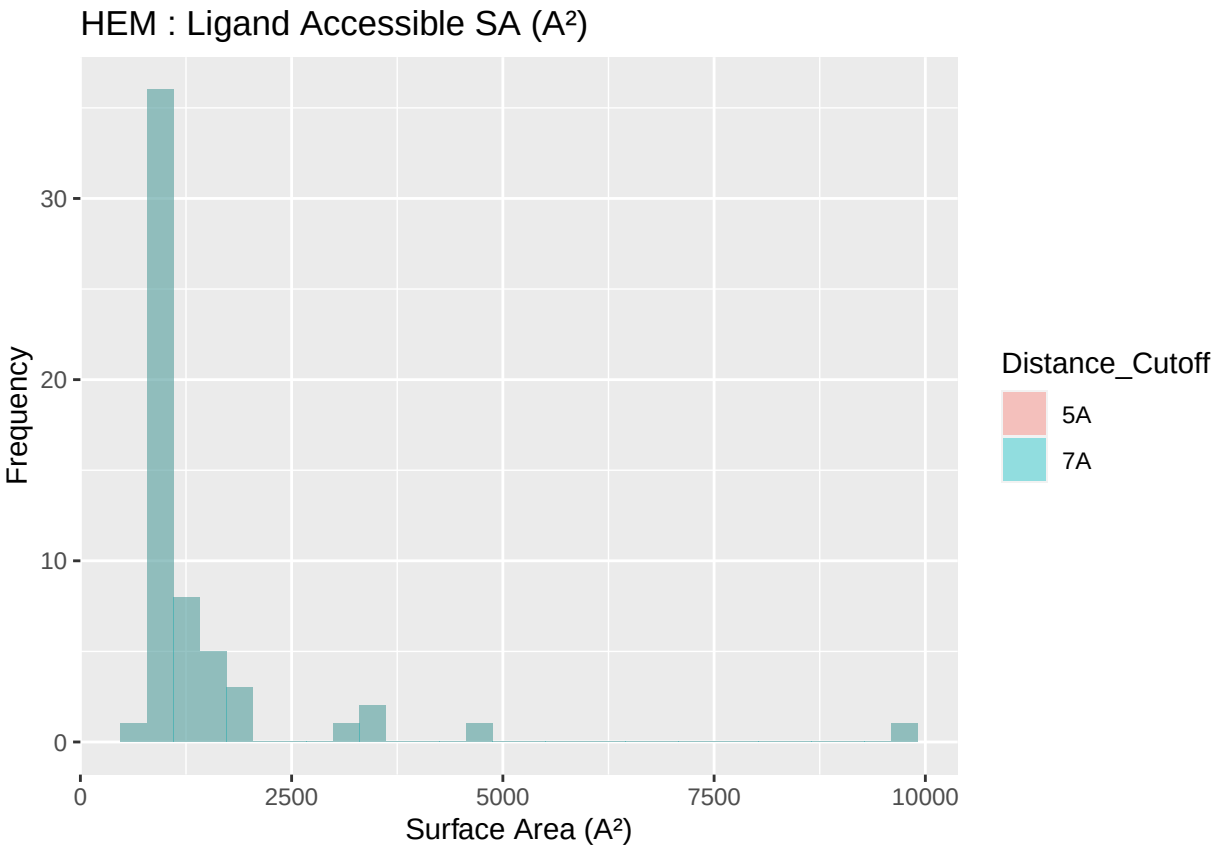

Figure A.13: HEM: Ligand Accessible Surface Area

Figure A.14: HEC: Ligand Accessible Surface Area

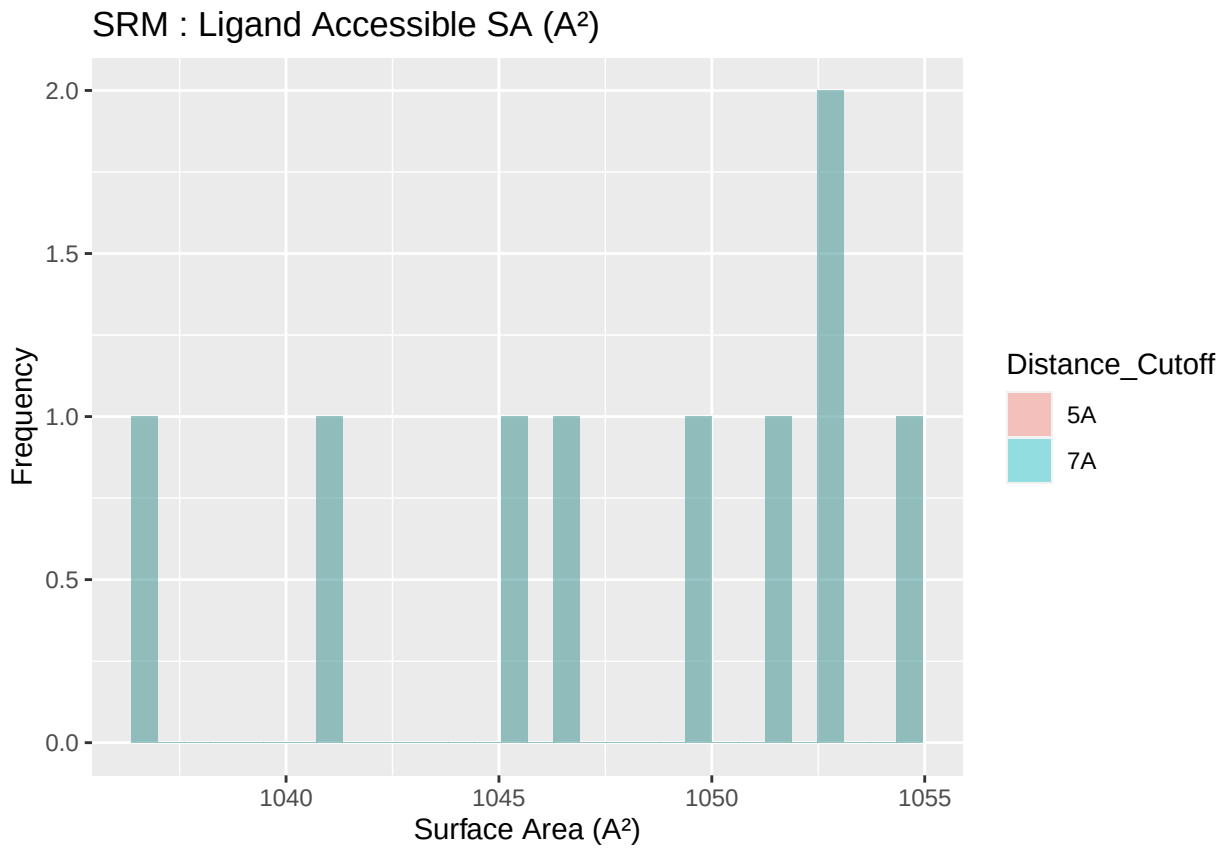

Figure A.15: SRM: Ligand Accessible Surface Area

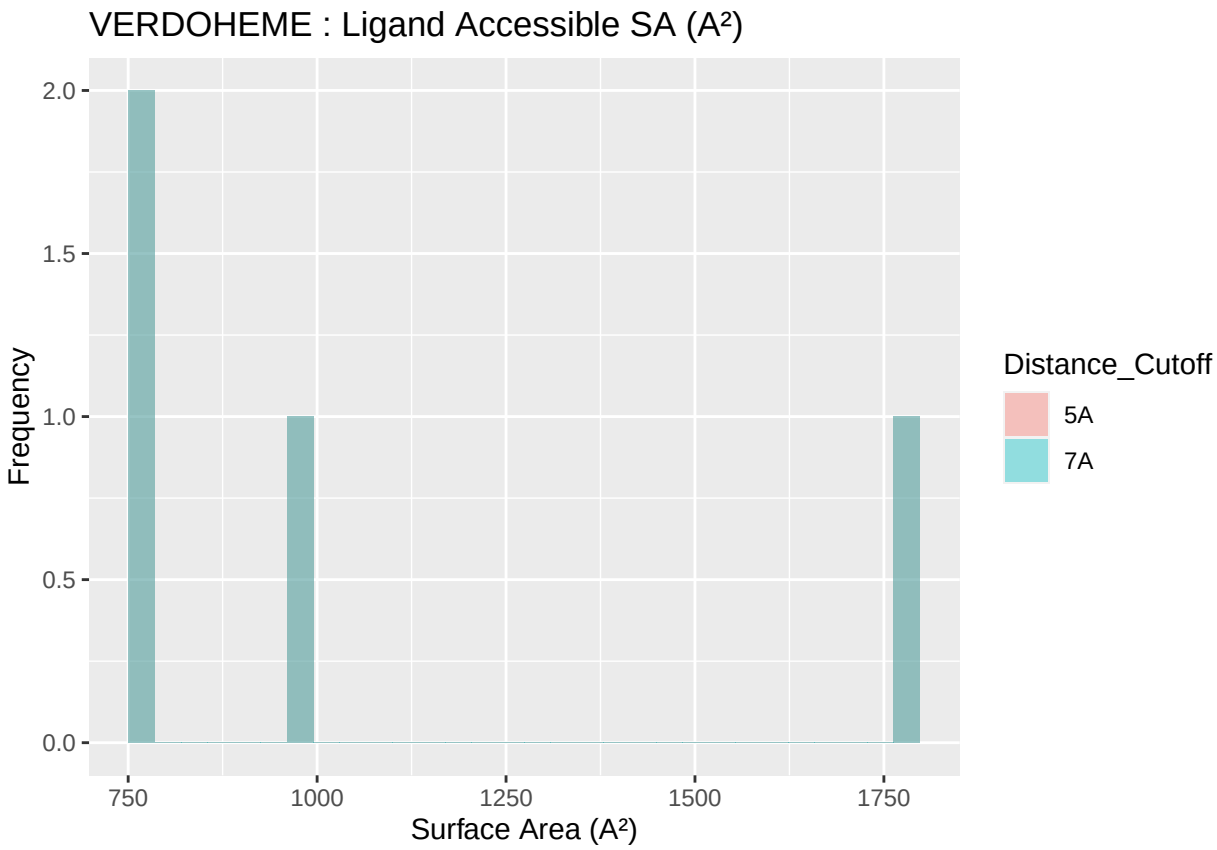

Figure A.16: VERDOHEME: Ligand Accessible Surface Area

A.5 Pocket Excluded Surface Area

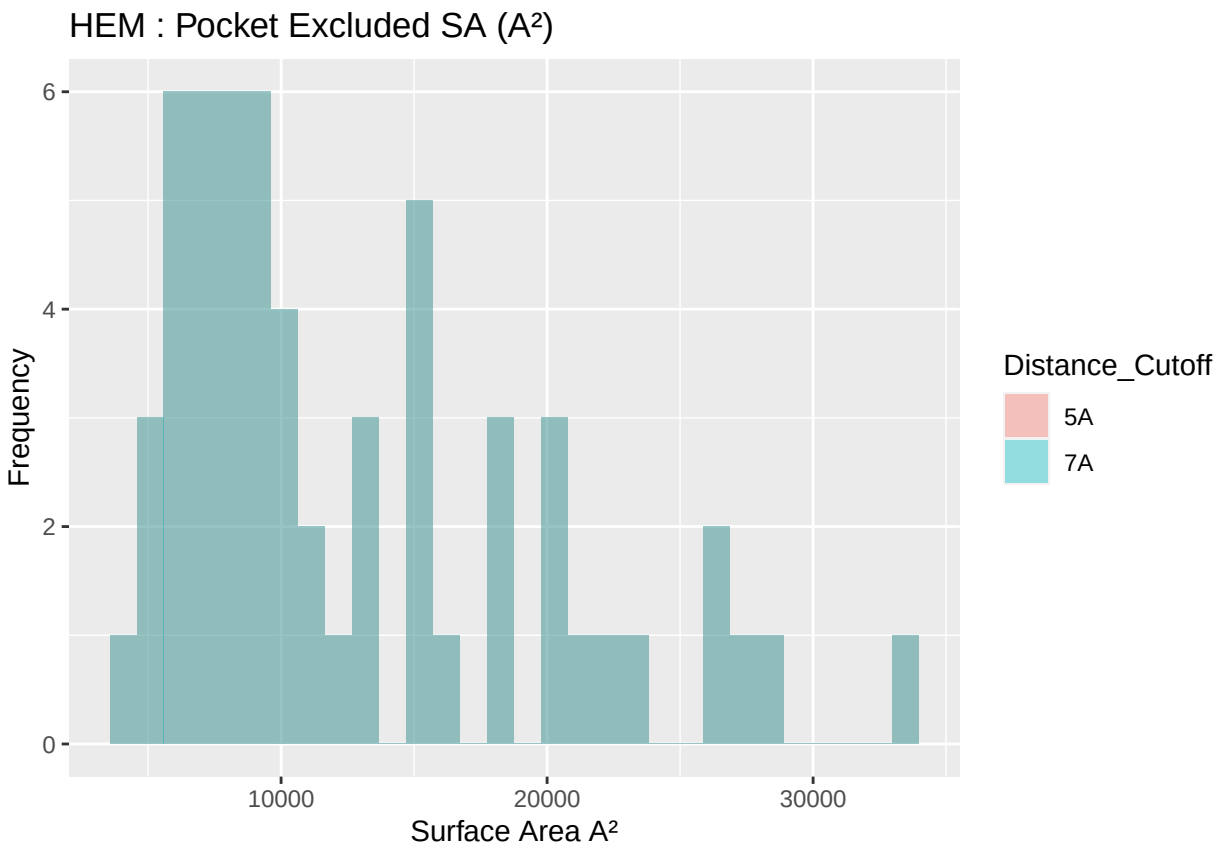

Figure A.17: HEM: Pocket Excluded Surface Area

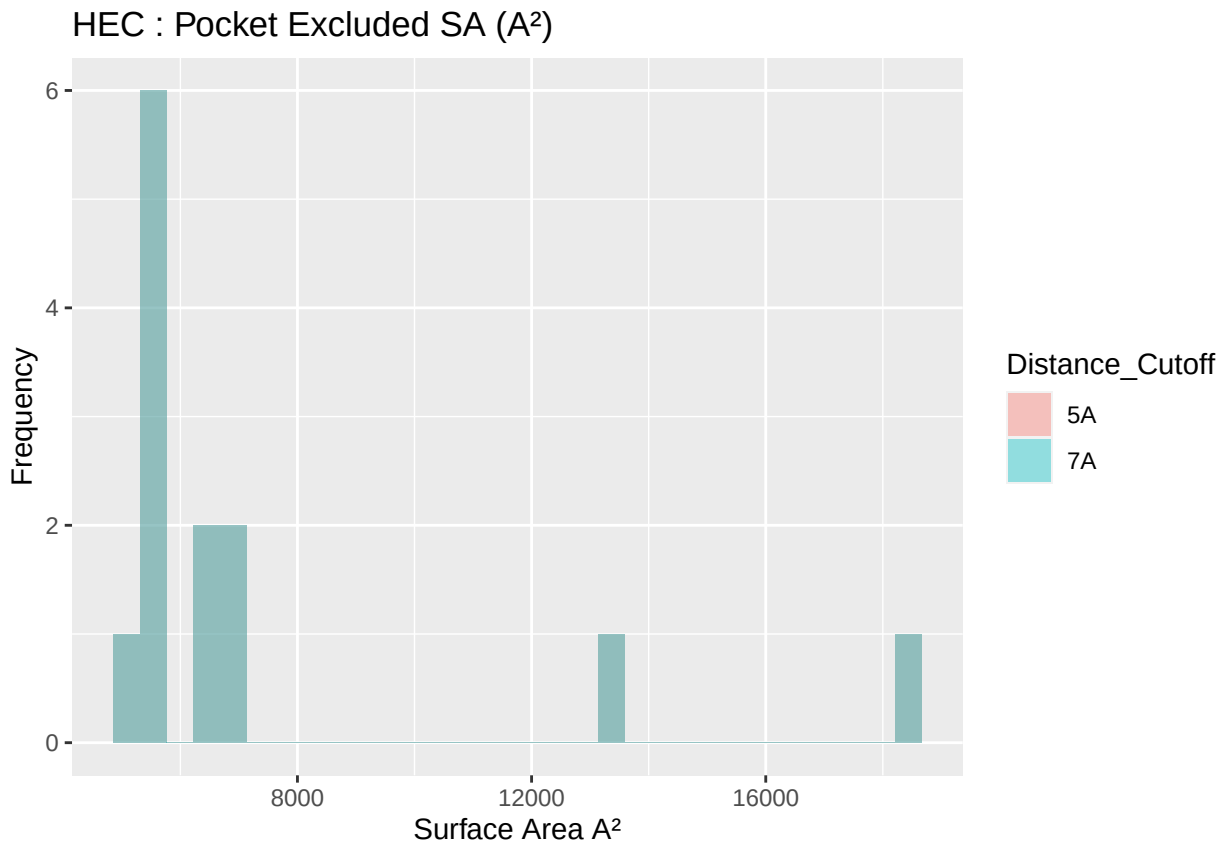

Figure A.18: HEC: Pocket Excluded Surface Area

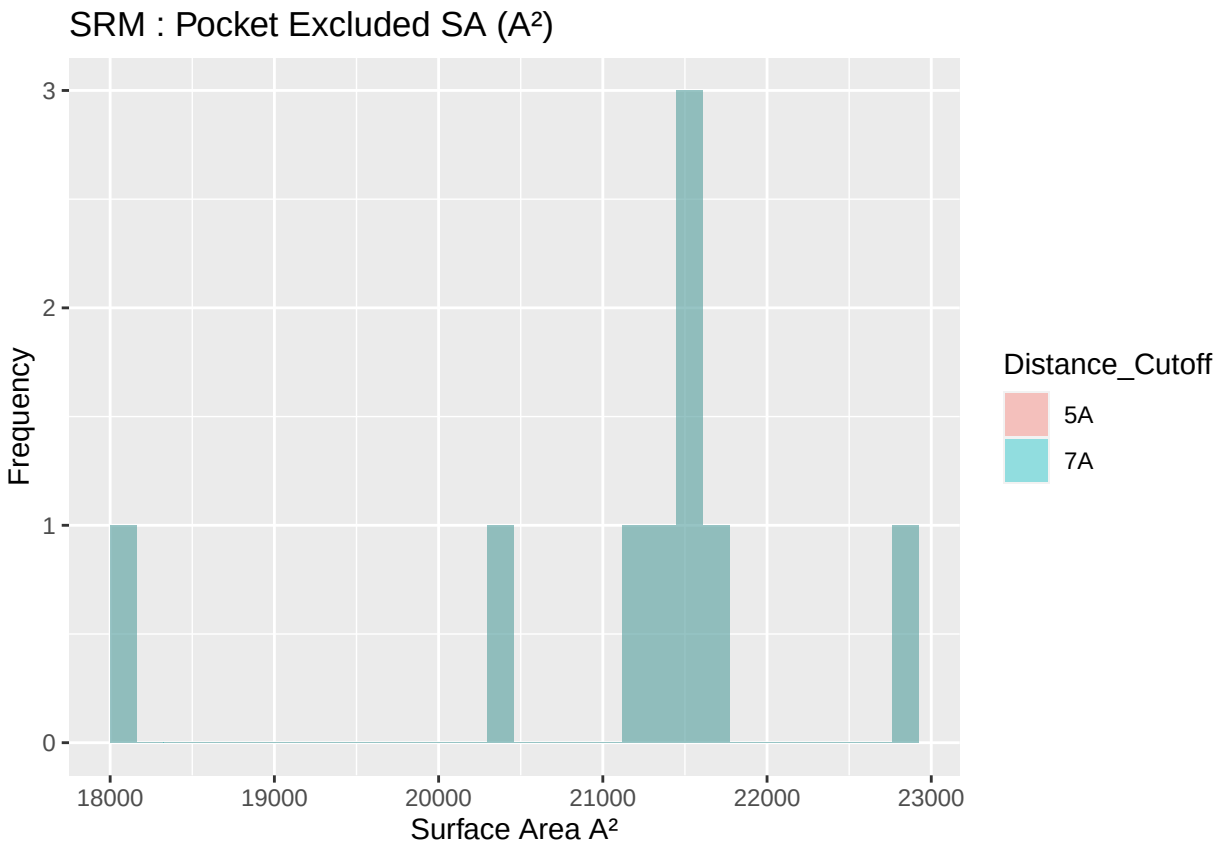

Figure A.19: SRM: Pocket Excluded Surface Area

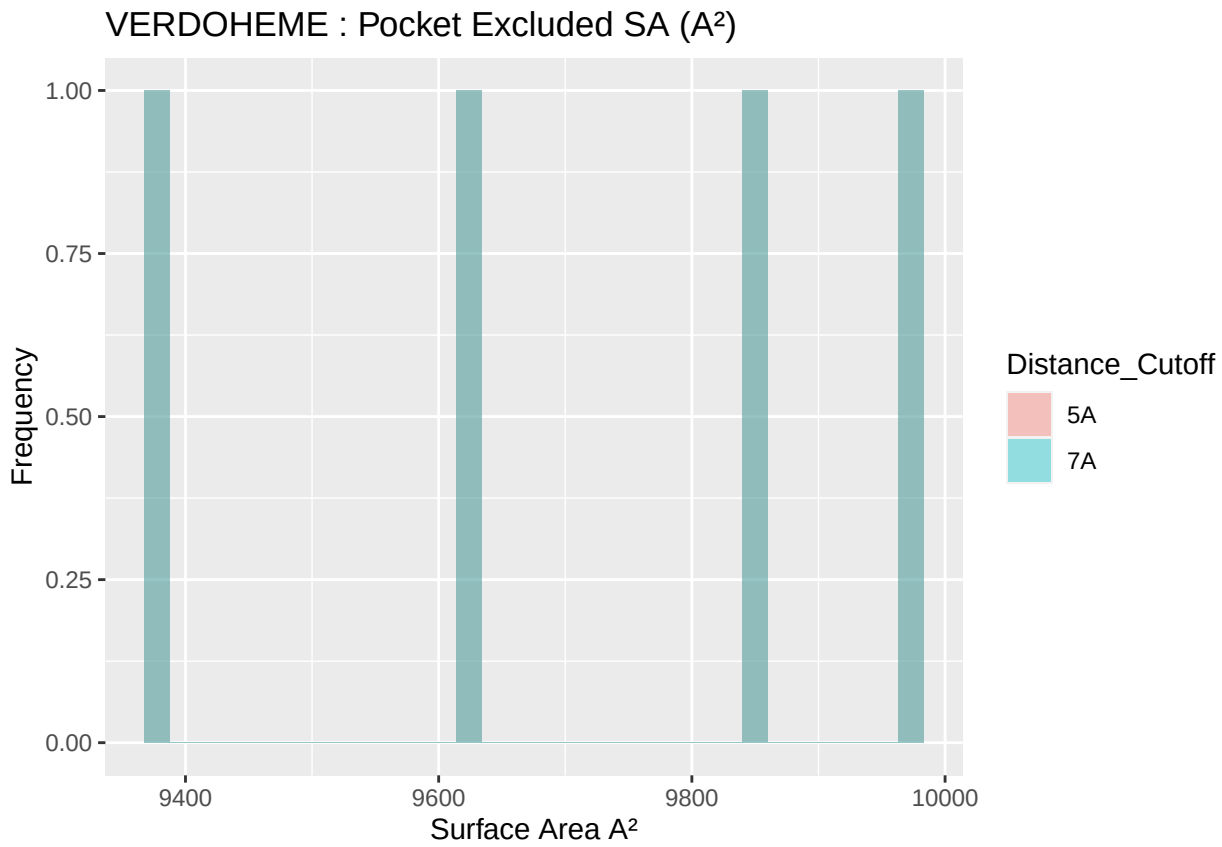

Figure A.20: VERDOHEME: Pocket Excluded Surface Area

A.6 Pocket Accessible Surface Area

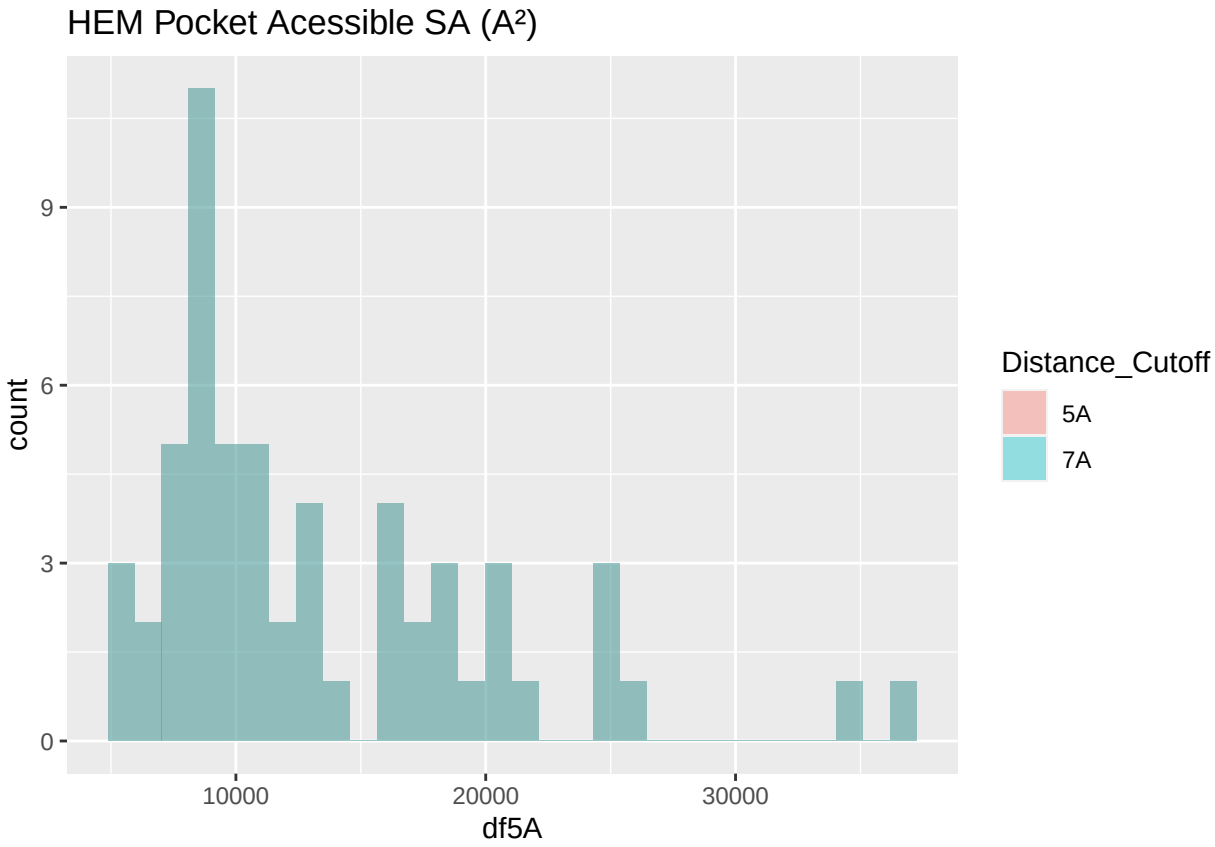

Figure A.21: HEM: Pocket Accessible Surface Area

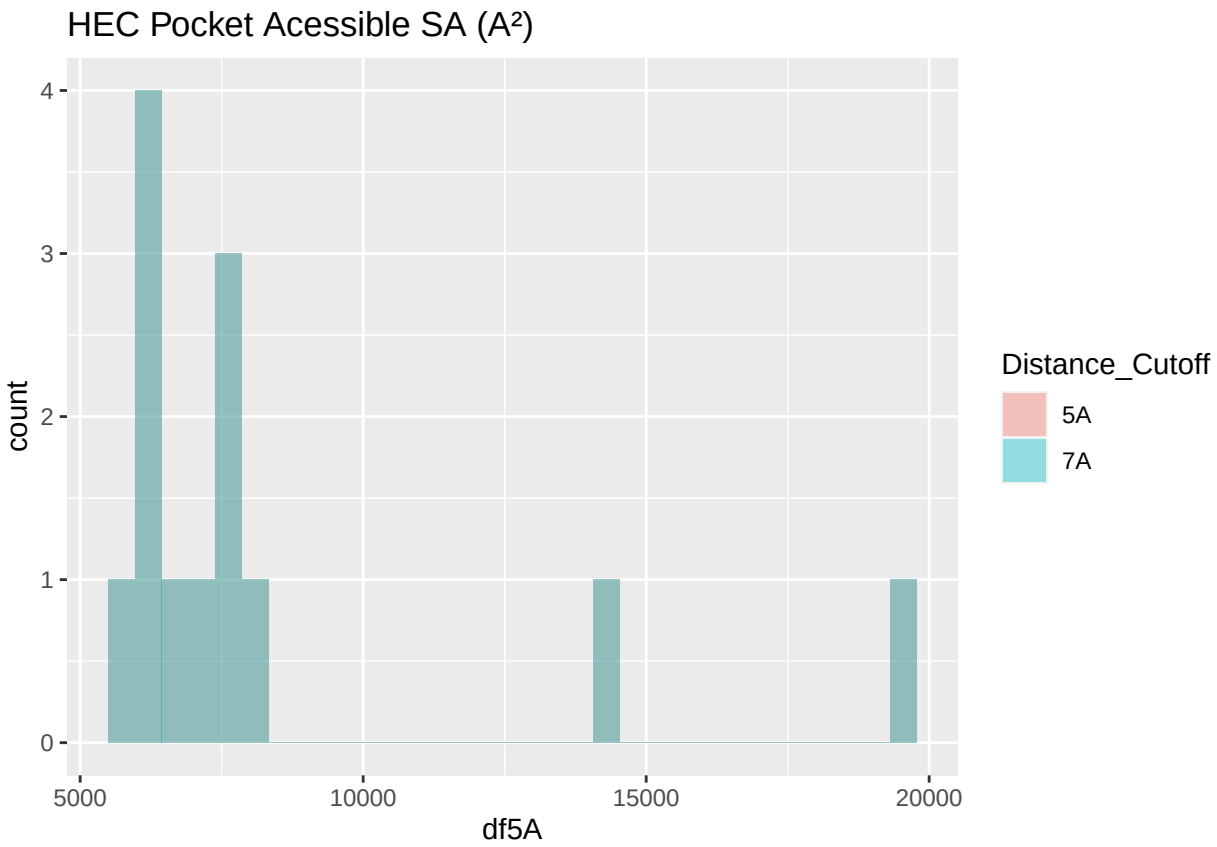

Figure A.22: HEC: Pocket Accessible Surface Area

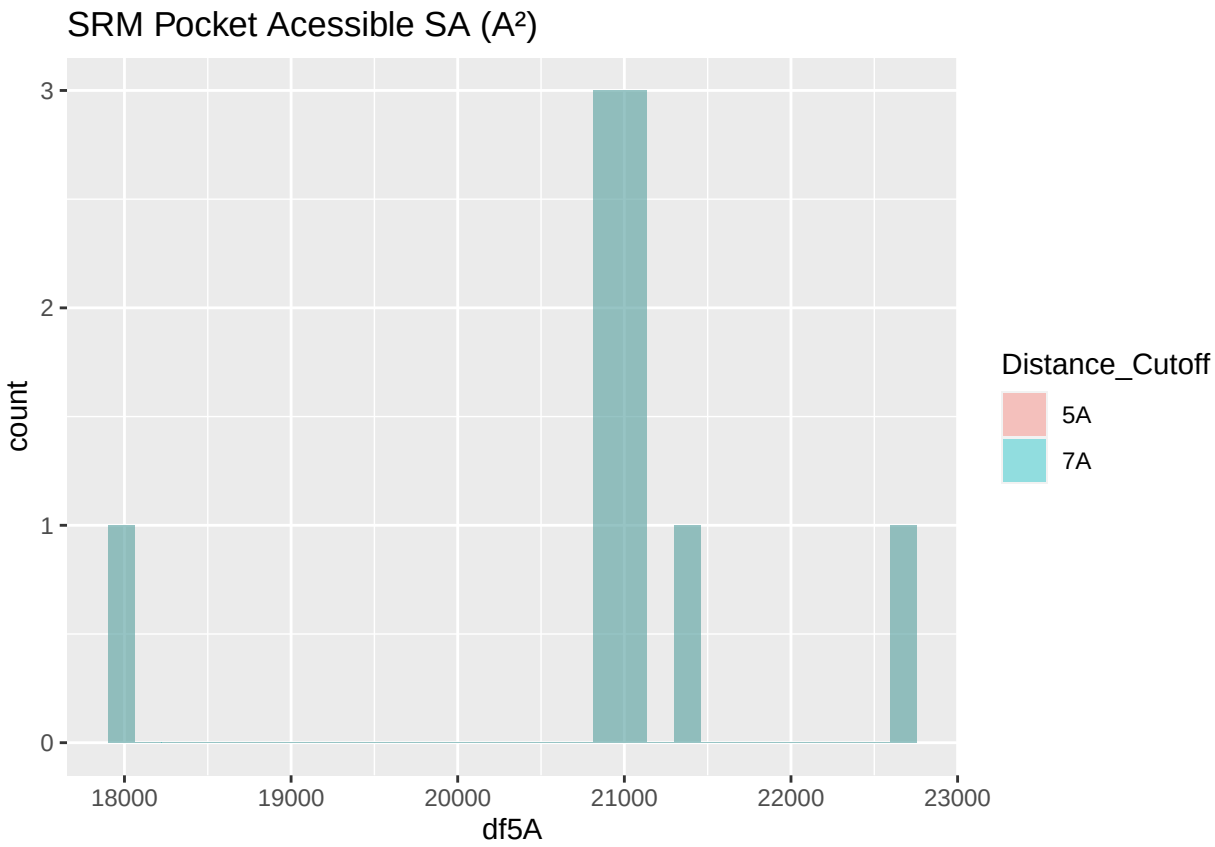

Figure A.23: SRM: Pocket Accessible Surface Area

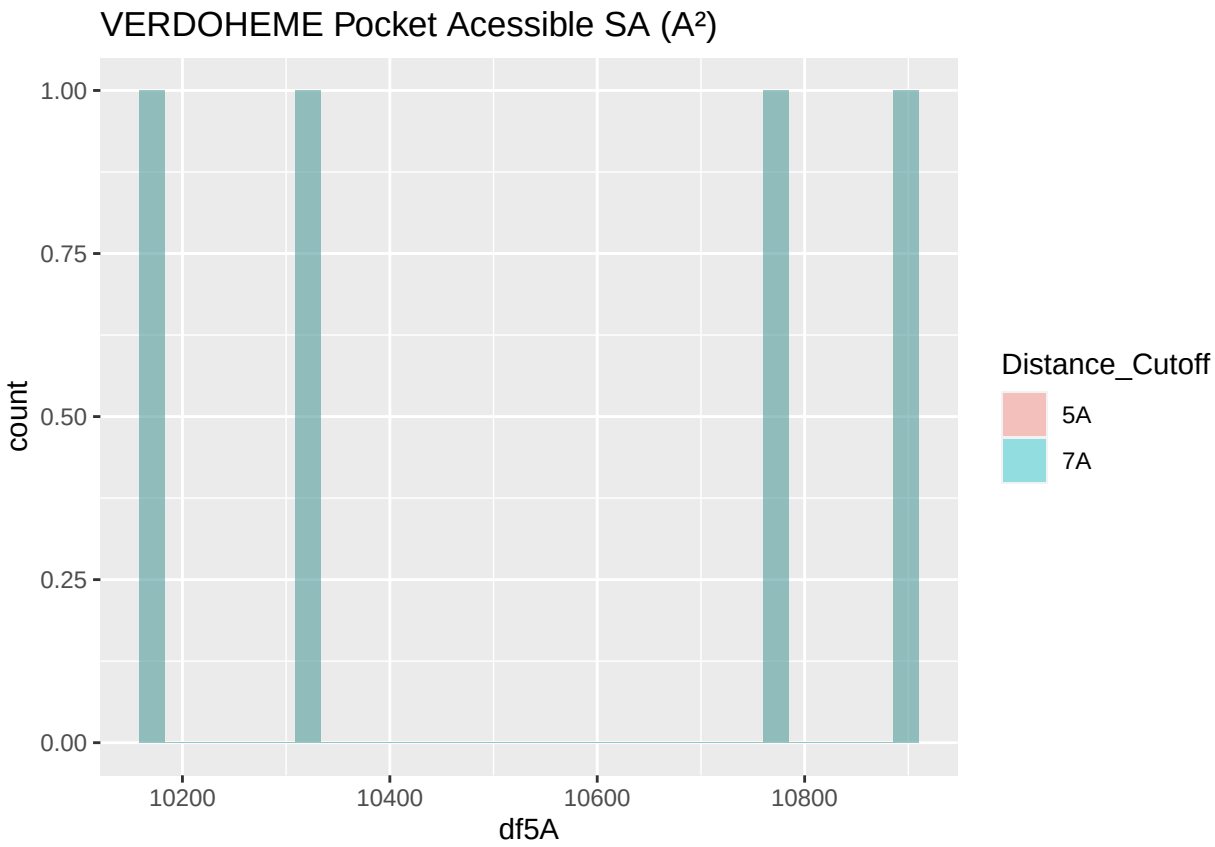

Figure A.24: VERDOHEME: Pocket Accessible Surface Area

A.7 All Planar Angles

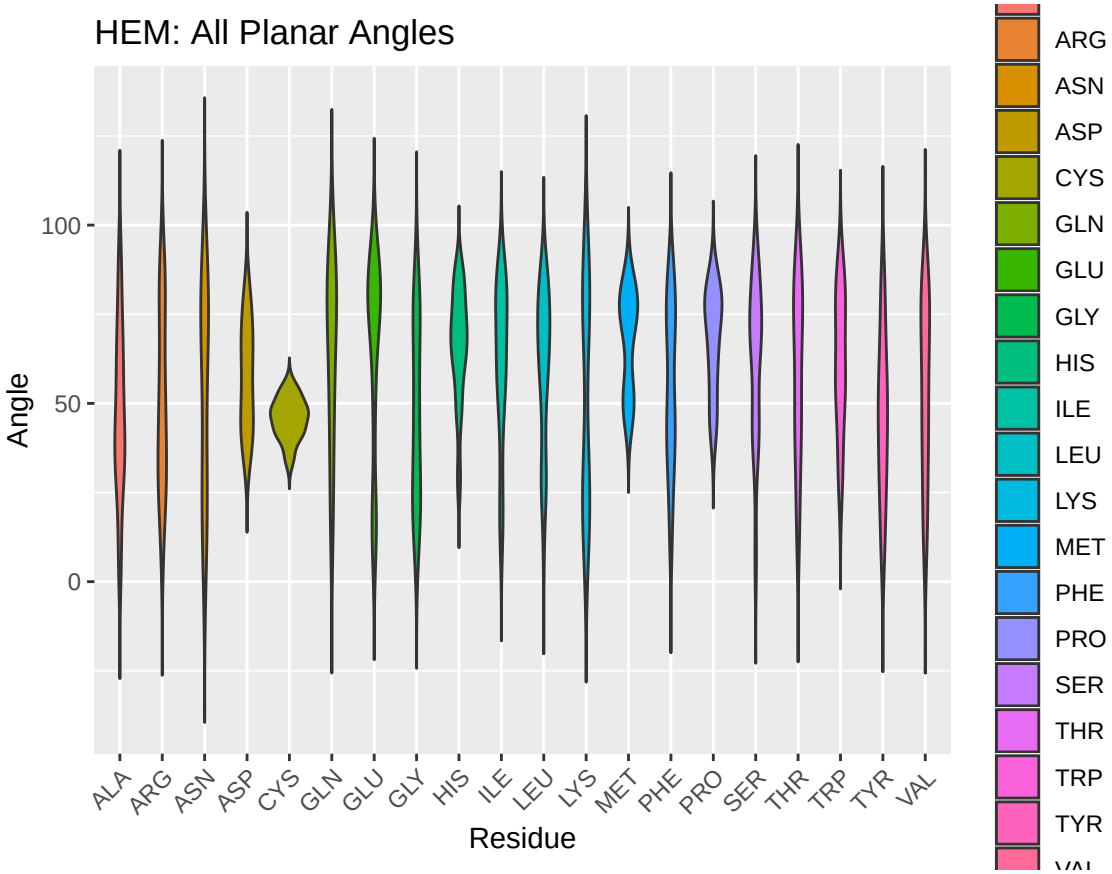

Figure A.25: HEM: All Planar Angles

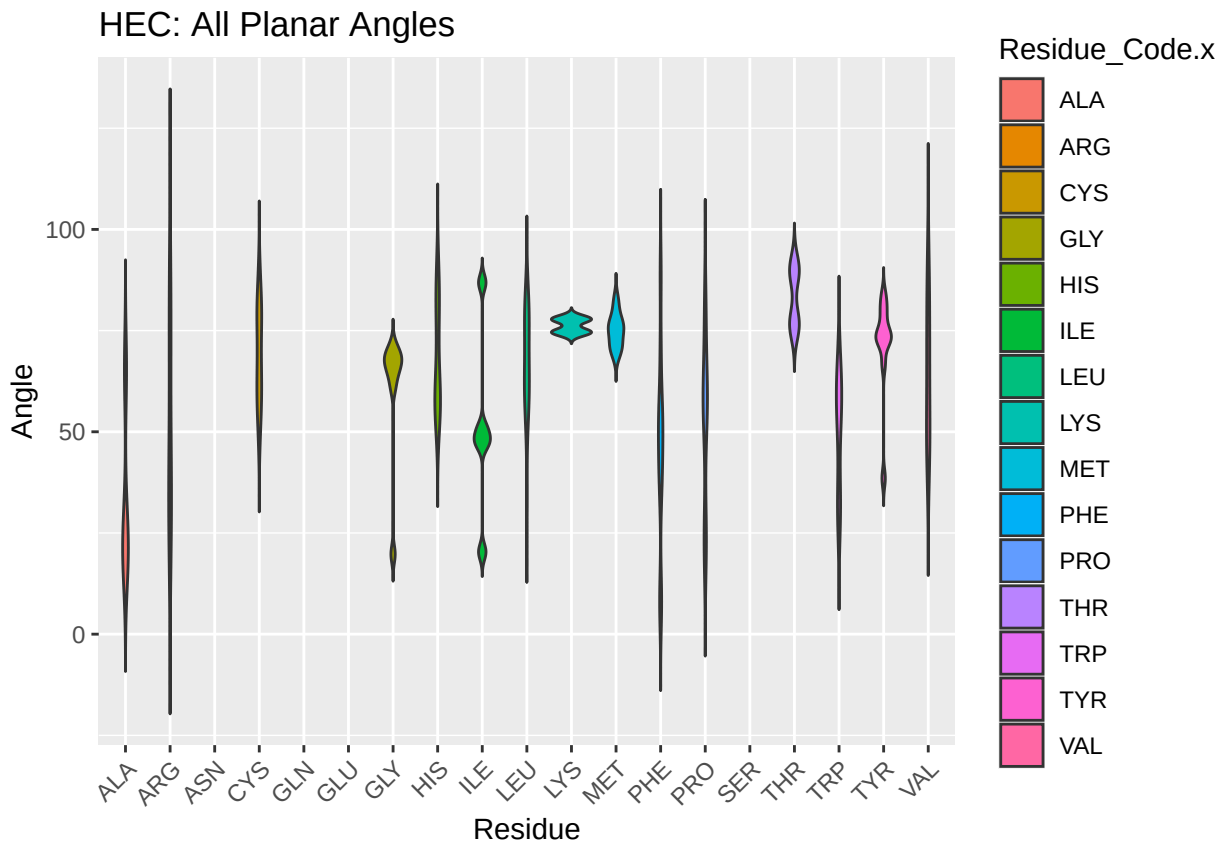

Figure A.26: HEC: All Planar Angles

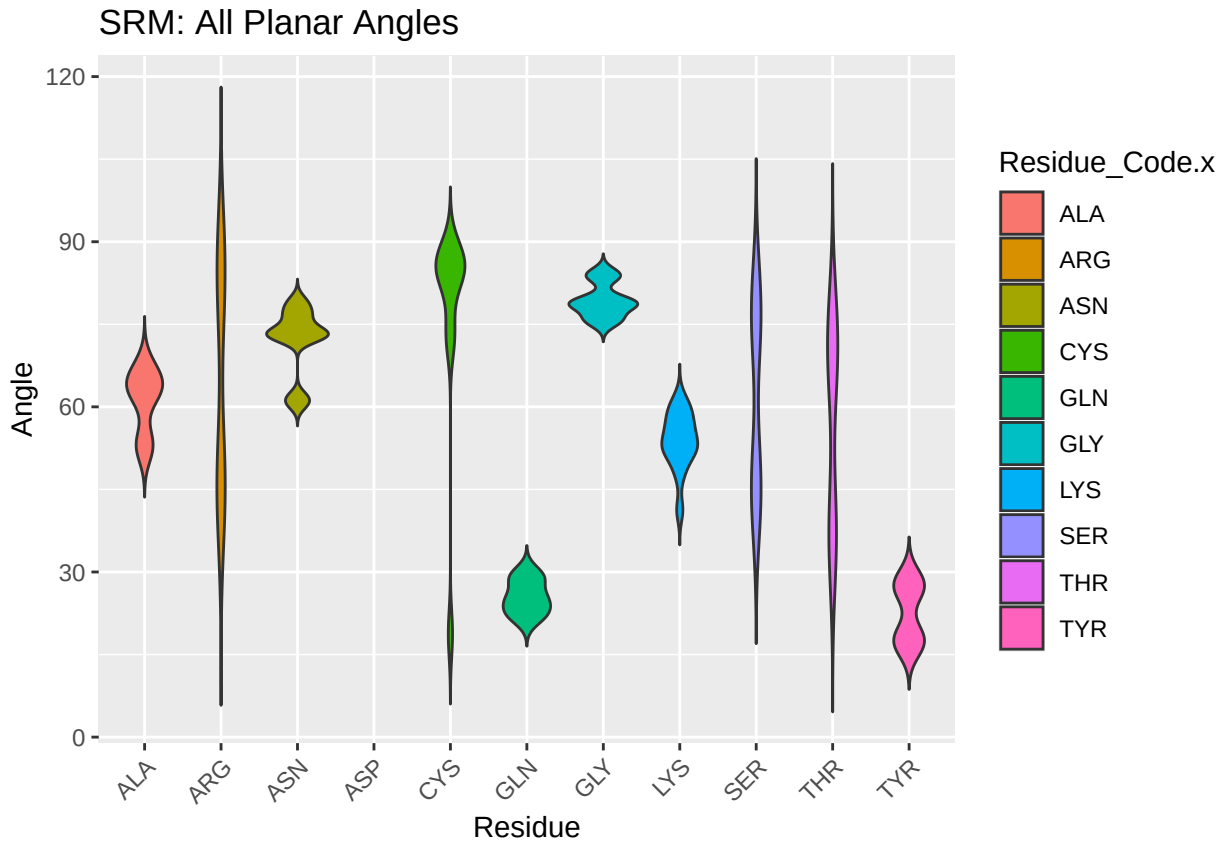

Figure A.27: SRM: All Planar Angles

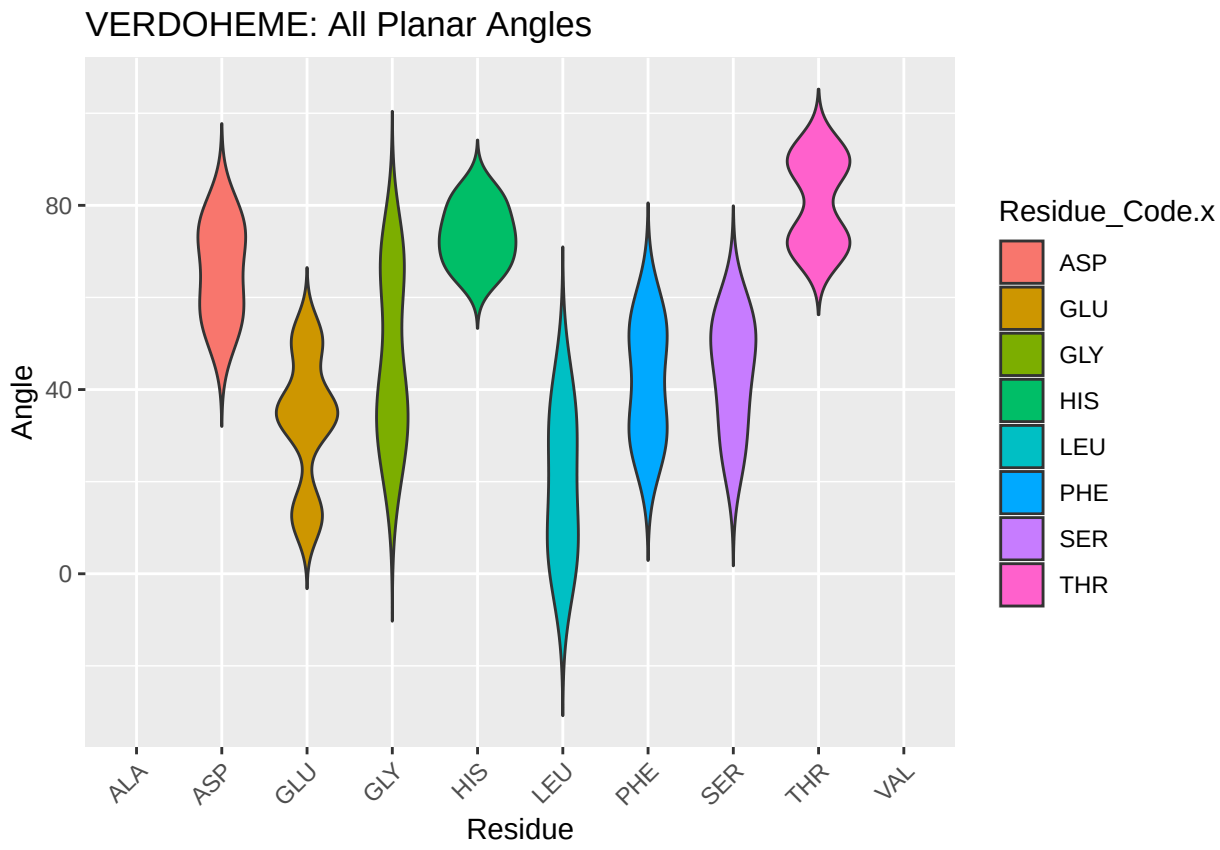

Figure A.28: VERDOHEME: All Planar Angles

A.8 Planar Angles of Closest Residues

Figure A.29: HEM: Planar Angles of Closest Residues

Figure A.30: HEC: Planar Angles of Closest Residues

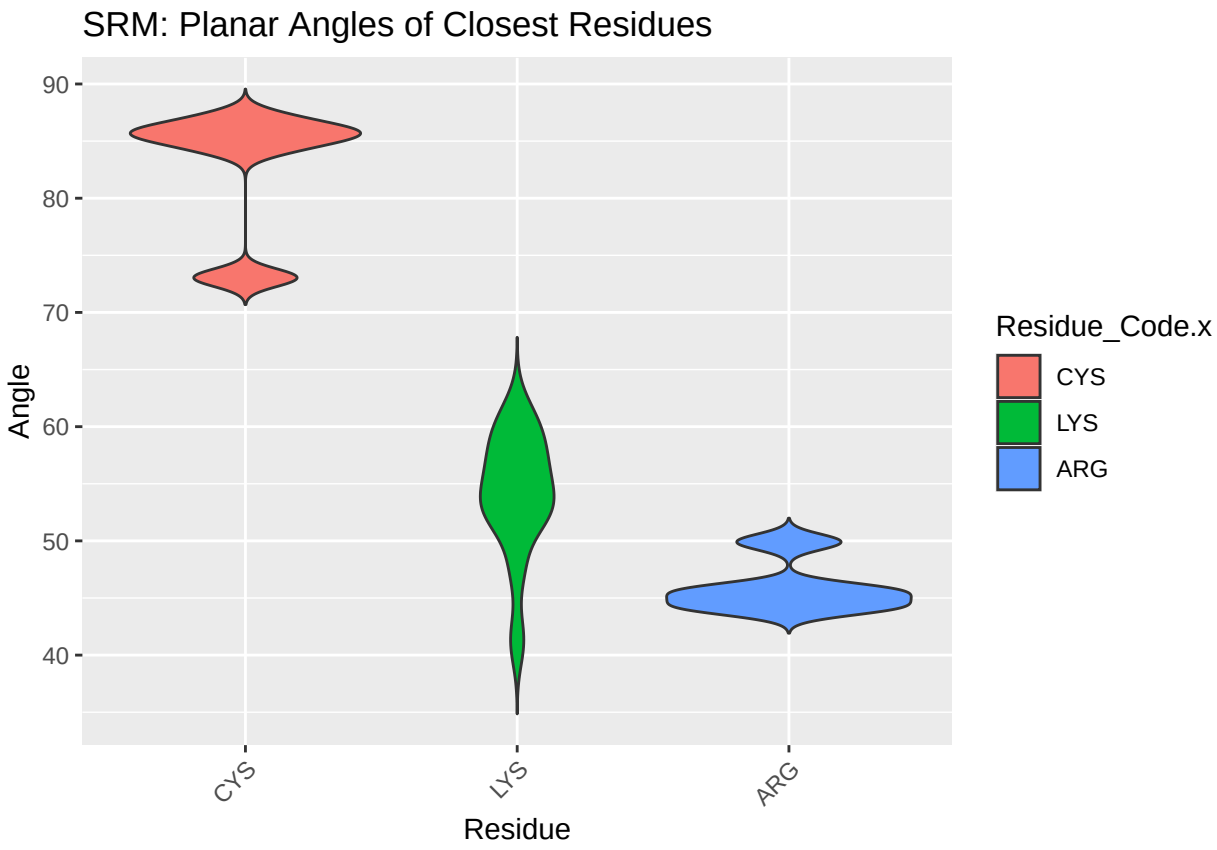

Figure A.31: SRM: Planar Angles of Closest Residues

Figure A.32: VERDOHEME: Planar Angles of Closest Residues

A.9 All CA-CB-Fe Angles

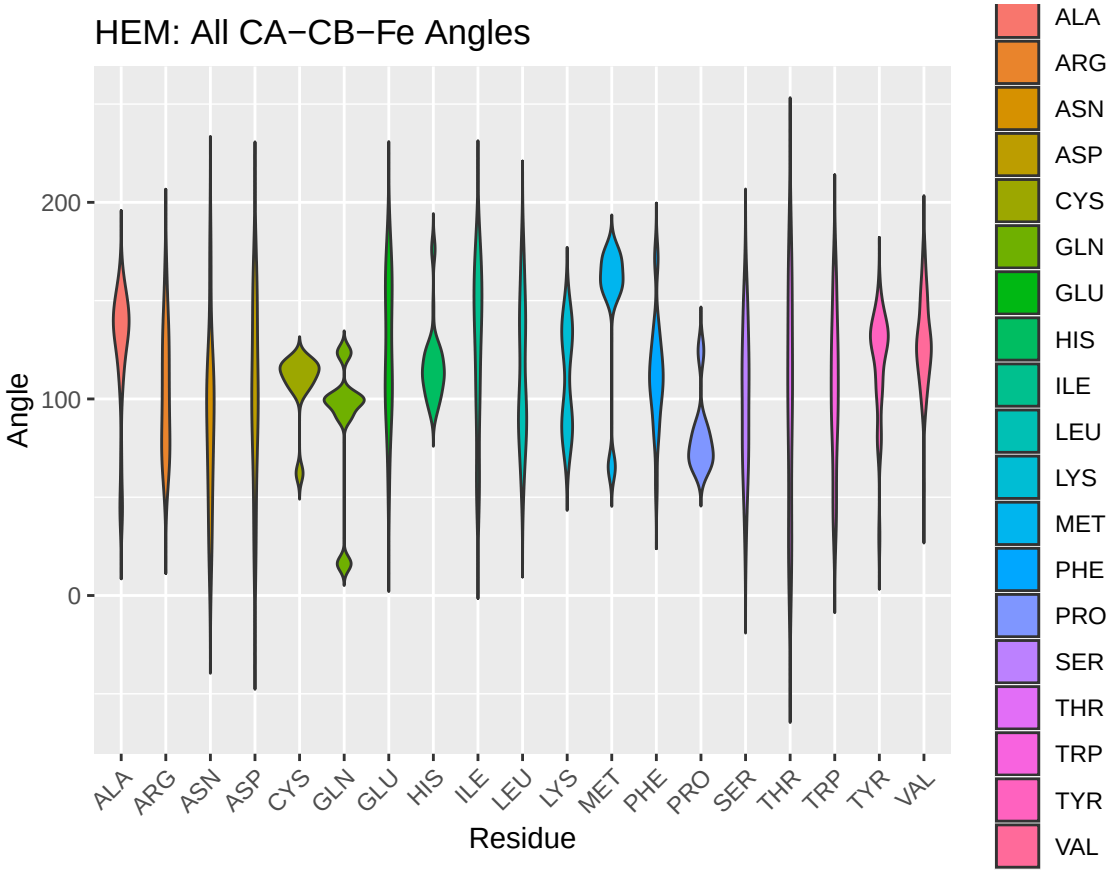

Figure A.33: HEM: All CA-CB-Fe Angles

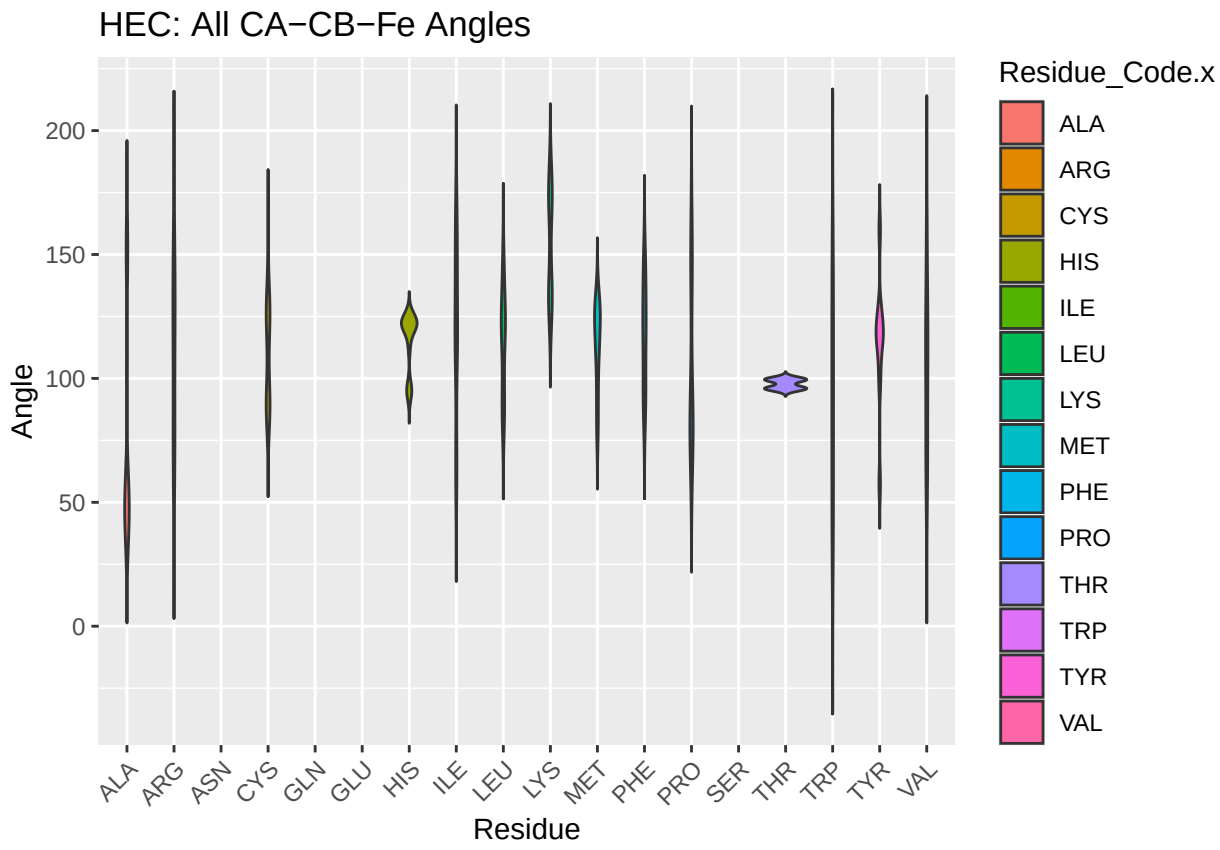

Figure A.34: HEC: All CA-CB-Fe Angles

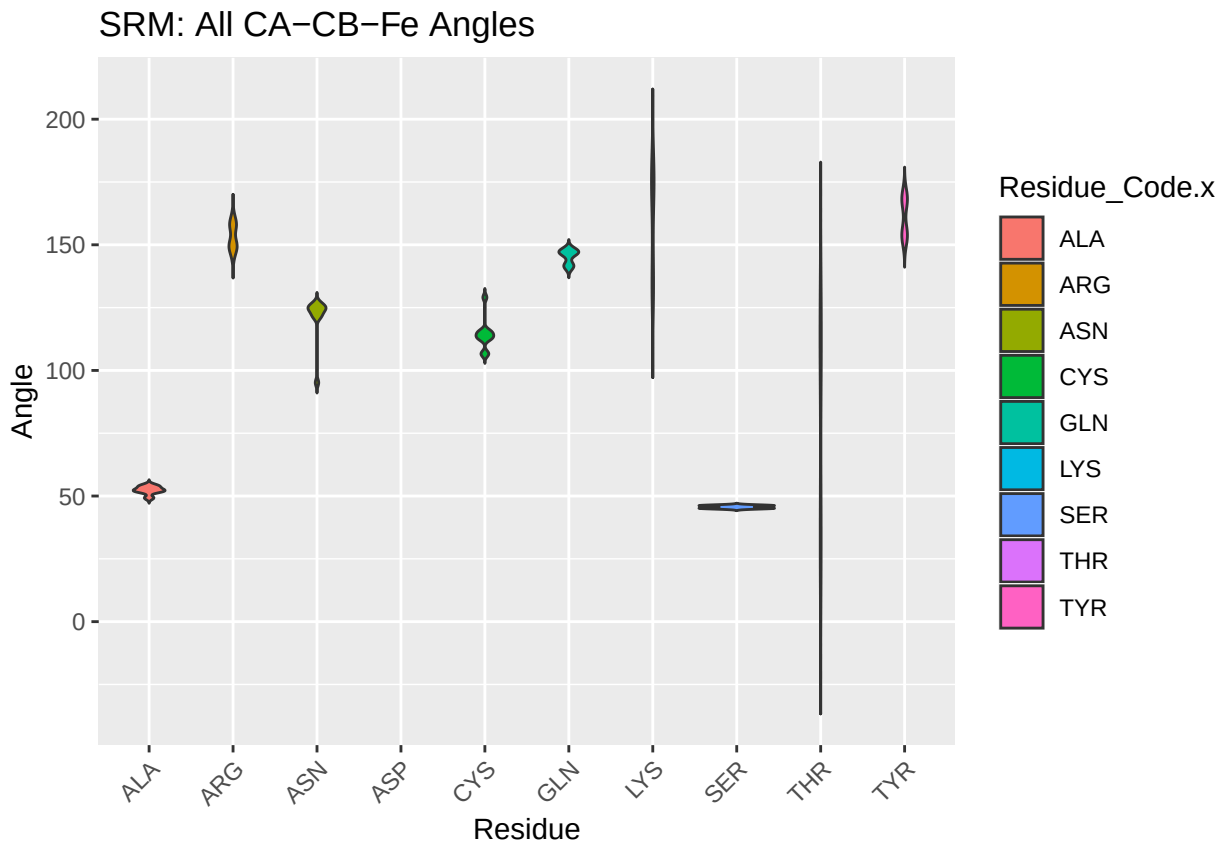

Figure A.35: SRM: All CA-CB-Fe Angles

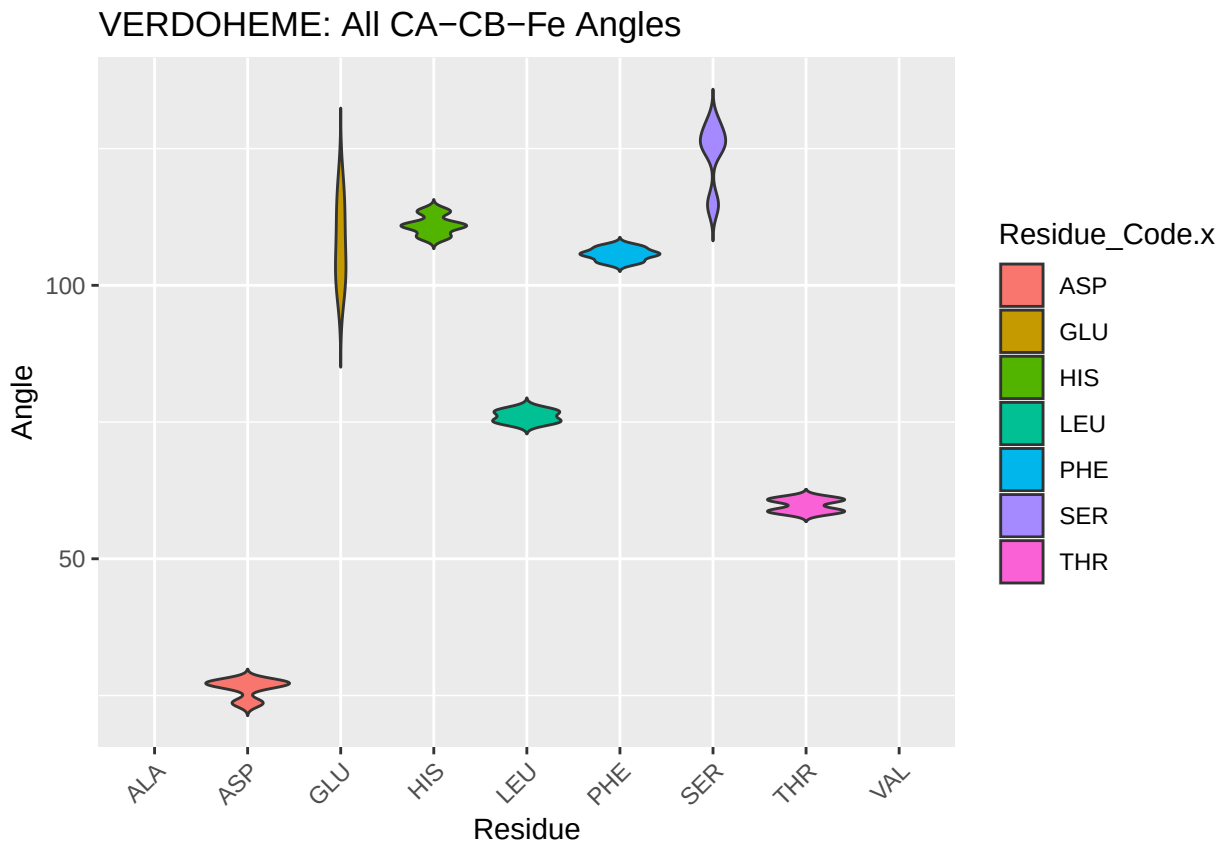

Figure A.36: VERDOHEME: All CA-CB-Fe Angles

A.10 CA-CB-Fe Angles of Closest Residues

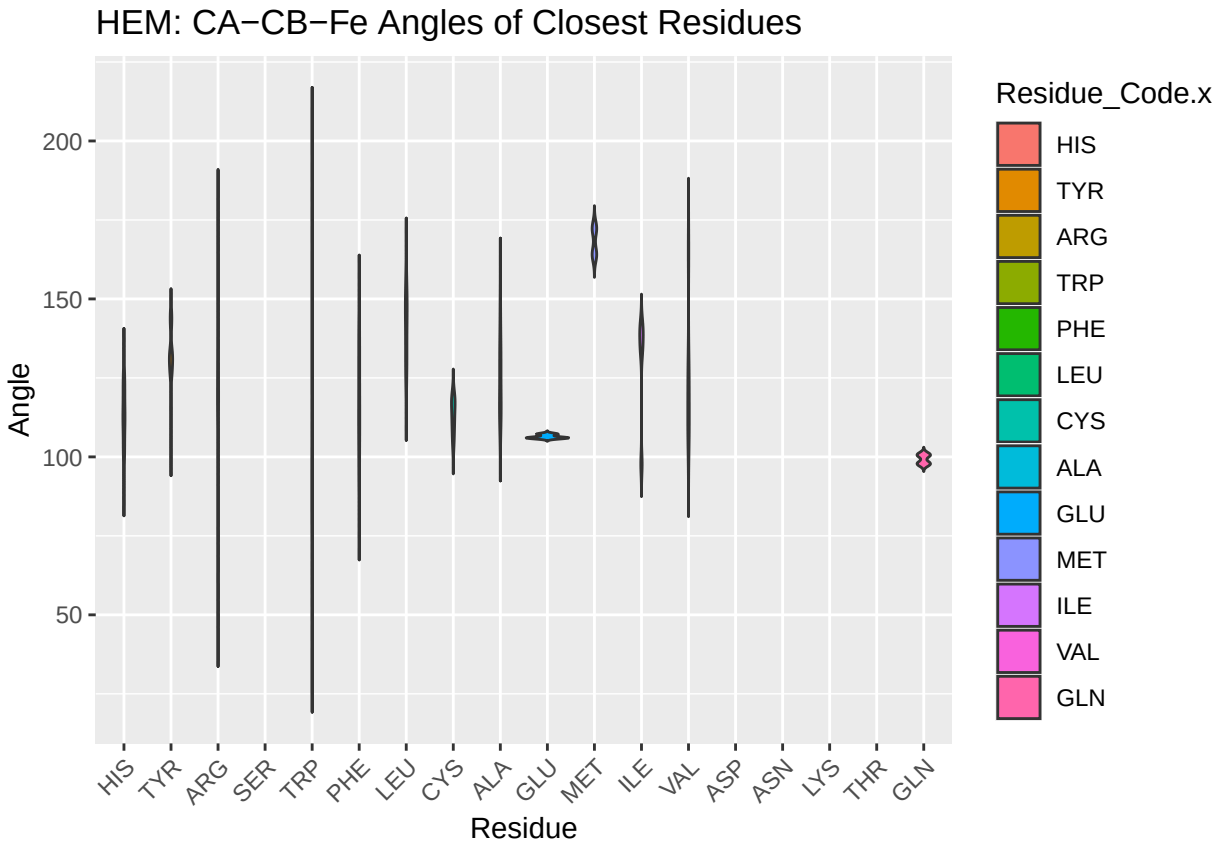

Figure A.37: HEM: CACBFe Angles of Closest Residues

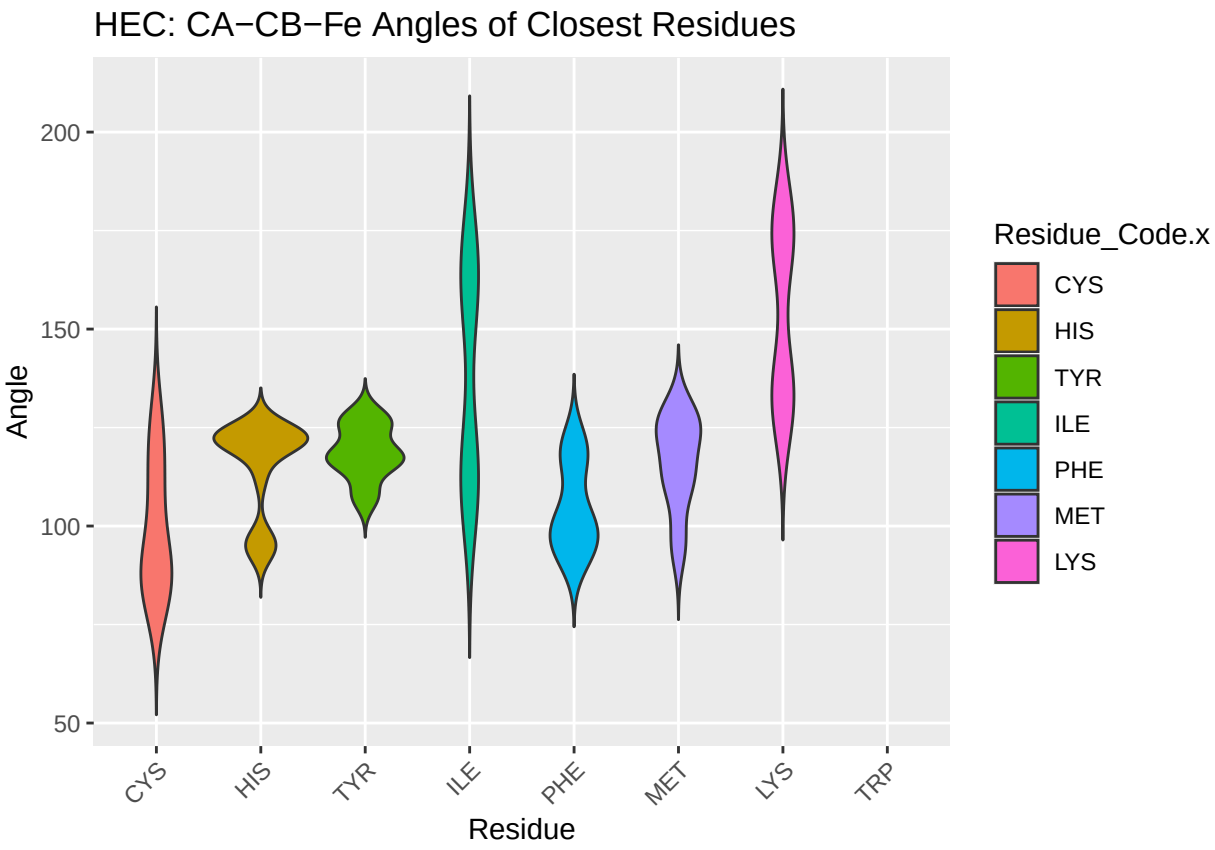

Figure A.38: HEC: CACBFe Angles of Closest Residues

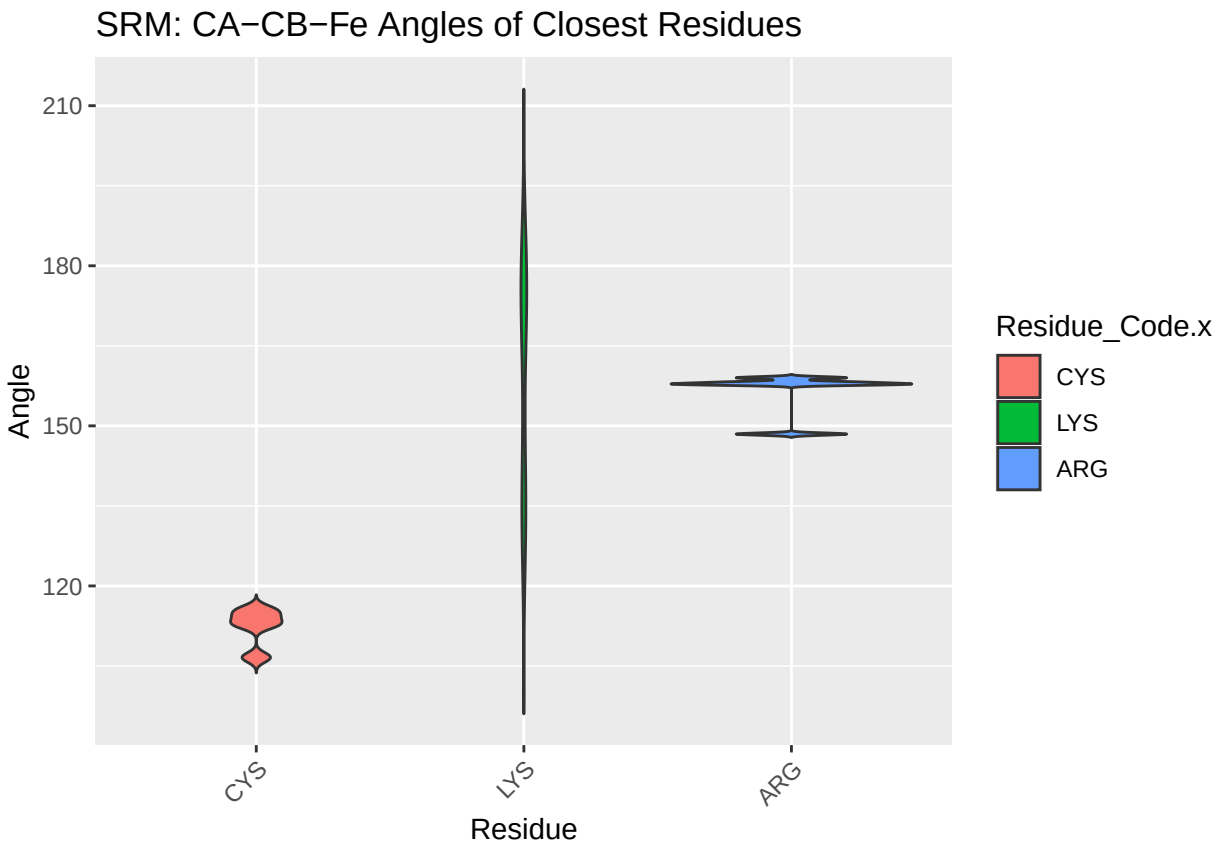

Figure A.39: SRM: CACBFe Angles of Closest Residues

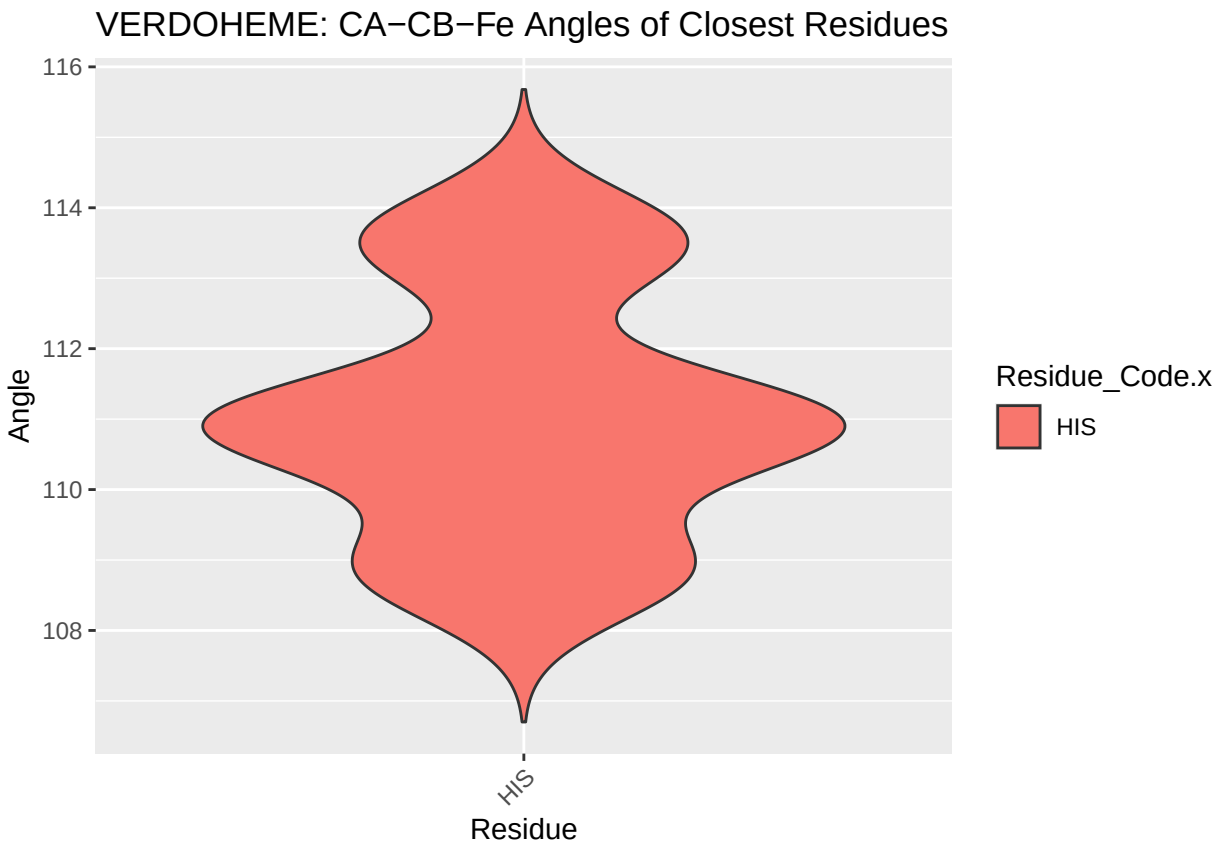

Figure A.40: VERDOHEME: CACBFe Angles of Closest Residues

B Tables

B.1 Molecule Names and Source Organisms

Table B.1: HEM: Molecules and Source Organisms

PDB_ID	Molecule_Name	Source_Organism
1B2V	PROTEIN (HEME-BINDING PROTEIN A);	SERRATIA MARCESCENS;
1B5M	CYTOCHROME B5;	RATTUS NORVEGICUS;
1DK0	HEME-BINDING PROTEIN A;	SERRATIA MARCESCENS;
1DKH	HEME-BINDING PROTEIN A;	SERRATIA MARCESCENS;
1ICC	CYTOCHROME B5 OUTER MITOCHONDRIAL MEMBRANE	RATTUS NORVEGICUS;
1IPH	CATALASE HPII;	ESCHERICHIA COLI;
1N45	HEME OXYGENASE 1;	HOMO SAPIENS;
1P3T	HEME OXYGENASE 1;	NEISSERIA MENINGITIDIS;

Table B.1: HEM: Molecules and Source Organisms *(continued)*

PDB_ID	Molecule_Name	Source_Organism
1QHU	PROTEIN (HEMOPEXIN);	ORYCTOLAGUS CUNICULUS;
1QJS	HEMOPEXIN;	ORYCTOLAGUS CUNICULUS;
1SI8	CATALASE;	ENTEROCOCCUS FAECALIS;
1SY2	NITROPHORIN 4;	RHODNIUS PROLIXUS;
1U9U	CYTOCHROME B5;	BOS TAURUS;
1VGI	HEME OXYGENASE 1;	RATTUS NORVEGICUS;
1ZVI	NITRIC-OXIDE SYNTHASE, BRAIN;	RATTUS NORVEGICUS;
2BHJ	NITRIC OXIDE SYNTHASE;	MUS MUSCULUS;
2CJ0	CHLOROPEROXIDASE;	CALDARIOMYCES FUMAGO;
2CN4	HEMOPHORE HASA;	SERRATIA MARCESCENS;
2CPO	CHLOROPEROXIDASE;	LEPTOXYPHIUM FUMAGO;
2E2Y	MYOGLOBIN;	PHYSETER CATODON;
2FC2	NITRIC OXIDE SYNTHASE;	BACILLUS SUBTILIS;
2IIZ	MELANIN BIOSYNTHESIS PROTEIN TYRA, PUTATIVE;	SHEWANELLA ONEIDENSIS;
2IPS	LACTOPEROXIDASE;	BOS TAURUS;
2J0P	HEMIN TRANSPORT PROTEIN HEMS;	YERSINIA ENTEROCOLITICA;
2J18	CHLOROPEROXIDASE;	CALDARIOMYCES FUMAGO;
2O6P	IRON-REGULATED SURFACE DETERMINANT PROTEIN C;	STAPHYLOCOCCUS AUREUS SUBSP. AUREUS;

Table B.1: HEM: Molecules and Source Organisms *(continued)*

PDB_ID	Molecule_Name	Source_Organism
2Q6N	CYTOCHROME P450 2B4;	ORYCTOLAGUS CUNICULUS;
2R7A	BACTERIAL HEME BINDING PROTEIN;	SHIGELLA DYSENTERIAE;
2SPL	MYOGLOBIN;	PHYSETER CATODON;
2VEB	PROTOGLOBIN;	METHANOSARCINA ACETIVORANS;
3HX9	PROTEIN RV3592;	MYCOBACTERIUM TUBERCULOSIS;
3MVF	NITROPHORIN-4;	RHODNIUS PROLIXUS;
3QZN	IRON-REGULATED SURFACE DETERMINANT PROTEIN A;	STAPHYLOCOCCUS AUREUS SUBSP. AUREUS;
3QZZ	METHANOSARCINA ACETIVORANS PROTOGLOBIN;	METHANOSARCINA ACETIVORANS;
3SIK	CONSERVED DOMAIN PROTEIN;	BACILLUS ANTHRACIS;
3TGC	NITROPHORIN-4;	RHODNIUS PROLIXUS;
3VP5	TRANSCRIPTIONAL REGULATOR;	LACTOCOCCUS LACTIS;
3ZJS	PROTOGLOBIN;	METHANOSARCINA ACETIVORANS;
4B8N	CYTOCHROME B5-HOST ORIGIN;	OSTREOCOCCUS TAURI VIRUS 2;
4CAT	CATALASE;	PENICILLIUM JANTHINELLUM;
4CDP	PUTATIVE HEME/HEMOGLOBIN TRANSPORT PROTEIN;	ESCHERICHIA COLI;
4I3Q	CYTOCHROME P450 3A4;	HOMO SAPIENS;
4JET	HEMOPHORE HASA;	YERSINIA PESTIS;

Table B.1: HEM: Molecules and Source Organisms *(continued)*

PDB_ID	Molecule_Name	Source_Organism
4MF9	HEMIN DEGRADING FACTOR;	PSEUDOMONAS AERUGINOSA;
4MYP	IRON-REGULATED SURFACE DETERMINANT PROTEIN A;	LISTERIA MONOCYTOGENES;
4NL5	HEME-DEGRADING MONOOXYGENASE HMOB;	MYCOBACTERIUM TUBERCULOSIS;
4UZV	HEMOGLOBIN;	THERMOBIFIDA FUSCA TM51;
4XZD	EXTRACELLULAR HEME ACQUISITION HEMOPHORE HASA;	YERSINIA PSEUDOTUBERCULOSIS IP 32953;
4Y1Q	EXTRACELLULAR HEME ACQUISITION HEMOPHORE HASA;	YERSINIA PSEUDOTUBERCULOSIS IP 32953;
5CN5	MYOGLOBIN;	EQUUS CABALLUS;
5GJ3	PERIPLASMIC BINDING PROTEIN;	ROSEIFLEXUS SP. RS-1;
5KZL	HEME OXYGENASE;	LEPTOSPIRA INTERROGANS;
5O1L	RUBBER OXYGENASE;	STREPTOMYCES SP. (STRAIN K30);
5O1M	RUBBER OXYGENASE;	STREPTOMYCES SP. (STRAIN K30);
5VEU	CYTOCHROME P450 3A5;	HOMO SAPIENS;
6A2J	HEME A SYNTHASE;	BACILLUS SUBTILIS (STRAIN 168);
7C74	LACTOPEROXIDASE;	BOS MUTUS;
7DMR	LACTOPEROXIDASE;	BOS MUTUS;

Table B.2: HEC: Molecules and Source Organisms

PDB_ID	Molecule_Name	Source_Organism
1BBH	CYTOCHROME C';	ALLOCHROMATIUM VINOSUM;
1S56	HEMOGLOBIN-LIKE PROTEIN HBN;	MYCOBACTERIUM TUBERCULOSIS;
1W2L	CYTOCHROME OXIDASE SUBUNIT II;	RHODOTHERMUS MARINUS;
2BC5	SOLUBLE CYTOCHROME B562;	ESCHERICHIA COLI;
2BH5	CYTOCHROME C-550;	PARACOCCUS VERSUTUS;
3EAH	NITRIC OXIDE SYNTHASE, ENDOTHELIAL;	HOMO SAPIENS;
3X15	CYTOCHROME C552;	AQUIFEX AEOLICUS VF5;
5KPF	CYTOCHROME C ISO-1;	SACCHAROMYCES CEREVISIAE;
5LFT	CYTOCHROME C ISO-1;	SACCHAROMYCES CEREVISIAE;
5T8W	CYC1P;	SACCHAROMYCES CEREVISIAE;
6VDQ	3-METHYL-L-TYROSINE PEROXYGENASE;	STREPTOMYCES LAVENDULAE;
6WZA	SOLUBLE CYTOCHROME B562;	ESCHERICHIA COLI;
6XNK	CYTOCHROME C;	HOMO SAPIENS;

Table B.3: SRM: Molecules and Source Organisms

PDB_ID	Molecule_Name	Source_Organism
1ZJ8	PROBABLE FERREDOXIN-DEPENDENT NITRITE REDUCTASE NIRA;	MYCOBACTERIUM TUBERCULOSIS;
2AKJ	FERREDOXIN–NITRITE REDUCTASE, CHLOROPLAST;	SPINACIA OLERACEA;
2AOP	SULFITE REDUCTASE HEMOPROTEIN;	ESCHERICHIA COLI;
3B0G	NITRITE REDUCTASE;	NICOTIANA TABACUM;
3VKP	NITRITE REDUCTASE;	NICOTIANA TABACUM;
3VLX	NITRITE REDUCTASE;	NICOTIANA TABACUM;
3VLY	NITRITE REDUCTASE;	NICOTIANA TABACUM;
3VLZ	NITRITE REDUCTASE;	NICOTIANA TABACUM;
5H8V	SULFITE REDUCTASE [FERREDOXIN], CHLOROPLASTIC;	ZEA MAYS;

Table B.4: VERDOHEME: Molecules and Source Organisms

PDB_ID	Molecule_Name	Source_Organism
2ZVU	HEME OXYGENASE 1;	RATTUS NORVEGICUS;
3MOO	HEME OXYGENASE;	CORYNEBACTERIUM DIPHTHERIAE;
1TWN	HEME OXYGENASE 1;	HOMO SAPIENS;
1TWR	HEME OXYGENASE 1;	HOMO SAPIENS;

B.2 Volume and Surface Areas

Table B.5: HEM: Volume and Surface Areas

PDB_ID	Volume_Data	HEM_Excluded_SA	HEM_Accessible_SA	Pocket_Excluded_SA	Pocket_Accessible_SA
1B2V	893.60	502.042	820.988	7276.09	8232.60
1B5M	672.79	490.050	800.780	4695.01	5512.20
1DK0	966.72	505.258	837.157	7237.94	8217.58
1DKH	1010.70	509.042	828.131	7402.34	8175.94
1ICC	1000.40	499.585	811.357	5079.72	6028.23
1IPH	1345.60	501.603	814.652	33983.80	34094.40
1N45	978.98	560.384	983.238	9944.50	10779.30
1P3T	987.05	509.939	829.611	9530.67	10410.80
1QHU	1389.20	573.686	1002.160	18503.10	18257.20
1QJS	1102.30	573.266	1000.380	18588.40	18584.10
1SI8	965.57	646.643	1184.070	23711.20	25120.40
1SY2	918.34	501.850	817.749	8960.76	9610.23
1U9U	738.55	496.132	813.773	4675.76	5632.32
1VGI	870.44	577.234	1002.530	9615.29	10248.20
1ZVI	1435.90	701.091	1129.540	19918.60	20968.20
2BHJ	1438.30	836.576	1290.530	20102.30	20762.60
2CJ0	809.62	2653.180	4835.280	12749.60	12892.20
2CN4	526.88	576.760	961.348	9617.23	11917.70
2CPO	886.17	1846.490	3329.540	13081.60	12995.60
2E2Y	994.92	811.270	1607.370	7531.94	8240.75
2FC2	1091.40	1011.190	1669.900	18383.50	18552.10
2IIZ	1015.60	731.342	1393.160	13651.70	14031.40
2IPS	1242.40	618.252	1075.560	27760.50	25814.10
2J0P	1281.80	1030.510	1873.810	15192.90	15871.10
2J18	841.67	1962.990	3556.340	12675.10	12779.00
2O6P	788.05	499.017	822.121	6234.84	7200.43
2Q6N	1030.10	644.365	1040.080	20051.10	19747.50
2R7A	1284.50	507.098	845.182	11255.10	12389.00
2SPL	1055.70	589.706	1029.660	7588.36	8105.94
2VEB	886.06	762.309	1454.750	9840.72	10401.80
3HX9	1844.50	785.442	1168.200	5819.08	7189.03

Table B.5: HEM: Volume and Surface Areas *(continued)*

PDB_ID	Volume_Data	HEM_Excluded_SA	HEM_Accessible_SA	Pocket_Excluded_SA	Pocket_Accessible_SA
3MVF	1271.40	576.502	1009.950	8559.24	9573.08
3QZN	726.52	664.858	1221.330	6133.24	7179.49
3QZZ	977.30	496.950	825.255	8523.59	9708.28
3SIK	492.15	498.621	823.565	6495.38	7739.06
3TGC	969.87	524.380	853.710	8712.77	9181.94
3VP5	1094.60	602.790	1050.820	9801.82	10810.80
3ZJS	788.74	528.419	860.137	9568.10	10130.40
4B8N	841.27	569.302	990.216	4560.39	5458.66
4CAT	1933.90	484.341	778.502	28372.40	36788.30
4CDP	1053.70	1425.050	3141.090	14733.50	15887.40
4I3Q	1220.50	510.623	845.108	21946.50	21093.70
4JET	1010.80	495.992	818.131	7887.81	8695.85
4MF9	1286.50	488.695	790.732	15669.80	16791.30
4MYP	610.72	963.019	1834.680	6285.40	7351.53
4NL5	1088.70	576.669	1003.400	5715.52	6894.72
4UZV	1184.10	526.584	844.058	7378.28	8322.74
4XZD	932.14	498.788	816.032	8028.32	8752.50
4Y1Q	952.23	494.939	806.960	7905.84	8785.04
5CN5	1070.30	663.162	1223.640	7629.45	8117.34
5GJ3	1108.20	756.603	1131.670	11394.00	12591.80
5KZL	914.22	483.760	805.567	9662.03	10431.00
5O1L	1438.70	801.519	1447.270	15538.20	16876.00
5O1M	1431.30	493.850	799.331	16096.90	15912.50
5VEU	964.76	993.578	1502.660	20900.80	20425.90
6A2J	1015.90	6183.450	9902.920	14870.30	15888.00
7C74	1155.10	497.527	820.381	26111.40	25094.20
7DMR	1083.40	1049.750	1916.950	26004.00	24563.80

Table B.6: HEC: Volume and Surface Areas

PDB_ID	Volume_Data	HEC_Excluded_SA	HEC_Accessible_SA	Pocket_Excluded_SA	Pocket_Accessible_SA
1BBH	969.51	514.130	829.817	6441.44	7514.06
1S56	1103.60	643.733	1075.840	6711.26	7477.96
1W2L	756.08	702.711	1240.680	5042.58	5485.50
2BC5	1166.20	569.905	997.324	5489.91	6306.02
2BH5	814.15	508.637	844.494	6359.51	6975.70
3EAH	1280.90	993.430	1697.130	18413.40	19313.80
3X15	823.59	496.328	802.584	5722.90	7493.62
5KPF	778.79	568.036	1007.680	5485.51	6155.84
5LFT	809.40	1720.870	2719.000	5539.47	6315.96
5T8W	858.74	511.519	848.952	5755.48	6458.40
6VDQ	977.52	510.534	846.299	13399.60	14076.40
6WZA	1040.10	713.997	1095.240	5529.40	6385.75
6XNK	2214.40	499.687	835.610	6737.92	8143.17

Table B.7: SRM: Volume and Surface Areas

PDB_ID	Volume_Data	SRM_Excluded_SA	SRM_Accessible_SA	Pocket_Excluded_SA	Pocket_Accessible_SA
1ZJ8	1960.2	656.508	1036.43	20388.7	21432.8
2AKJ	1810.2	659.667	1041.00	21673.6	20933.7
2AOP	1040.5	682.170	1045.18	18119.8	18016.0
3B0G	1189.9	666.995	1054.40	21496.8	21033.9
3VKP	1178.0	675.050	1049.85	21279.3	20964.9
3VLX	1164.8	667.013	1052.76	21470.0	21037.0
3VLY	1061.8	675.293	1046.41	21476.6	21022.1
3VLZ	1123.2	676.360	1051.40	21433.5	20901.8
5H8V	1360.8	685.850	1052.56	22885.9	22713.3

Table B.8: VERDOHEME: Volume and Surface Areas

PDB_ID	Volume_Data	VERDOHEME_EXCLUDED_SA	VERDOHEME_ACCESSIBLE_SA	POCKET_EXCLUDED_SA	POCKET_ACCESSIBLE_SA
2ZVU	984.51	560.791	969.143	9633.81	10317.3
3MOO	864.48	870.228	1772.07	9371.88	10170.3
1TWN	1145	448.81	759.632	9966.97	10896.8
1TWR	1426	469.982	783.313	9854.01	10775.6

B.3 All Planar Angles

Table B.9: HEM: All Planar Angles

PDB_ID	Residue_Number	Residue_Code.x	Mean_Distance	Angle	Residue_Code.y
1N45	28	ALA	6.981230	51.517	ALA
2CJ0	31	ALA	5.440871	54.576	ALA
2CPO	31	ALA	5.505123	50.842	ALA
2J18	31	ALA	5.457126	52.882	ALA
1SY2	42	ALA	6.006055	38.441	ALA
3MVF	42	ALA	5.827660	37.714	ALA
3TGC	42	ALA	6.033598	36.906	ALA
2O6P	49	ALA	6.356063	33.301	ALA
4B8N	54	ALA	6.390793	40.757	ALA
1B5M	67	ALA	5.797296	4.944	ALA
1ICC	67	ALA	6.085233	8.515	ALA
1U9U	67	ALA	6.016697	3.989	ALA
2CJ0	71	ALA	6.531120	88.775	ALA
2CPO	71	ALA	6.539227	89.067	ALA
2J18	71	ALA	6.477348	89.793	ALA
3HX9	71	ALA	6.230664	24.118	ALA

Table B.9: HEM: All Planar Angles *(continued)*

PDB_ID	Residue_Number	Residue_Code.x	Mean_Distance	Angle	Residue_Code.y
4NL5	71	ALA	6.805378	12.006	ALA
4Y1Q	75	ALA	6.722226	65.239	ALA
1P3T	121	ALA	6.382367	68.509	ALA
3SIK	138	ALA	6.231014	84.490	ALA
3QZN	166	ALA	6.907969	73.637	ALA
2R7A	169	ALA	5.223004	39.141	ALA
6A2J	180	ALA	6.687029	46.961	ALA
2BHJ	191	ALA	6.261711	68.057	ALA
6A2J	220	ALA	5.986896	31.915	ALA
6A2J	259	ALA	6.937825	66.152	ALA
4MYP	282	ALA	6.581195	36.442	ALA
4MYP	293	ALA	6.207799	64.118	ALA
2Q6N	298	ALA	5.672036	28.414	ALA
4I3Q	305	ALA	5.305272	55.811	ALA
5VEU	305	ALA	6.219660	37.021	ALA
1ZVI	412	ALA	6.481380	68.137	ALA
2Q6N	442	ALA	6.935846	35.011	ALA
5VEU	447	ALA	6.667315	35.226	ALA
4I3Q	448	ALA	6.441232	28.736	ALA
4JET	40	ARG	5.660400	8.293	ARG
4XZD	40	ARG	5.892195	23.940	ARG
4Y1Q	40	ARG	5.725205	11.586	ARG
3SIK	54	ARG	6.090293	58.962	ARG
2FC2	61	ARG	6.072553	27.736	ARG
2FC2	65	ARG	6.459491	31.691	ARG
4CDP	100	ARG	5.360373	82.404	ARG
2J0P	102	ARG	5.002395	83.046	ARG
4UZV	105	ARG	6.689489	51.468	ARG
4MF9	112	ARG	5.056393	85.919	ARG
5GJ3	142	ARG	9.016294	44.325	ARG
4JET	144	ARG	6.239587	45.482	ARG
4XZD	144	ARG	6.335714	52.771	ARG
4Y1Q	144	ARG	6.425880	45.332	ARG
2BHJ	193	ARG	5.745098	22.913	ARG
2BHJ	197	ARG	6.221230	38.014	ARG

Table B.9: HEM: All Planar Angles *(continued)*

PDB_ID	Residue_Number	Residue_Code.x	Mean_Distance	Angle	Residue_Code.y
4I3Q	212	ARG	6.392849	65.236	ARG
1QHU	214	ARG	6.588734	53.531	ARG
1QJS	214	ARG	6.249190	87.831	ARG
6A2J	217	ARG	6.781589	69.272	ARG
5GJ3	241	ARG	5.542517	89.231	ARG
2IIZ	242	ARG	5.236889	71.798	ARG
1SI8	333	ARG	5.247624	87.335	ARG
2IPS	348	ARG	6.336679	28.401	ARG
7C74	348	ARG	6.274279	28.825	ARG
7DMR	348	ARG	6.250958	34.360	ARG
1IPH	411	ARG	5.321024	79.235	ARG
1ZVI	414	ARG	5.799426	24.112	ARG
1ZVI	418	ARG	6.259544	32.179	ARG
3HX9	7	ASN	9.030558	67.240	ASN
4NL5	7	ASN	5.402231	60.999	ASN
1B2V	41	ASN	6.894251	9.238	ASN
1DK0	41	ASN	6.870425	7.885	ASN
1P3T	118	ASN	6.625279	81.885	ASN
1SI8	127	ASN	6.666708	88.346	ASN
1IPH	201	ASN	6.396844	80.526	ASN
2BHJ	364	ASN	6.955669	54.701	ASN
2IPS	437	ASN	6.276979	27.543	ASN
7C74	437	ASN	6.653391	27.901	ASN
7DMR	437	ASN	6.591349	28.625	ASN
5VEU	440	ASN	6.408862	78.050	ASN
4I3Q	441	ASN	6.139159	80.458	ASN
1P3T	27	ASP	6.267807	39.072	ASP
2E2Y	64	ASP	6.865050	39.668	ASP
2IPS	108	ASP	5.870986	78.247	ASP
7C74	108	ASP	6.017401	74.114	ASP
7DMR	108	ASP	6.266021	79.901	ASP
5KZL	129	ASP	6.318347	48.961	ASP
1N45	140	ASP	6.389011	51.996	ASP
1VGI	140	ASP	6.566393	62.088	ASP
2IIZ	151	ASP	5.861207	42.941	ASP

Table B.9: HEM: All Planar Angles *(continued)*

PDB_ID	Residue_Number	Residue_Code.x	Mean_Distance	Angle	Residue_Code.y
4CDP	191	ASP	6.789427	37.522	ASP
2J0P	194	ASP	6.862392	50.396	ASP
1QHU	203	ASP	6.920576	64.837	ASP
1QJS	203	ASP	6.878437	64.521	ASP
2IIZ	284	ASP	6.598336	68.375	ASP
2CJ0	29	CYS	4.390905	47.217	CYS
2CPO	29	CYS	4.443549	49.291	CYS
2J18	29	CYS	4.359887	47.527	CYS
2FC2	62	CYS	4.482879	54.005	CYS
1P3T	113	CYS	6.881310	41.741	CYS
2BHJ	194	CYS	4.487497	52.816	CYS
1ZVI	415	CYS	4.181834	46.871	CYS
2Q6N	436	CYS	4.305637	40.993	CYS
5VEU	441	CYS	4.349464	42.614	CYS
4I3Q	442	CYS	4.085782	34.781	CYS
2IPS	105	GLN	5.981590	87.342	GLN
7C74	105	GLN	5.667218	84.879	GLN
7DMR	105	GLN	5.517249	82.031	GLN
5GJ3	141	GLN	9.940999	57.821	GLN
2R7A	253	GLN	6.081153	19.452	GLN
6A2J	258	GLN	5.803666	43.028	GLN
4MYP	292	GLN	6.537566	73.527	GLN
5KZL	19	GLU	5.803913	14.669	GLU
1N45	29	GLU	6.277510	13.488	GLU
1VGI	29	GLU	6.279863	19.844	GLU
5O1L	148	GLU	6.440638	81.093	GLU
2CJ0	183	GLU	5.716050	77.664	GLU
2CPO	183	GLU	5.799506	78.548	GLU
2J18	183	GLU	5.722472	78.531	GLU
1QHU	225	GLU	6.177350	81.356	GLU
1QJS	226	GLU	6.465511	78.730	GLU
2IPS	258	GLU	6.388898	83.283	GLU
7C74	258	GLU	6.258582	88.863	GLU
7DMR	258	GLU	6.172262	88.960	GLU
2Q6N	439	GLU	6.270464	60.625	GLU

Table B.9: HEM: All Planar Angles *(continued)*

PDB_ID	Residue_Number	Residue_Code.x	Mean_Distance	Angle	Residue_Code.y
1ZVI	592	GLU	6.601349	48.481	GLU
1B5M	41	GLY	5.388127	72.708	GLY
1ICC	41	GLY	5.723853	72.752	GLY
1U9U	41	GLY	5.723510	83.944	GLY
1B5M	42	GLY	6.533917	10.848	GLY
1ICC	42	GLY	6.657462	8.777	GLY
1U9U	42	GLY	6.689632	17.633	GLY
4B8N	50	GLY	5.464969	87.471	GLY
4B8N	51	GLY	6.462950	23.037	GLY
1B5M	62	GLY	6.365897	81.093	GLY
2FC2	64	GLY	5.882725	21.989	GLY
1P3T	116	GLY	5.737222	80.192	GLY
1P3T	120	GLY	4.843774	41.129	GLY
5KZL	128	GLY	5.130966	70.591	GLY
5KZL	132	GLY	5.705062	50.430	GLY
1N45	139	GLY	5.251379	58.119	GLY
1VGI	139	GLY	5.155470	60.437	GLY
1N45	143	GLY	5.882948	37.778	GLY
1VGI	143	GLY	5.279720	32.760	GLY
1VGI	144	GLY	5.974807	66.493	GLY
2R7A	170	GLY	5.922307	19.803	GLY
6A2J	179	GLY	5.548597	36.551	GLY
2BHJ	196	GLY	5.667103	19.625	GLY
2FC2	233	GLY	6.517575	77.972	GLY
6A2J	262	GLY	5.820895	75.177	GLY
4MYP	291	GLY	6.624699	50.662	GLY
2Q6N	299	GLY	6.518431	10.616	GLY
4I3Q	306	GLY	6.573103	20.924	GLY
2IPS	350	GLY	6.712596	52.440	GLY
7C74	350	GLY	6.606591	46.520	GLY
7DMR	350	GLY	6.694618	48.519	GLY
2BHJ	365	GLY	6.617587	80.698	GLY
1ZVI	417	GLY	5.404983	24.763	GLY
2Q6N	438	GLY	5.615678	28.366	GLY
5VEU	443	GLY	5.482822	27.362	GLY

Table B.9: HEM: All Planar Angles *(continued)*

PDB_ID	Residue_Number	Residue_Code.x	Mean_Distance	Angle	Residue_Code.y
4I3Q	444	GLY	5.222394	22.218	GLY
1ZVI	586	GLY	6.997972	72.788	GLY
5KZL	15	HIS	4.819650	59.949	HIS
1P3T	23	HIS	4.573926	67.542	HIS
1N45	25	HIS	4.545004	69.116	HIS
1VGI	25	HIS	4.646180	72.142	HIS
1B2V	32	HIS	4.667618	51.415	HIS
1DK0	32	HIS	4.556145	48.497	HIS
1DKH	32	HIS	5.099382	50.187	HIS
1B5M	39	HIS	4.456809	87.693	HIS
1ICC	39	HIS	4.542187	78.752	HIS
1U9U	39	HIS	4.589294	80.451	HIS
4B8N	48	HIS	4.479396	87.524	HIS
1SI8	54	HIS	5.688888	26.890	HIS
1SY2	59	HIS	4.045387	85.351	HIS
3MVF	59	HIS	4.066882	87.977	HIS
3TGC	59	HIS	4.100823	87.207	HIS
1B5M	63	HIS	4.211990	71.272	HIS
1ICC	63	HIS	4.451283	57.814	HIS
1U9U	63	HIS	4.417873	66.393	HIS
2SPL	64	HIS	5.889080	73.719	HIS
5CN5	64	HIS	5.804727	84.840	HIS
4B8N	71	HIS	4.416116	70.933	HIS
3VP5	72	HIS	4.371971	45.918	HIS
3HX9	75	HIS	4.195649	50.709	HIS
4NL5	75	HIS	4.473936	46.347	HIS
4JET	81	HIS	5.381133	54.183	HIS
4XZD	81	HIS	5.263108	67.684	HIS
4Y1Q	81	HIS	5.294289	61.474	HIS
1B2V	83	HIS	5.366599	56.778	HIS
1DK0	83	HIS	5.314133	62.320	HIS
1DKH	83	HIS	5.223800	43.522	HIS
2CN4	83	HIS	5.251875	61.039	HIS
3QZN	83	HIS	4.660500	67.495	HIS
2E2Y	93	HIS	4.514535	86.534	HIS

Table B.9: HEM: All Planar Angles *(continued)*

PDB_ID	Residue_Number	Residue_Code.x	Mean_Distance	Angle	Residue_Code.y
2SPL	93	HIS	4.578545	88.954	HIS
5CN5	93	HIS	4.575365	82.799	HIS
2E2Y	97	HIS	5.917056	68.715	HIS
2SPL	97	HIS	5.997752	67.846	HIS
5CN5	97	HIS	5.966408	71.762	HIS
4UZV	106	HIS	4.502311	79.507	HIS
2IPS	109	HIS	5.924623	73.103	HIS
7C74	109	HIS	5.952700	70.733	HIS
7DMR	109	HIS	5.699226	62.306	HIS
2VEB	120	HIS	4.471709	79.839	HIS
3QZZ	120	HIS	4.599066	74.693	HIS
3ZJS	120	HIS	4.427156	73.923	HIS
1IPH	128	HIS	5.713777	33.997	HIS
2O6P	134	HIS	6.496593	61.077	HIS
3VP5	149	HIS	4.350835	49.264	HIS
3QZN	168	HIS	6.973181	70.767	HIS
4CDP	193	HIS	4.417630	74.031	HIS
2J0P	196	HIS	4.310325	75.104	HIS
5O1L	198	HIS	4.305405	66.467	HIS
5O1M	198	HIS	4.392715	64.463	HIS
4MF9	209	HIS	4.606487	63.203	HIS
1QHU	213	HIS	4.734866	79.430	HIS
1QJS	213	HIS	4.696712	82.802	HIS
6A2J	216	HIS	4.601722	63.468	HIS
1QHU	222	HIS	6.740296	77.401	HIS
2IIZ	224	HIS	4.533607	61.464	HIS
1QHU	265	HIS	4.200094	83.910	HIS
1QJS	266	HIS	4.484379	82.026	HIS
6A2J	278	HIS	4.655598	63.931	HIS
2IPS	351	HIS	4.125792	28.391	HIS
7C74	351	HIS	4.494179	25.953	HIS
7DMR	351	HIS	4.201640	31.126	HIS
3HX9	9	ILE	9.558396	78.071	ILE
4NL5	9	ILE	5.756873	80.656	ILE
4JET	30	ILE	6.988601	55.096	ILE

Table B.9: HEM: All Planar Angles *(continued)*

PDB_ID	Residue_Number	Residue_Code.x	Mean_Distance	Angle	Residue_Code.y
2O6P	48	ILE	5.365972	44.466	ILE
4B8N	55	ILE	5.758462	70.943	ILE
2FC2	63	ILE	6.106378	69.135	ILE
2E2Y	68	ILE	5.517060	80.623	ILE
3VP5	71	ILE	6.407016	71.208	ILE
2E2Y	99	ILE	6.130795	52.979	ILE
2SPL	99	ILE	6.223033	48.696	ILE
5CN5	99	ILE	6.410362	54.086	ILE
2E2Y	107	ILE	6.704700	16.195	ILE
2SPL	107	ILE	6.505472	17.465	ILE
5CN5	107	ILE	6.767432	16.093	ILE
4UZV	111	ILE	5.897899	46.982	ILE
2Q6N	114	ILE	6.560571	9.779	ILE
2VEB	116	ILE	6.573571	81.358	ILE
3QZZ	116	ILE	6.472356	81.312	ILE
3ZJS	116	ILE	6.518950	85.700	ILE
2O6P	121	ILE	6.852081	79.662	ILE
3SIK	129	ILE	6.189129	72.935	ILE
3SIK	131	ILE	6.481115	75.292	ILE
2VEB	137	ILE	6.361213	61.323	ILE
3QZZ	137	ILE	6.393964	65.377	ILE
3ZJS	137	ILE	6.315026	65.712	ILE
3QZN	159	ILE	5.866079	87.212	ILE
3QZN	164	ILE	6.384201	78.779	ILE
2BHJ	195	ILE	6.216303	34.244	ILE
2FC2	214	ILE	6.545905	59.848	ILE
5O1L	222	ILE	6.024951	24.897	ILE
5O1M	222	ILE	6.241067	30.392	ILE
2IIZ	225	ILE	6.430481	80.524	ILE
5O1L	227	ILE	6.973430	56.638	ILE
4CDP	252	ILE	6.178209	87.181	ILE
2J0P	255	ILE	6.197370	88.613	ILE
6A2J	265	ILE	6.271826	86.089	ILE
4MF9	268	ILE	6.092502	87.522	ILE
2Q6N	363	ILE	6.794813	63.519	ILE

Table B.9: HEM: All Planar Angles *(continued)*

PDB_ID	Residue_Number	Residue_Code.x	Mean_Distance	Angle	Residue_Code.y
2Q6N	435	ILE	6.531691	62.893	ILE
5VEU	442	ILE	6.119535	59.766	ILE
4I3Q	443	ILE	5.985023	55.615	ILE
2CJ0	32	LEU	5.757197	86.436	LEU
2CPO	32	LEU	5.913058	85.779	LEU
2J18	32	LEU	5.760472	86.600	LEU
1B5M	46	LEU	5.848737	58.371	LEU
1ICC	46	LEU	5.941384	55.221	LEU
1U9U	46	LEU	5.958763	65.230	LEU
1SY2	57	LEU	6.145372	80.845	LEU
3MVF	57	LEU	6.242544	82.824	LEU
3TGC	57	LEU	6.147624	82.612	LEU
4B8N	70	LEU	6.456250	84.030	LEU
1B2V	77	LEU	6.429830	74.863	LEU
1DK0	77	LEU	6.502332	70.907	LEU
1DKH	77	LEU	6.345588	81.197	LEU
2CN4	77	LEU	6.548785	64.950	LEU
4UZV	79	LEU	6.352126	32.691	LEU
2E2Y	89	LEU	6.167984	57.194	LEU
2SPL	89	LEU	6.446644	54.572	LEU
5CN5	89	LEU	6.607510	81.740	LEU
4CDP	90	LEU	6.499175	53.089	LEU
4UZV	102	LEU	6.801707	80.742	LEU
2E2Y	104	LEU	6.384225	42.486	LEU
2SPL	104	LEU	6.518599	49.950	LEU
5CN5	104	LEU	6.517400	40.971	LEU
1P3T	119	LEU	6.709401	29.938	LEU
1SY2	123	LEU	5.902915	71.098	LEU
3MVF	123	LEU	5.891492	77.839	LEU
3TGC	123	LEU	5.908675	73.018	LEU
5KZL	127	LEU	6.731689	26.021	LEU
1SY2	133	LEU	6.241713	67.620	LEU
3MVF	133	LEU	6.341681	74.740	LEU
3TGC	133	LEU	6.315080	69.684	LEU
5KZL	136	LEU	6.422701	84.272	LEU

Table B.9: HEM: All Planar Angles *(continued)*

PDB_ID	Residue_Number	Residue_Code.x	Mean_Distance	Angle	Residue_Code.y
1N45	138	LEU	6.717099	17.508	LEU
1VGI	138	LEU	6.110494	28.406	LEU
2VEB	142	LEU	6.331426	30.581	LEU
3QZZ	142	LEU	6.534813	26.402	LEU
3ZJS	142	LEU	6.289922	24.952	LEU
1N45	147	LEU	6.115862	65.024	LEU
2R7A	167	LEU	6.508147	65.218	LEU
5O1L	171	LEU	5.743071	78.726	LEU
2IIZ	255	LEU	6.075868	6.622	LEU
2R7A	257	LEU	5.559331	26.488	LEU
2IIZ	286	LEU	5.566800	60.469	LEU
2IPS	417	LEU	6.792313	68.323	LEU
2IPS	433	LEU	5.458537	63.062	LEU
7C74	433	LEU	5.275537	56.669	LEU
7DMR	433	LEU	5.225161	71.791	LEU
2Q6N	437	LEU	5.864970	68.730	LEU
3VP5	145	LYS	5.832567	22.419	LYS
5O1M	167	LYS	5.125712	80.116	LYS
3QZN	84	MET	6.337233	82.368	MET
1B2V	140	MET	6.218846	78.617	MET
1DK0	140	MET	6.185917	75.977	MET
1DKH	140	MET	6.519598	80.084	MET
2CN4	140	MET	5.816277	79.067	MET
4JET	147	MET	5.810508	82.720	MET
4XZD	147	MET	6.297861	74.779	MET
4Y1Q	147	MET	6.115760	72.668	MET
4UZV	151	MET	5.908059	50.673	MET
4CDP	241	MET	6.340896	51.184	MET
2J0P	244	MET	6.821994	47.273	MET
4MF9	257	MET	6.826627	47.678	MET
5VEU	444	MET	6.285199	69.820	MET
4I3Q	445	MET	5.975507	54.809	MET
3HX9	23	PHE	8.679990	57.262	PHE
4NL5	23	PHE	5.580423	79.989	PHE
2SPL	29	PHE	6.129536	67.992	PHE

Table B.9: HEM: All Planar Angles *(continued)*

PDB_ID	Residue_Number	Residue_Code.x	Mean_Distance	Angle	Residue_Code.y
1B5M	35	PHE	5.848448	51.666	PHE
1ICC	35	PHE	6.276818	51.071	PHE
1U9U	35	PHE	6.094672	55.366	PHE
2SPL	43	PHE	5.815167	43.358	PHE
5CN5	43	PHE	5.981197	45.242	PHE
4B8N	44	PHE	6.120000	52.229	PHE
4JET	50	PHE	6.875792	36.195	PHE
4Y1Q	50	PHE	6.555816	41.424	PHE
4UZV	53	PHE	6.941930	87.835	PHE
2CJ0	57	PHE	6.484645	35.572	PHE
2CPO	57	PHE	6.473913	37.630	PHE
2J18	57	PHE	6.534471	36.396	PHE
1B5M	58	PHE	6.096500	79.544	PHE
1ICC	58	PHE	6.182239	87.840	PHE
4B8N	67	PHE	6.248829	74.088	PHE
4UZV	67	PHE	5.984317	67.843	PHE
1SY2	68	PHE	6.098374	86.062	PHE
3MVF	68	PHE	6.146303	85.237	PHE
3TGC	68	PHE	6.152796	84.376	PHE
2VEB	74	PHE	6.405384	85.523	PHE
3QZZ	74	PHE	6.218919	81.733	PHE
3ZJS	74	PHE	6.270262	76.080	PHE
3VP5	76	PHE	6.844578	44.869	PHE
4JET	77	PHE	6.310922	82.490	PHE
4XZD	77	PHE	6.275751	87.170	PHE
4Y1Q	77	PHE	6.412846	87.126	PHE
2VEB	93	PHE	5.810118	22.043	PHE
3QZZ	93	PHE	6.033470	11.038	PHE
3ZJS	93	PHE	5.922481	16.833	PHE
2CJ0	103	PHE	6.182880	27.021	PHE
2CPO	103	PHE	6.396792	28.962	PHE
2J18	103	PHE	6.235843	27.909	PHE
3VP5	112	PHE	6.509162	68.707	PHE
4UZV	119	PHE	5.820671	52.586	PHE
1SI8	132	PHE	6.553242	35.834	PHE

Table B.9: HEM: All Planar Angles *(continued)*

PDB_ID	Residue_Number	Residue_Code.x	Mean_Distance	Angle	Residue_Code.y
1SI8	140	PHE	5.575451	44.222	PHE
2VEB	145	PHE	6.211153	71.125	PHE
3QZZ	145	PHE	6.192963	67.209	PHE
3ZJS	145	PHE	6.059949	63.965	PHE
1P3T	181	PHE	5.974488	28.002	PHE
2CJ0	186	PHE	5.833496	74.907	PHE
2CPO	186	PHE	5.891089	74.604	PHE
2J18	186	PHE	5.882819	73.963	PHE
5KZL	195	PHE	6.351090	26.366	PHE
2J0P	199	PHE	6.468406	77.213	PHE
1IPH	206	PHE	6.665963	47.799	PHE
1N45	207	PHE	5.975984	35.914	PHE
1VGI	207	PHE	6.238995	35.601	PHE
1IPH	214	PHE	5.767678	38.797	PHE
2FC2	231	PHE	6.129726	47.062	PHE
4CDP	243	PHE	5.994465	75.432	PHE
2J0P	246	PHE	6.155004	71.919	PHE
2IIZ	257	PHE	5.749045	43.524	PHE
4MF9	259	PHE	5.680334	67.502	PHE
7C74	347	PHE	6.478230	66.212	PHE
7DMR	347	PHE	6.671472	71.799	PHE
2BHJ	363	PHE	5.980185	49.593	PHE
2Q6N	429	PHE	6.192258	16.599	PHE
5VEU	434	PHE	6.084164	6.989	PHE
4I3Q	435	PHE	6.161681	12.310	PHE
1ZVI	584	PHE	6.009975	47.157	PHE
2CJ0	28	PRO	6.127671	77.384	PRO
2CPO	28	PRO	6.018197	79.394	PRO
2J18	28	PRO	6.103023	75.350	PRO
2CJ0	30	PRO	5.960531	45.202	PRO
2CPO	30	PRO	6.017188	43.004	PRO
2J18	30	PRO	5.936382	46.559	PRO
1B5M	40	PRO	6.032548	64.686	PRO
1ICC	40	PRO	6.016737	74.979	PRO
1U9U	40	PRO	6.149502	62.201	PRO

Table B.9: HEM: All Planar Angles *(continued)*

PDB_ID	Residue_Number	Residue_Code.x	Mean_Distance	Angle	Residue_Code.y
4B8N	49	PRO	6.182011	55.551	PRO
1SI8	315	PRO	6.539721	79.646	PRO
1IPH	393	PRO	6.703993	79.546	PRO
2Q6N	428	PRO	6.945175	64.749	PRO
5VEU	433	PRO	6.574196	84.362	PRO
4I3Q	434	PRO	6.893037	81.173	PRO
1B2V	42	SER	6.443386	37.867	SER
1DK0	42	SER	6.540219	66.931	SER
1DKH	42	SER	6.070312	84.431	SER
2FC2	59	SER	6.581787	68.948	SER
2E2Y	92	SER	6.454585	87.015	SER
2SPL	92	SER	6.650791	83.681	SER
5CN5	92	SER	6.529632	89.481	SER
1P3T	117	SER	5.531584	72.173	SER
5GJ3	124	SER	10.238794	71.645	SER
5KZL	131	SER	6.438631	67.739	SER
1N45	142	SER	6.525024	45.908	SER
1VGI	142	SER	5.700272	44.929	SER
4MYP	205	SER	6.655356	71.936	SER
6A2J	261	SER	6.949581	69.073	SER
1QHU	266	SER	6.680148	46.159	SER
1QJS	267	SER	6.730283	37.983	SER
1IPH	414	SER	6.728176	7.127	SER
1DK0	33	THR	6.991008	82.730	THR
2R7A	52	THR	5.945515	75.272	THR
2E2Y	67	THR	6.891096	23.524	THR
3VP5	68	THR	6.164947	65.743	THR
4XZD	82	THR	6.830323	42.191	THR
1B2V	84	THR	6.798527	48.773	THR
1DK0	84	THR	6.799510	46.371	THR
1DKH	84	THR	6.267175	13.394	THR
2CN4	84	THR	6.804573	47.318	THR
1SY2	121	THR	6.333312	76.088	THR
3MVF	121	THR	6.595150	73.083	THR
3TGC	121	THR	6.343084	72.698	THR

Table B.9: HEM: All Planar Angles *(continued)*

PDB_ID	Residue_Number	Residue_Code.x	Mean_Distance	Angle	Residue_Code.y
3VP5	130	THR	5.980868	66.884	THR
1N45	135	THR	6.713859	87.717	THR
1VGI	135	THR	6.883314	86.934	THR
5O1M	168	THR	6.373467	86.011	THR
6A2J	178	THR	6.772182	40.134	THR
5O1L	194	THR	6.305648	88.159	THR
5O1M	194	THR	6.409916	87.811	THR
4MF9	208	THR	6.202558	72.980	THR
5O1L	230	THR	6.574103	56.973	THR
5O1M	230	THR	6.603918	48.514	THR
2Q6N	302	THR	5.748396	11.940	THR
4I3Q	309	THR	6.214341	29.056	THR
5VEU	309	THR	5.895842	31.467	THR
2E2Y	43	TRP	5.845537	63.663	TRP
2FC2	56	TRP	5.737975	58.198	TRP
3QZZ	60	TRP	6.491833	87.108	TRP
3ZJS	60	TRP	6.366999	80.062	TRP
3HX9	66	TRP	7.852796	51.391	TRP
4NL5	66	TRP	6.235302	53.548	TRP
2R7A	68	TRP	6.192116	56.988	TRP
1QHU	171	TRP	6.147194	45.734	TRP
1QJS	171	TRP	6.211700	40.663	TRP
2VEB	185	TRP	5.717992	82.552	TRP
3QZZ	185	TRP	6.111800	87.248	TRP
3ZJS	185	TRP	5.960798	85.251	TRP
2BHJ	188	TRP	6.049049	55.507	TRP
2CJ0	213	TRP	6.764355	72.064	TRP
2J18	213	TRP	6.782850	71.352	TRP
2FC2	234	TRP	6.837576	33.085	TRP
1QHU	267	TRP	5.987630	76.604	TRP
1QJS	268	TRP	6.230710	77.078	TRP
2BHJ	366	TRP	6.764735	26.115	TRP
1ZVI	409	TRP	5.660275	56.622	TRP
1ZVI	587	TRP	6.843603	29.680	TRP
1SY2	40	TYR	5.887937	30.456	TYR

Table B.9: HEM: All Planar Angles *(continued)*

PDB_ID	Residue_Number	Residue_Code.x	Mean_Distance	Angle	Residue_Code.y
3MVF	40	TYR	6.759408	4.606	TYR
3TGC	40	TYR	5.967215	29.632	TYR
2O6P	52	TYR	6.682161	77.760	TYR
2CN4	55	TYR	6.806239	16.581	TYR
4JET	55	TYR	6.877273	11.357	TYR
4XZD	55	TYR	6.821652	12.231	TYR
4Y1Q	55	TYR	6.699820	8.751	TYR
1SY2	58	TYR	6.964531	86.657	TYR
1U9U	58	TYR	6.232812	76.301	TYR
3ZJS	61	TYR	6.548411	42.808	TYR
2R7A	67	TYR	4.159993	73.259	TYR
1B2V	75	TYR	4.251885	39.160	TYR
1DK0	75	TYR	4.346840	40.042	TYR
1DKH	75	TYR	4.792830	45.976	TYR
2CN4	75	TYR	4.345054	45.523	TYR
4JET	75	TYR	4.420106	47.089	TYR
4XZD	75	TYR	4.329954	46.839	TYR
3QZN	87	TYR	6.251729	84.821	TYR
3VP5	91	TYR	6.574739	32.406	TYR
2O6P	132	TYR	4.055037	56.191	TYR
2O6P	136	TYR	5.148558	86.464	TYR
3SIK	136	TYR	4.260470	52.942	TYR
1B2V	137	TYR	6.232518	27.438	TYR
1DK0	137	TYR	6.186950	32.086	TYR
1DKH	137	TYR	6.409147	26.390	TYR
2CN4	137	TYR	6.142879	28.073	TYR
3SIK	140	TYR	5.120136	63.829	TYR
5GJ3	140	TYR	7.520130	58.494	TYR
3QZN	170	TYR	5.718488	72.518	TYR
1QHU	204	TYR	6.239544	47.589	TYR
1QJS	204	TYR	6.225721	48.525	TYR
5GJ3	239	TYR	4.170326	62.993	TYR
4MYP	280	TYR	4.465249	56.836	TYR
4MYP	289	TYR	5.900895	20.187	TYR
1SI8	337	TYR	3.976560	58.339	TYR

Table B.9: HEM: All Planar Angles *(continued)*

PDB_ID	Residue_Number	Residue_Code.x	Mean_Distance	Angle	Residue_Code.y
1IPH	415	TYR	4.218561	62.200	TYR
1P3T	26	VAL	6.716946	70.533	VAL
1SY2	36	VAL	6.479806	81.825	VAL
3TGC	36	VAL	6.135653	80.270	VAL
1B2V	37	VAL	5.425221	76.657	VAL
1DK0	37	VAL	5.400636	79.308	VAL
1DKH	37	VAL	5.642973	85.568	VAL
1B5M	45	VAL	5.846522	22.834	VAL
1ICC	45	VAL	5.992035	10.185	VAL
1U9U	45	VAL	6.500194	23.361	VAL
1SI8	53	VAL	6.238869	22.937	VAL
3HX9	53	VAL	10.092943	16.301	VAL
4NL5	53	VAL	5.909472	26.973	VAL
1B5M	61	VAL	6.074911	50.909	VAL
1ICC	61	VAL	5.726742	49.678	VAL
1U9U	61	VAL	6.163696	55.756	VAL
2SPL	68	VAL	5.598014	66.196	VAL
5CN5	68	VAL	5.556498	70.253	VAL
4B8N	75	VAL	6.033658	36.289	VAL
2VEB	89	VAL	5.917494	83.599	VAL
3QZZ	89	VAL	5.927268	83.889	VAL
3ZJS	89	VAL	5.790982	89.427	VAL
2O6P	119	VAL	6.176593	82.298	VAL
5KZL	124	VAL	6.607237	84.454	VAL
1SI8	125	VAL	6.016899	42.150	VAL
1IPH	127	VAL	6.256166	18.034	VAL
3VP5	131	VAL	5.568423	66.180	VAL
3VP5	148	VAL	6.888565	79.860	VAL
5O1L	152	VAL	6.293389	50.217	VAL
5O1M	152	VAL	6.250877	42.675	VAL
3QZN	161	VAL	6.290827	78.263	VAL
6A2J	175	VAL	6.202413	9.481	VAL
6A2J	182	VAL	6.679490	6.095	VAL
4CDP	192	VAL	5.600764	66.470	VAL
2J0P	195	VAL	6.307524	65.521	VAL

Table B.9: HEM: All Planar Angles *(continued)*

PDB_ID	Residue_Number	Residue_Code.x	Mean_Distance	Angle	Residue_Code.y
5O1L	197	VAL	6.648164	58.183	VAL
5O1M	197	VAL	6.631076	62.092	VAL
1IPH	199	VAL	6.294207	46.553	VAL
2IIZ	228	VAL	5.315815	34.144	VAL
2BHJ	346	VAL	6.643571	65.072	VAL
2IPS	354	VAL	6.655642	42.876	VAL
5VEU	369	VAL	6.886497	38.286	VAL
1ZVI	416	VAL	5.960795	36.384	VAL

Table B.10: HEC: All Planar Angles

PDB_ID	Residue_Number	Residue_Code.x	Mean_Distance	Angle	Residue_Code.y
5KPF	81	ALA	6.517051	19.673	ALA
5LFT	81	ALA	6.400723	27.359	ALA
5T8W	81	ALA	6.484127	17.792	ALA
3EAH	147	ALA	6.240842	65.476	ALA
2BC5	106	ARG	5.961420	72.519	ARG
6WZA	106	ARG	6.631682	36.834	ARG
1BBH	129	ARG	5.790808	84.690	ARG
3EAH	149	ARG	5.803314	30.280	ARG
3EAH	153	ARG	6.514542	31.482	ARG
2BC5	99	ASN	6.936196	74.457	ASN
3X15	12	CYS	6.451594	75.877	CYS
5KPF	14	CYS	6.631432	78.361	CYS
5LFT	14	CYS	6.598389	78.924	CYS
5T8W	14	CYS	6.647516	80.130	CYS
6XNK	14	CYS	6.275930	83.242	CYS
2BH5	15	CYS	6.513509	80.908	CYS
3X15	15	CYS	6.178945	60.268	CYS
5KPF	17	CYS	6.098545	57.159	CYS
5LFT	17	CYS	6.056595	55.965	CYS
5T8W	17	CYS	6.188739	57.751	CYS

Table B.10: HEC: All Planar Angles *(continued)*

PDB_ID	Residue_Number	Residue_Code.x	Mean_Distance	Angle	Residue_Code.y
6XNK	17	CYS	5.903640	67.256	CYS
1W2L	18	CYS	6.554906	79.901	CYS
2BH5	18	CYS	6.369197	56.447	CYS
1W2L	21	CYS	6.223591	50.740	CYS
2BC5	98	CYS	5.957326	62.529	CYS
6WZA	98	CYS	5.774303	65.838	CYS
2BC5	101	CYS	6.394766	89.234	CYS
6WZA	101	CYS	6.455707	88.190	CYS
1BBH	121	CYS	5.737156	69.070	CYS
1BBH	124	CYS	6.272059	73.170	CYS
3EAH	150	CYS	4.247423	47.992	CYS
6VDQ	317	CYS	6.231170	64.036	CYS
1S56	58	GLN	6.005777	46.505	GLN
1BBH	17	GLU	6.940695	44.648	GLU
3X15	24	GLY	6.352237	71.150	GLY
5KPF	29	GLY	6.052599	68.487	GLY
5LFT	29	GLY	6.048126	64.422	GLY
5T8W	29	GLY	6.153313	65.660	GLY
6XNK	29	GLY	5.786913	67.542	GLY
1W2L	31	GLY	6.565877	60.959	GLY
2BH5	36	GLY	6.126048	68.830	GLY
3EAH	152	GLY	5.627214	19.760	GLY
3X15	16	HIS	4.360557	56.339	HIS
5KPF	18	HIS	4.310334	57.026	HIS
5LFT	18	HIS	4.342999	57.434	HIS
5T8W	18	HIS	4.334295	56.673	HIS
6XNK	18	HIS	4.599701	53.280	HIS
2BH5	19	HIS	4.283790	56.825	HIS
1W2L	22	HIS	4.350769	62.051	HIS
1S56	81	HIS	4.475028	80.865	HIS
2BC5	102	HIS	4.186908	82.850	HIS
6WZA	102	HIS	4.440577	87.413	HIS
1BBH	125	HIS	4.218890	89.456	HIS
6VDQ	274	HIS	4.500421	76.928	HIS
6VDQ	313	HIS	4.120545	68.371	HIS

Table B.10: HEC: All Planar Angles *(continued)*

PDB_ID	Residue_Number	Residue_Code.x	Mean_Distance	Angle	Residue_Code.y
3X15	30	ILE	6.412845	48.363	ILE
1W2L	61	ILE	6.839545	86.856	ILE
6XNK	75	ILE	6.412701	20.309	ILE
1S56	86	ILE	5.878780	46.879	ILE
6VDQ	278	ILE	5.358791	51.036	ILE
2BC5	3	LEU	6.742954	75.724	LEU
6WZA	3	LEU	6.697674	65.670	LEU
2BC5	10	LEU	6.154091	81.531	LEU
6WZA	10	LEU	6.067786	77.978	LEU
5KPF	32	LEU	6.145036	62.380	LEU
5LFT	32	LEU	6.106815	62.454	LEU
5T8W	32	LEU	5.994375	61.079	LEU
6XNK	32	LEU	6.085909	58.350	LEU
2BH5	39	LEU	5.728784	68.293	LEU
1S56	54	LEU	5.947501	53.661	LEU
5KPF	68	LEU	6.268124	82.295	LEU
5LFT	68	LEU	6.315525	79.956	LEU
5T8W	68	LEU	6.123569	78.343	LEU
6VDQ	238	LEU	6.409586	33.875	LEU
6VDQ	277	LEU	6.506868	55.119	LEU
6XNK	79	LYS	3.938274	74.591	LYS
2BH5	100	LYS	4.313747	77.818	LYS
2BC5	7	MET	4.661903	78.629	MET
6WZA	7	MET	4.611608	76.023	MET
1BBH	19	MET	6.049470	76.193	MET
1W2L	76	MET	4.403618	74.807	MET
1S56	77	MET	6.187616	82.400	MET
5KPF	80	MET	4.692154	69.191	MET
5LFT	80	MET	4.757864	70.970	MET
5T8W	80	MET	4.693021	71.981	MET
1W2L	34	PHE	5.935685	47.542	PHE
3X15	44	PHE	6.024333	88.840	PHE
1S56	46	PHE	5.938368	40.237	PHE
2BC5	65	PHE	6.201901	7.130	PHE
6WZA	65	PHE	6.184290	8.954	PHE

Table B.10: HEC: All Planar Angles *(continued)*

PDB_ID	Residue_Number	Residue_Code.x	Mean_Distance	Angle	Residue_Code.y
5KPF	82	PHE	6.311357	54.389	PHE
5LFT	82	PHE	6.466458	54.125	PHE
5T8W	82	PHE	6.527249	55.006	PHE
2BH5	102	PHE	6.736126	35.502	PHE
3EAH	319	PHE	6.137327	43.608	PHE
6VDQ	320	PHE	6.121894	69.729	PHE
3X15	25	PRO	6.252857	53.365	PRO
5KPF	30	PRO	6.184028	58.382	PRO
5LFT	30	PRO	6.179273	58.317	PRO
5T8W	30	PRO	6.138272	60.452	PRO
6XNK	30	PRO	5.900245	78.500	PRO
1W2L	32	PRO	6.457693	61.577	PRO
2BH5	37	PRO	6.202537	54.969	PRO
5KPF	71	PRO	6.976183	22.212	PRO
5LFT	71	PRO	6.983064	24.358	PRO
5T8W	71	PRO	6.909375	23.188	PRO
1W2L	77	PRO	6.071845	79.721	PRO
1W2L	60	SER	6.470812	29.839	SER
6XNK	28	THR	6.983672	89.881	THR
6VDQ	309	THR	6.443589	76.554	THR
3EAH	144	TRP	5.647844	55.208	TRP
6VDQ	271	TRP	5.880644	62.992	TRP
3EAH	322	TRP	6.529256	31.513	TRP
1BBH	16	TYR	4.795494	83.790	TYR
1S56	33	TYR	6.252015	73.693	TYR
1BBH	58	TYR	6.554347	74.986	TYR
5KPF	67	TYR	5.922923	73.698	TYR
5LFT	67	TYR	5.919346	72.327	TYR
5T8W	67	TYR	5.858639	72.392	TYR
6XNK	67	TYR	5.613420	78.584	TYR
2BH5	79	TYR	5.535216	66.731	TYR
1W2L	80	TYR	6.249808	80.939	TYR
6VDQ	310	TYR	6.768220	38.505	TYR
1W2L	75	VAL	6.753821	70.180	VAL
1S56	80	VAL	6.205932	89.256	VAL

Table B.10: HEC: All Planar Angles *(continued)*

PDB_ID	Residue_Number	Residue_Code.x	Mean_Distance	Angle	Residue_Code.y
2BH5	80	VAL	6.887770	66.644	VAL
6XNK	83	VAL	6.004096	49.708	VAL
1S56	94	VAL	6.626107	47.118	VAL
1S56	126	VAL	6.029592	82.902	VAL
3EAH	151	VAL	6.103944	46.478	VAL

Table B.11: SRM: All Planar Angles

PDB_ID	Residue_Number	Residue_Code.x	Mean_Distance	Angle	Residue_Code.y
1ZJ8	468	ALA	6.774896	67.235	ALA
3B0G	486	ALA	6.469408	53.215	ALA
3VKP	486	ALA	6.471195	63.024	ALA
3VLX	486	ALA	6.481752	63.686	ALA
3VLY	486	ALA	6.503895	62.464	ALA
3VLZ	486	ALA	6.507235	52.788	ALA
5H8V	545	ALA	6.528336	65.454	ALA
2AOP	83	ARG	5.905472	47.714	ARG
1ZJ8	97	ARG	5.632921	36.797	ARG
2AKJ	109	ARG	5.624044	45.808	ARG
3B0G	109	ARG	5.714505	49.905	ARG
3VKP	109	ARG	5.727950	45.457	ARG
3VLX	109	ARG	5.657293	44.382	ARG
3VLY	109	ARG	5.670401	44.269	ARG
3VLZ	109	ARG	5.666461	48.083	ARG
5H8V	124	ARG	5.731236	44.003	ARG
2AOP	153	ARG	6.898322	85.374	ARG
1ZJ8	166	ARG	6.411696	86.955	ARG
2AKJ	179	ARG	6.270969	87.072	ARG
3B0G	179	ARG	6.332302	75.820	ARG
3VKP	179	ARG	6.261289	85.962	ARG
3VLX	179	ARG	6.332845	87.012	ARG

Table B.11: SRM: All Planar Angles *(continued)*

PDB_ID	Residue_Number	Residue_Code.x	Mean_Distance	Angle	Residue_Code.y
3VLY	179	ARG	6.349458	86.279	ARG
3VLZ	179	ARG	6.432708	75.861	ARG
5H8V	193	ARG	6.748373	86.970	ARG
2AOP	116	ASN	6.627004	77.523	ASN
1ZJ8	465	ASN	6.589731	74.338	ASN
2AOP	481	ASN	6.568014	76.265	ASN
3B0G	483	ASN	6.105308	61.801	ASN
3VKP	483	ASN	6.093849	72.638	ASN
3VLX	483	ASN	6.149563	73.596	ASN
3VLY	483	ASN	6.199685	72.914	ASN
3VLZ	483	ASN	6.172324	60.497	ASN
2AKJ	484	ASN	6.180565	72.711	ASN
5H8V	542	ASN	6.517505	79.233	ASN
1ZJ8	129	ASP	6.873987	67.150	ASP
1ZJ8	467	CYS	4.642760	87.220	CYS
2AOP	483	CYS	4.593058	85.931	CYS
3B0G	485	CYS	4.334547	73.017	CYS
3VKP	485	CYS	4.338921	84.887	CYS
3VLX	485	CYS	4.333556	85.502	CYS
3VLY	485	CYS	4.349260	84.134	CYS
3VLZ	485	CYS	4.361247	73.065	CYS
2AKJ	486	CYS	4.400598	86.391	CYS
5H8V	494	CYS	6.918908	18.748	CYS
5H8V	544	CYS	4.294361	85.621	CYS
2AOP	121	GLN	6.832109	25.136	GLN
1ZJ8	134	GLN	6.870508	22.173	GLN
5H8V	161	GLN	6.725078	29.150	GLN
2AOP	482	GLY	6.644058	75.745	GLY
2AOP	484	GLY	6.751562	83.876	GLY
2AKJ	487	GLY	6.536313	79.167	GLY
5H8V	543	GLY	6.487994	78.451	GLY
1ZJ8	207	LYS	5.279599	51.736	LYS
1ZJ8	209	LYS	5.254105	61.416	LYS
2AOP	215	LYS	5.521547	41.259	LYS
2AOP	217	LYS	5.485034	57.432	LYS

Table B.11: SRM: All Planar Angles *(continued)*

PDB_ID	Residue_Number	Residue_Code.x	Mean_Distance	Angle	Residue_Code.y
2AKJ	224	LYS	5.292960	53.525	LYS
3B0G	224	LYS	5.579947	59.557	LYS
3VKP	224	LYS	5.500133	56.004	LYS
3VLX	224	LYS	5.605021	56.372	LYS
3VLY	224	LYS	5.637976	59.364	LYS
3VLZ	224	LYS	5.601385	52.886	LYS
3VLY	226	LYS	5.485627	52.123	LYS
3VLZ	226	LYS	5.641233	47.713	LYS
5H8V	276	LYS	5.805329	50.247	LYS
5H8V	278	LYS	5.495851	53.934	LYS
1ZJ8	466	SER	6.539429	45.045	SER
2AKJ	485	SER	6.504302	77.035	SER
2AKJ	142	THR	6.814343	68.034	THR
3B0G	142	THR	6.442796	66.277	THR
3VKP	142	THR	6.428882	73.086	THR
3VLX	142	THR	6.455248	73.866	THR
3VLY	142	THR	6.452740	72.255	THR
3VLZ	142	THR	6.394057	69.555	THR
5H8V	156	THR	6.490994	74.765	THR
3B0G	484	THR	6.402854	34.005	THR
3VKP	484	THR	6.412766	38.529	THR
3VLX	484	THR	6.401875	38.523	THR
3VLY	484	THR	6.414362	37.480	THR
3VLZ	484	THR	6.437540	35.092	THR
1ZJ8	69	TYR	6.963349	17.492	TYR
5H8V	106	TYR	6.992106	27.541	TYR

Table B.12: VERDOHEME: All Planar Angles

PDB_ID	Residue_Number	Residue_Code.x	Mean_Distance	Angle	Residue_Code.y
2ZVU	28	ALA	6.962159	60.211	ALA
3MOO	136	ASP	6.778611	59.636	ASP
2ZVU	140	ASP	6.674210	53.858	ASP
3MOO	24	GLU	6.275511	34.237	GLU
2ZVU	29	GLU	6.221641	12.615	GLU
3MOO	135	GLY	5.288496	66.356	GLY
2ZVU	139	GLY	5.265696	66.938	GLY
3MOO	139	GLY	5.369017	35.165	GLY
3MOO	140	GLY	6.027517	69.523	GLY
2ZVU	143	GLY	5.436145	32.937	GLY
2ZVU	144	GLY	5.902504	68.684	GLY
3MOO	20	HIS	4.614778	65.389	HIS
2ZVU	25	HIS	4.603252	70.790	HIS
3MOO	134	LEU	6.100073	27.652	LEU
2ZVU	138	LEU	6.249768	37.499	LEU
3MOO	201	PHE	5.958999	31.400	PHE
2ZVU	207	PHE	6.037412	29.522	PHE
3MOO	138	SER	5.886820	52.337	SER
2ZVU	142	SER	6.048311	54.957	SER
2ZVU	135	THR	6.765195	89.631	THR
3MOO	131	VAL	6.796515	89.945	VAL
1TWN	140	ASP	6.273979	75.887	ASP
1TWR	140	ASP	6.553790	73.555	ASP
1TWN	29	GLU	6.123574	35.411	GLU
1TWR	29	GLU	6.517157	50.624	GLU
1TWN	139	GLY	5.092800	37.268	GLY
1TWR	139	GLY	5.369385	36.457	GLY
1TWN	143	GLY	5.231213	20.583	GLY
1TWR	143	GLY	5.836559	26.276	GLY
1TWN	144	GLY	6.024952	48.406	GLY
1TWN	25	HIS	4.673370	82.070	HIS
1TWR	25	HIS	4.786588	75.802	HIS
1TWN	138	LEU	6.399559	8.072	LEU
1TWR	138	LEU	6.579770	2.665	LEU
1TWN	207	PHE	6.263716	53.897	PHE

Table B.12: VERDOHEME: All Planar Angles *(continued)*

PDB_ID	Residue_Number	Residue_Code.x	Mean_Distance	Angle	Residue_Code.y
1TWR	207	PHE	6.447849	51.949	PHE
1TWN	142	SER	6.035867	26.649	SER
1TWR	142	SER	6.195017	40.009	SER
1TWN	135	THR	6.865192	71.849	THR

B.4 Planar Angles of Closest Residues

Table B.13: HEM: Planar Angles of Closest Residues

PDB_ID	Residue_Number	Residue_Code.x	Mean_Distance	Angle	Residue_Code.y
1B2V	75	TYR	4.251885	39.160	TYR
1B2V	32	HIS	4.667618	51.415	HIS
1B2V	83	HIS	5.366599	56.778	HIS
1B5M	63	HIS	4.211990	71.272	HIS
1B5M	39	HIS	4.456809	87.693	HIS
1B5M	41	GLY	5.388127	72.708	GLY
1DK0	75	TYR	4.346840	40.042	TYR
1DK0	32	HIS	4.556145	48.497	HIS
1DK0	83	HIS	5.314133	62.320	HIS
1DKH	75	TYR	4.792830	45.976	TYR
1DKH	32	HIS	5.099382	50.187	HIS
1DKH	83	HIS	5.223800	43.522	HIS
1ICC	63	HIS	4.451283	57.814	HIS
1ICC	39	HIS	4.542187	78.752	HIS
1ICC	41	GLY	5.723853	72.752	GLY
1IPH	415	TYR	4.218561	62.200	TYR
1IPH	411	ARG	5.321024	79.235	ARG
1IPH	128	HIS	5.713777	33.997	HIS
1N45	25	HIS	4.545004	69.116	HIS
1N45	139	GLY	5.251379	58.119	GLY

Table B.13: HEM: Planar Angles of Closest Residues *(continued)*

PDB_ID	Residue_Number	Residue_Code.x	Mean_Distance	Angle	Residue_Code.y
1N45	143	GLY	5.882948	37.778	GLY
1P3T	23	HIS	4.573926	67.542	HIS
1P3T	120	GLY	4.843774	41.129	GLY
1P3T	117	SER	5.531584	72.173	SER
1QHU	265	HIS	4.200094	83.910	HIS
1QHU	213	HIS	4.734866	79.430	HIS
1QHU	267	TRP	5.987630	76.604	TRP
1QJS	266	HIS	4.484379	82.026	HIS
1QJS	213	HIS	4.696712	82.802	HIS
1QJS	171	TRP	6.211700	40.663	TRP
1SI8	337	TYR	3.976560	58.339	TYR
1SI8	333	ARG	5.247624	87.335	ARG
1SI8	140	PHE	5.575451	44.222	PHE
1SY2	59	HIS	4.045387	85.351	HIS
1SY2	40	TYR	5.887937	30.456	TYR
1SY2	123	LEU	5.902915	71.098	LEU
1U9U	63	HIS	4.417873	66.393	HIS
1U9U	39	HIS	4.589294	80.451	HIS
1U9U	41	GLY	5.723510	83.944	GLY
1VGI	25	HIS	4.646180	72.142	HIS
1VGI	139	GLY	5.155470	60.437	GLY
1VGI	143	GLY	5.279720	32.760	GLY
1ZVI	415	CYS	4.181834	46.871	CYS
1ZVI	417	GLY	5.404983	24.763	GLY
1ZVI	409	TRP	5.660275	56.622	TRP
2BHJ	194	CYS	4.487497	52.816	CYS
2BHJ	196	GLY	5.667103	19.625	GLY
2BHJ	193	ARG	5.745098	22.913	ARG
2CJ0	29	CYS	4.390905	47.217	CYS
2CJ0	31	ALA	5.440871	54.576	ALA
2CJ0	183	GLU	5.716050	77.664	GLU
2CN4	75	TYR	4.345054	45.523	TYR
2CN4	83	HIS	5.251875	61.039	HIS
2CN4	140	MET	5.816277	79.067	MET
2CPO	29	CYS	4.443549	49.291	CYS

Table B.13: HEM: Planar Angles of Closest Residues *(continued)*

PDB_ID	Residue_Number	Residue_Code.x	Mean_Distance	Angle	Residue_Code.y
2CPO	31	ALA	5.505123	50.842	ALA
2CPO	183	GLU	5.799506	78.548	GLU
2E2Y	93	HIS	4.514535	86.534	HIS
2E2Y	68	ILE	5.517060	80.623	ILE
2E2Y	43	TRP	5.845537	63.663	TRP
2FC2	62	CYS	4.482879	54.005	CYS
2FC2	56	TRP	5.737975	58.198	TRP
2FC2	64	GLY	5.882725	21.989	GLY
2IIZ	224	HIS	4.533607	61.464	HIS
2IIZ	242	ARG	5.236889	71.798	ARG
2IIZ	228	VAL	5.315815	34.144	VAL
2IPS	351	HIS	4.125792	28.391	HIS
2IPS	433	LEU	5.458537	63.062	LEU
2IPS	108	ASP	5.870986	78.247	ASP
2J0P	196	HIS	4.310325	75.104	HIS
2J0P	102	ARG	5.002395	83.046	ARG
2J0P	246	PHE	6.155004	71.919	PHE
2J18	29	CYS	4.359887	47.527	CYS
2J18	31	ALA	5.457126	52.882	ALA
2J18	183	GLU	5.722472	78.531	GLU
2O6P	132	TYR	4.055037	56.191	TYR
2O6P	136	TYR	5.148558	86.464	TYR
2O6P	48	ILE	5.365972	44.466	ILE
2Q6N	436	CYS	4.305637	40.993	CYS
2Q6N	438	GLY	5.615678	28.366	GLY
2Q6N	298	ALA	5.672036	28.414	ALA
2R7A	67	TYR	4.159993	73.259	TYR
2R7A	169	ALA	5.223004	39.141	ALA
2R7A	257	LEU	5.559331	26.488	LEU
2SPL	93	HIS	4.578545	88.954	HIS
2SPL	68	VAL	5.598014	66.196	VAL
2SPL	43	PHE	5.815167	43.358	PHE
2VEB	120	HIS	4.471709	79.839	HIS
2VEB	185	TRP	5.717992	82.552	TRP
2VEB	93	PHE	5.810118	22.043	PHE

Table B.13: HEM: Planar Angles of Closest Residues *(continued)*

PDB_ID	Residue_Number	Residue_Code.x	Mean_Distance	Angle	Residue_Code.y
3HX9	75	HIS	4.195649	50.709	HIS
3HX9	71	ALA	6.230664	24.118	ALA
3HX9	66	TRP	7.852796	51.391	TRP
3MVF	59	HIS	4.066882	87.977	HIS
3MVF	42	ALA	5.827660	37.714	ALA
3MVF	123	LEU	5.891492	77.839	LEU
3QZN	83	HIS	4.660500	67.495	HIS
3QZN	170	TYR	5.718488	72.518	TYR
3QZN	159	ILE	5.866079	87.212	ILE
3QZZ	120	HIS	4.599066	74.693	HIS
3QZZ	89	VAL	5.927268	83.889	VAL
3QZZ	93	PHE	6.033470	11.038	PHE
3SIK	136	TYR	4.260470	52.942	TYR
3SIK	140	TYR	5.120136	63.829	TYR
3SIK	54	ARG	6.090293	58.962	ARG
3TGC	59	HIS	4.100823	87.207	HIS
3TGC	123	LEU	5.908675	73.018	LEU
3TGC	40	TYR	5.967215	29.632	TYR
3VP5	149	HIS	4.350835	49.264	HIS
3VP5	72	HIS	4.371971	45.918	HIS
3VP5	131	VAL	5.568423	66.180	VAL
3ZJS	120	HIS	4.427156	73.923	HIS
3ZJS	89	VAL	5.790982	89.427	VAL
3ZJS	93	PHE	5.922481	16.833	PHE
4B8N	71	HIS	4.416116	70.933	HIS
4B8N	48	HIS	4.479396	87.524	HIS
4B8N	50	GLY	5.464969	87.471	GLY
4CDP	193	HIS	4.417630	74.031	HIS
4CDP	100	ARG	5.360373	82.404	ARG
4CDP	192	VAL	5.600764	66.470	VAL
4I3Q	442	CYS	4.085782	34.781	CYS
4I3Q	444	GLY	5.222394	22.218	GLY
4I3Q	305	ALA	5.305272	55.811	ALA
4JET	75	TYR	4.420106	47.089	TYR
4JET	81	HIS	5.381133	54.183	HIS

Table B.13: HEM: Planar Angles of Closest Residues *(continued)*

PDB_ID	Residue_Number	Residue_Code.x	Mean_Distance	Angle	Residue_Code.y
4JET	40	ARG	5.660400	8.293	ARG
4MF9	209	HIS	4.606487	63.203	HIS
4MF9	112	ARG	5.056393	85.919	ARG
4MF9	259	PHE	5.680334	67.502	PHE
4MYP	280	TYR	4.465249	56.836	TYR
4MYP	289	TYR	5.900895	20.187	TYR
4MYP	293	ALA	6.207799	64.118	ALA
4NL5	75	HIS	4.473936	46.347	HIS
4NL5	7	ASN	5.402231	60.999	ASN
4NL5	23	PHE	5.580423	79.989	PHE
4UZV	106	HIS	4.502311	79.507	HIS
4UZV	119	PHE	5.820671	52.586	PHE
4UZV	111	ILE	5.897899	46.982	ILE
4XZD	75	TYR	4.329954	46.839	TYR
4XZD	81	HIS	5.263108	67.684	HIS
4XZD	40	ARG	5.892195	23.940	ARG
4Y1Q	81	HIS	5.294289	61.474	HIS
4Y1Q	40	ARG	5.725205	11.586	ARG
4Y1Q	147	MET	6.115760	72.668	MET
5CN5	93	HIS	4.575365	82.799	HIS
5CN5	68	VAL	5.556498	70.253	VAL
5CN5	64	HIS	5.804727	84.840	HIS
5GJ3	239	TYR	4.170326	62.993	TYR
5GJ3	241	ARG	5.542517	89.231	ARG
5GJ3	140	TYR	7.520130	58.494	TYR
5KZL	15	HIS	4.819650	59.949	HIS
5KZL	128	GLY	5.130966	70.591	GLY
5KZL	132	GLY	5.705062	50.430	GLY
5O1L	198	HIS	4.305405	66.467	HIS
5O1L	171	LEU	5.743071	78.726	LEU
5O1L	222	ILE	6.024951	24.897	ILE
5O1M	198	HIS	4.392715	64.463	HIS
5O1M	167	LYS	5.125712	80.116	LYS
5O1M	222	ILE	6.241067	30.392	ILE
5VEU	441	CYS	4.349464	42.614	CYS

Table B.13: HEM: Planar Angles of Closest Residues *(continued)*

PDB_ID	Residue_Number	Residue_Code.x	Mean_Distance	Angle	Residue_Code.y
5VEU	443	GLY	5.482822	27.362	GLY
5VEU	309	THR	5.895842	31.467	THR
6A2J	216	HIS	4.601722	63.468	HIS
6A2J	278	HIS	4.655598	63.931	HIS
6A2J	179	GLY	5.548597	36.551	GLY
7C74	351	HIS	4.494179	25.953	HIS
7C74	433	LEU	5.275537	56.669	LEU
7C74	105	GLN	5.667218	84.879	GLN
7DMR	351	HIS	4.201640	31.126	HIS
7DMR	433	LEU	5.225161	71.791	LEU
7DMR	105	GLN	5.517249	82.031	GLN

Table B.14: HEC: Planar Angles of Closest Residues

PDB_ID	Residue_Number	Residue_Code.x	Mean_Distance	Angle	Residue_Code.y
1BBH	125	HIS	4.218890	89.456	HIS
1BBH	16	TYR	4.795494	83.790	TYR
1BBH	121	CYS	5.737156	69.070	CYS
1S56	81	HIS	4.475028	80.865	HIS
1S56	86	ILE	5.878780	46.879	ILE
1S56	46	PHE	5.938368	40.237	PHE
1W2L	22	HIS	4.350769	62.051	HIS
1W2L	76	MET	4.403618	74.807	MET
1W2L	34	PHE	5.935685	47.542	PHE
2BC5	102	HIS	4.186908	82.850	HIS
2BC5	7	MET	4.661903	78.629	MET
2BC5	98	CYS	5.957326	62.529	CYS
2BH5	19	HIS	4.283790	56.825	HIS
2BH5	100	LYS	4.313747	77.818	LYS
2BH5	79	TYR	5.535216	66.731	TYR
3EAH	150	CYS	4.247423	47.992	CYS

Table B.14: HEC: Planar Angles of Closest Residues *(continued)*

PDB_ID	Residue_Number	Residue_Code.x	Mean_Distance	Angle	Residue_Code.y
3EAH	152	GLY	5.627214	19.760	GLY
3EAH	144	TRP	5.647844	55.208	TRP
3X15	16	HIS	4.360557	56.339	HIS
3X15	44	PHE	6.024333	88.840	PHE
3X15	15	CYS	6.178945	60.268	CYS
5KPF	18	HIS	4.310334	57.026	HIS
5KPF	80	MET	4.692154	69.191	MET
5KPF	67	TYR	5.922923	73.698	TYR
5LFT	18	HIS	4.342999	57.434	HIS
5LFT	80	MET	4.757864	70.970	MET
5LFT	67	TYR	5.919346	72.327	TYR
5T8W	18	HIS	4.334295	56.673	HIS
5T8W	80	MET	4.693021	71.981	MET
5T8W	67	TYR	5.858639	72.392	TYR
6VDQ	313	HIS	4.120545	68.371	HIS
6VDQ	274	HIS	4.500421	76.928	HIS
6VDQ	278	ILE	5.358791	51.036	ILE
6WZA	102	HIS	4.440577	87.413	HIS
6WZA	7	MET	4.611608	76.023	MET
6WZA	98	CYS	5.774303	65.838	CYS
6XNK	79	LYS	3.938274	74.591	LYS
6XNK	18	HIS	4.599701	53.280	HIS
6XNK	67	TYR	5.613420	78.584	TYR

Table B.15: SRM: Planar Angles of Closest Residues

PDB_ID	Residue_Number	Residue_Code.x	Mean_Distance	Angle	Residue_Code.y
1ZJ8	467	CYS	4.642760	87.220	CYS
1ZJ8	209	LYS	5.254105	61.416	LYS
1ZJ8	207	LYS	5.279599	51.736	LYS
2AKJ	486	CYS	4.400598	86.391	CYS
2AKJ	224	LYS	5.292960	53.525	LYS

Table B.15: SRM: Planar Angles of Closest Residues *(continued)*

PDB_ID	Residue_Number	Residue_Code.x	Mean_Distance	Angle	Residue_Code.y
2AKJ	109	ARG	5.624044	45.808	ARG
2AOP	483	CYS	4.593058	85.931	CYS
2AOP	217	LYS	5.485034	57.432	LYS
2AOP	215	LYS	5.521547	41.259	LYS
3B0G	485	CYS	4.334547	73.017	CYS
3B0G	224	LYS	5.579947	59.557	LYS
3B0G	109	ARG	5.714505	49.905	ARG
3VKP	485	CYS	4.338921	84.887	CYS
3VKP	224	LYS	5.500133	56.004	LYS
3VKP	109	ARG	5.727950	45.457	ARG
3VLX	485	CYS	4.333556	85.502	CYS
3VLX	224	LYS	5.605021	56.372	LYS
3VLX	109	ARG	5.657293	44.382	ARG
3VLY	485	CYS	4.349260	84.134	CYS
3VLY	226	LYS	5.485627	52.123	LYS
3VLY	224	LYS	5.637976	59.364	LYS
3VLZ	485	CYS	4.361247	73.065	CYS
3VLZ	224	LYS	5.601385	52.886	LYS
3VLZ	226	LYS	5.641233	47.713	LYS
5H8V	544	CYS	4.294361	85.621	CYS
5H8V	278	LYS	5.495851	53.934	LYS
5H8V	124	ARG	5.731236	44.003	ARG

Table B.16: VERDOHEME: Planar Angles of Closest Residues

PDB_ID	Residue_Number	Residue_Code.x	Mean_Distance	Angle	Residue_Code.y
2ZVU	25	HIS	4.603252	70.790	HIS
2ZVU	139	GLY	5.265696	66.938	GLY
2ZVU	143	GLY	5.436145	32.937	GLY
3MOO	20	HIS	4.614778	65.389	HIS
3MOO	135	GLY	5.288496	66.356	GLY

Table B.16: VERDOHEME: Planar Angles of Closest Residues *(continued)*

PDB_ID	Residue_Number	Residue_Code.x	Mean_Distance	Angle	Residue_Code.y
3MOO	139	GLY	5.369017	35.165	GLY
1TWN	25	HIS	4.673370	82.070	HIS
1TWN	139	GLY	5.092800	37.268	GLY
1TWN	143	GLY	5.231213	20.583	GLY
1TWR	25	HIS	4.786588	75.802	HIS
1TWR	139	GLY	5.369385	36.457	GLY
1TWR	143	GLY	5.836559	26.276	GLY

B.5 All CA-CB-Fe Angles

Table B.17: HEM: All CA-CB-Fe Angles

PDB_ID	Residue_Number	Residue_Code.x	Mean_Distance	Residue_Code.y	Angle
1N45	28	ALA	6.981230	ALA	133.1800
2CJ0	31	ALA	5.440871	ALA	114.8710
2CPO	31	ALA	5.505123	ALA	115.0400
2J18	31	ALA	5.457126	ALA	114.2550
1SY2	42	ALA	6.006055	ALA	148.0360
3MVF	42	ALA	5.827660	ALA	147.3790
3TGC	42	ALA	6.033598	ALA	151.3290
2O6P	49	ALA	6.356063	ALA	69.6260
4B8N	54	ALA	6.390793	ALA	135.4860
1B5M	67	ALA	5.797296	ALA	143.9450
1ICC	67	ALA	6.085233	ALA	131.3420
1U9U	67	ALA	6.016697	ALA	136.6100
2CJ0	71	ALA	6.531120	ALA	140.1920
2CPO	71	ALA	6.539227	ALA	137.2830
2J18	71	ALA	6.477348	ALA	139.0360
4NL5	71	ALA	6.805378	ALA	99.7605
4Y1Q	75	ALA	6.722226	ALA	130.5910

Table B.17: HEM: All CA-CB-Fe Angles *(continued)*

PDB_ID	Residue_Number	Residue_Code.x	Mean_Distance	Residue_Code.y	Angle
1P3T	121	ALA	6.382367	ALA	48.9641
3SIK	138	ALA	6.231014	ALA	159.2210
2R7A	169	ALA	5.223004	ALA	132.6020
6A2J	180	ALA	6.687029	ALA	43.4302
2BHJ	191	ALA	6.261711	ALA	163.9660
6A2J	220	ALA	5.986896	ALA	140.0610
6A2J	259	ALA	6.937825	ALA	40.3063
4MYP	282	ALA	6.581195	ALA	153.2720
4MYP	293	ALA	6.207799	ALA	133.2580
2Q6N	298	ALA	5.672036	ALA	129.8410
4I3Q	305	ALA	5.305272	ALA	115.6050
5VEU	305	ALA	6.219660	ALA	130.5820
1ZVI	412	ALA	6.481380	ALA	147.8760
2Q6N	442	ALA	6.935846	ALA	147.6550
5VEU	447	ALA	6.667315	ALA	149.4040
4I3Q	448	ALA	6.441232	ALA	146.6870
4JET	40	ARG	5.660400	ARG	117.6700
4XZD	40	ARG	5.892195	ARG	118.8830
4Y1Q	40	ARG	5.725205	ARG	121.1480
3SIK	54	ARG	6.090293	ARG	163.0460
2FC2	61	ARG	6.072553	ARG	76.2562
2FC2	65	ARG	6.459491	ARG	70.9521
4CDP	100	ARG	5.360373	ARG	139.0430
2J0P	102	ARG	5.002395	ARG	139.6090
4UZV	105	ARG	6.689489	ARG	101.6930
4MF9	112	ARG	5.056393	ARG	134.9890
4JET	144	ARG	6.239587	ARG	94.9228
4XZD	144	ARG	6.335714	ARG	98.1313
4Y1Q	144	ARG	6.425880	ARG	98.5684
2BHJ	193	ARG	5.745098	ARG	61.6429
2BHJ	197	ARG	6.221230	ARG	67.6390
4I3Q	212	ARG	6.392849	ARG	133.1990
1QHU	214	ARG	6.588734	ARG	137.0270
1QJS	214	ARG	6.249190	ARG	70.2144
6A2J	217	ARG	6.781589	ARG	54.8831

Table B.17: HEM: All CA-CB-Fe Angles *(continued)*

PDB_ID	Residue_Number	Residue_Code.x	Mean_Distance	Residue_Code.y	Angle
2IIZ	242	ARG	5.236889	ARG	162.0190
1SI8	333	ARG	5.247624	ARG	116.1170
2IPS	348	ARG	6.336679	ARG	87.8395
7C74	348	ARG	6.274279	ARG	78.0301
7DMR	348	ARG	6.250958	ARG	82.5509
1IPH	411	ARG	5.321024	ARG	108.2630
1ZVI	414	ARG	5.799426	ARG	71.6516
1ZVI	418	ARG	6.259544	ARG	69.7795
4NL5	7	ASN	5.402231	ASN	170.5520
1B2V	41	ASN	6.894251	ASN	79.4068
1DK0	41	ASN	6.870425	ASN	80.6960
1P3T	118	ASN	6.625279	ASN	26.9658
1SI8	127	ASN	6.666708	ASN	103.3680
1IPH	201	ASN	6.396844	ASN	101.2860
2BHJ	364	ASN	6.955669	ASN	23.4362
2IPS	437	ASN	6.276979	ASN	111.3700
7C74	437	ASN	6.653391	ASN	112.3740
7DMR	437	ASN	6.591349	ASN	110.5710
5VEU	440	ASN	6.408862	ASN	56.4019
4I3Q	441	ASN	6.139159	ASN	60.3712
1P3T	27	ASP	6.267807	ASP	103.4810
2E2Y	64	ASP	6.865050	ASP	101.7770
2IPS	108	ASP	5.870986	ASP	152.6010
7C74	108	ASP	6.017401	ASP	160.5440
7DMR	108	ASP	6.266021	ASP	151.6240
1N45	140	ASP	6.389011	ASP	35.7360
1VGI	140	ASP	6.566393	ASP	22.5121
2IIZ	151	ASP	5.861207	ASP	97.0879
4CDP	191	ASP	6.789427	ASP	101.3160
2J0P	194	ASP	6.862392	ASP	107.8210
1QHU	203	ASP	6.920576	ASP	76.4671
1QJS	203	ASP	6.878437	ASP	70.4888
2IIZ	284	ASP	6.598336	ASP	144.2720
2CJ0	29	CYS	4.390905	CYS	117.5660
2CPO	29	CYS	4.443549	CYS	118.1890

Table B.17: HEM: All CA-CB-Fe Angles *(continued)*

PDB_ID	Residue_Number	Residue_Code.x	Mean_Distance	Residue_Code.y	Angle
2J18	29	CYS	4.359887	CYS	118.4250
2FC2	62	CYS	4.482879	CYS	112.5820
1P3T	113	CYS	6.881310	CYS	62.2220
2BHJ	194	CYS	4.487497	CYS	118.0500
1ZVI	415	CYS	4.181834	CYS	112.7440
2Q6N	436	CYS	4.305637	CYS	109.8240
5VEU	441	CYS	4.349464	CYS	106.7690
4I3Q	442	CYS	4.085782	CYS	103.9950
2IPS	105	GLN	5.981590	GLN	100.5170
7C74	105	GLN	5.667218	GLN	97.8161
7DMR	105	GLN	5.517249	GLN	100.6130
2R7A	253	GLN	6.081153	GLN	123.5700
6A2J	258	GLN	5.803666	GLN	91.0438
4MYP	292	GLN	6.537566	GLN	16.1591
1N45	29	GLU	6.277510	GLU	93.8698
1VGI	29	GLU	6.279863	GLU	118.3990
5O1L	148	GLU	6.440638	GLU	94.5791
2CJ0	183	GLU	5.716050	GLU	106.0810
2CPO	183	GLU	5.799506	GLU	105.9460
2J18	183	GLU	5.722472	GLU	107.1960
1QHU	225	GLU	6.177350	GLU	167.2860
1QJS	226	GLU	6.465511	GLU	155.6740
2IPS	258	GLU	6.388898	GLU	174.0360
7C74	258	GLU	6.258582	GLU	160.0830
7DMR	258	GLU	6.172262	GLU	155.5410
2Q6N	439	GLU	6.270464	GLU	58.8909
1ZVI	592	GLU	6.601349	GLU	140.0500
1P3T	23	HIS	4.573926	HIS	111.7580
1N45	25	HIS	4.545004	HIS	112.7600
1VGI	25	HIS	4.646180	HIS	113.1630
1B2V	32	HIS	4.667618	HIS	116.3150
1DK0	32	HIS	4.556145	HIS	116.4470
1DKH	32	HIS	5.099382	HIS	121.3750
1B5M	39	HIS	4.456809	HIS	101.8130
1ICC	39	HIS	4.542187	HIS	101.5070

Table B.17: HEM: All CA-CB-Fe Angles *(continued)*

PDB_ID	Residue_Number	Residue_Code.x	Mean_Distance	Residue_Code.y	Angle
1U9U	39	HIS	4.589294	HIS	102.2750
4B8N	48	HIS	4.479396	HIS	104.9040
1SI8	54	HIS	5.688888	HIS	131.6120
1SY2	59	HIS	4.045387	HIS	126.3700
3MVF	59	HIS	4.066882	HIS	126.0770
3TGC	59	HIS	4.100823	HIS	124.3700
1B5M	63	HIS	4.211990	HIS	125.8380
1ICC	63	HIS	4.451283	HIS	114.1290
1U9U	63	HIS	4.417873	HIS	116.0130
2SPL	64	HIS	5.889080	HIS	103.2250
5CN5	64	HIS	5.804727	HIS	107.1420
4B8N	71	HIS	4.416116	HIS	119.3920
3VP5	72	HIS	4.371971	HIS	101.6570
4NL5	75	HIS	4.473936	HIS	117.7090
4JET	81	HIS	5.381133	HIS	121.2740
4XZD	81	HIS	5.263108	HIS	114.4420
4Y1Q	81	HIS	5.294289	HIS	126.8310
1B2V	83	HIS	5.366599	HIS	102.9160
1DK0	83	HIS	5.314133	HIS	102.7520
1DKH	83	HIS	5.223800	HIS	122.9600
2CN4	83	HIS	5.251875	HIS	107.5140
2E2Y	93	HIS	4.514535	HIS	114.4980
2SPL	93	HIS	4.578545	HIS	112.4730
5CN5	93	HIS	4.575365	HIS	113.1870
2E2Y	97	HIS	5.917056	HIS	177.1860
2SPL	97	HIS	5.997752	HIS	176.0860
5CN5	97	HIS	5.966408	HIS	177.3970
4UZV	106	HIS	4.502311	HIS	110.2430
2IPS	109	HIS	5.924623	HIS	93.6174
7C74	109	HIS	5.952700	HIS	93.3571
7DMR	109	HIS	5.699226	HIS	93.5665
2VEB	120	HIS	4.471709	HIS	110.4880
3QZZ	120	HIS	4.599066	HIS	109.3460
3ZJS	120	HIS	4.427156	HIS	110.7000
1IPH	128	HIS	5.713777	HIS	129.2180

Table B.17: HEM: All CA-CB-Fe Angles *(continued)*

PDB_ID	Residue_Number	Residue_Code.x	Mean_Distance	Residue_Code.y	Angle
2O6P	134	HIS	6.496593	HIS	146.7790
3VP5	149	HIS	4.350835	HIS	100.8200
4CDP	193	HIS	4.417630	HIS	109.7720
2J0P	196	HIS	4.310325	HIS	111.1620
5O1L	198	HIS	4.305405	HIS	102.4410
5O1M	198	HIS	4.392715	HIS	100.3070
4MF9	209	HIS	4.606487	HIS	108.6490
1QHU	213	HIS	4.734866	HIS	114.5350
1QJS	213	HIS	4.696712	HIS	122.0930
6A2J	216	HIS	4.601722	HIS	122.2890
1QHU	222	HIS	6.740296	HIS	173.7070
2IIZ	224	HIS	4.533607	HIS	124.3380
1QHU	265	HIS	4.200094	HIS	121.1810
1QJS	266	HIS	4.484379	HIS	120.9930
6A2J	278	HIS	4.655598	HIS	124.6210
2IPS	351	HIS	4.125792	HIS	94.9759
7C74	351	HIS	4.494179	HIS	92.7950
7DMR	351	HIS	4.201640	HIS	96.7615
4NL5	9	ILE	5.756873	ILE	125.9250
4JET	30	ILE	6.988601	ILE	147.5590
2O6P	48	ILE	5.365972	ILE	141.3220
4B8N	55	ILE	5.758462	ILE	101.7060
2FC2	63	ILE	6.106378	ILE	55.1533
2E2Y	68	ILE	5.517060	ILE	97.7283
3VP5	71	ILE	6.407016	ILE	105.2440
2E2Y	99	ILE	6.130795	ILE	160.7990
2SPL	99	ILE	6.223033	ILE	157.6520
5CN5	99	ILE	6.410362	ILE	160.0190
2E2Y	107	ILE	6.704700	ILE	171.6940
2SPL	107	ILE	6.505472	ILE	170.3470
5CN5	107	ILE	6.767432	ILE	172.1900
4UZV	111	ILE	5.897899	ILE	140.3930
2Q6N	114	ILE	6.560571	ILE	116.0170
2VEB	116	ILE	6.573571	ILE	101.7820
3QZZ	116	ILE	6.472356	ILE	100.9480

Table B.17: HEM: All CA-CB-Fe Angles *(continued)*

PDB_ID	Residue_Number	Residue_Code.x	Mean_Distance	Residue_Code.y	Angle
3ZJS	116	ILE	6.518950	ILE	103.0000
2O6P	121	ILE	6.852081	ILE	132.2050
3SIK	129	ILE	6.189129	ILE	165.5190
3SIK	131	ILE	6.481115	ILE	134.1420
2VEB	137	ILE	6.361213	ILE	179.1050
3QZZ	137	ILE	6.393964	ILE	177.4290
3ZJS	137	ILE	6.315026	ILE	177.5600
2BHJ	195	ILE	6.216303	ILE	54.9628
2FC2	214	ILE	6.545905	ILE	136.6930
5O1L	222	ILE	6.024951	ILE	133.4090
5O1M	222	ILE	6.241067	ILE	136.2240
2IIZ	225	ILE	6.430481	ILE	59.8660
5O1L	227	ILE	6.973430	ILE	87.0131
4CDP	252	ILE	6.178209	ILE	160.7780
2J0P	255	ILE	6.197370	ILE	154.1260
6A2J	265	ILE	6.271826	ILE	147.7330
4MF9	268	ILE	6.092502	ILE	155.0200
2Q6N	363	ILE	6.794813	ILE	150.8430
2Q6N	435	ILE	6.531691	ILE	50.7026
5VEU	442	ILE	6.119535	ILE	59.4678
4I3Q	443	ILE	5.985023	ILE	55.5209
2CJ0	32	LEU	5.757197	LEU	97.6039
2CPO	32	LEU	5.913058	LEU	99.3621
2J18	32	LEU	5.760472	LEU	96.2823
1B5M	46	LEU	5.848737	LEU	104.5310
1ICC	46	LEU	5.941384	LEU	99.3266
1U9U	46	LEU	5.958763	LEU	99.9911
1SY2	57	LEU	6.145372	LEU	142.4070
3MVF	57	LEU	6.242544	LEU	143.0050
3TGC	57	LEU	6.147624	LEU	140.8920
4B8N	70	LEU	6.456250	LEU	123.0540
1B2V	77	LEU	6.429830	LEU	57.1497
1DK0	77	LEU	6.502332	LEU	58.1793
1DKH	77	LEU	6.345588	LEU	66.1552
2CN4	77	LEU	6.548785	LEU	53.5337

Table B.17: HEM: All CA-CB-Fe Angles *(continued)*

PDB_ID	Residue_Number	Residue_Code.x	Mean_Distance	Residue_Code.y	Angle
4UZV	79	LEU	6.352126	LEU	105.2350
2E2Y	89	LEU	6.167984	LEU	89.7887
2SPL	89	LEU	6.446644	LEU	83.4261
5CN5	89	LEU	6.607510	LEU	97.7142
4CDP	90	LEU	6.499175	LEU	152.7650
4UZV	102	LEU	6.801707	LEU	85.2040
2E2Y	104	LEU	6.384225	LEU	87.1682
2SPL	104	LEU	6.518599	LEU	83.9530
5CN5	104	LEU	6.517400	LEU	86.5002
1P3T	119	LEU	6.709401	LEU	90.3174
1SY2	123	LEU	5.902915	LEU	147.6300
3MVF	123	LEU	5.891492	LEU	147.9850
3TGC	123	LEU	5.908675	LEU	148.3100
1SY2	133	LEU	6.241713	LEU	171.7810
3MVF	133	LEU	6.341681	LEU	176.8730
3TGC	133	LEU	6.315080	LEU	175.4300
1N45	138	LEU	6.717099	LEU	68.2659
1VGI	138	LEU	6.110494	LEU	81.0454
2VEB	142	LEU	6.331426	LEU	87.5695
3QZZ	142	LEU	6.534813	LEU	83.8050
3ZJS	142	LEU	6.289922	LEU	80.1179
1N45	147	LEU	6.115862	LEU	123.9670
2R7A	167	LEU	6.508147	LEU	132.6910
5O1L	171	LEU	5.743071	LEU	140.5170
2IIZ	255	LEU	6.075868	LEU	168.3090
2R7A	257	LEU	5.559331	LEU	156.1720
2IIZ	286	LEU	5.566800	LEU	170.9810
2IPS	417	LEU	6.792313	LEU	133.2130
2IPS	433	LEU	5.458537	LEU	130.0630
7C74	433	LEU	5.275537	LEU	124.6650
7DMR	433	LEU	5.225161	LEU	132.7140
2Q6N	437	LEU	5.864970	LEU	72.0648
3VP5	145	LYS	5.832567	LYS	85.9178
5O1M	167	LYS	5.125712	LYS	134.4970
1B2V	140	MET	6.218846	MET	173.7920

Table B.17: HEM: All CA-CB-Fe Angles *(continued)*

PDB_ID	Residue_Number	Residue_Code.x	Mean_Distance	Residue_Code.y	Angle
1DK0	140	MET	6.185917	MET	173.4760
1DKH	140	MET	6.519598	MET	172.2070
2CN4	140	MET	5.816277	MET	172.2930
4JET	147	MET	5.810508	MET	164.8890
4XZD	147	MET	6.297861	MET	157.8890
4Y1Q	147	MET	6.115760	MET	164.0570
4UZV	151	MET	5.908059	MET	159.1620
4CDP	241	MET	6.340896	MET	157.1200
2J0P	244	MET	6.821994	MET	155.7900
4MF9	257	MET	6.826627	MET	151.6460
5VEU	444	MET	6.285199	MET	65.6856
4I3Q	445	MET	5.975507	MET	65.1655
4NL5	23	PHE	5.580423	PHE	91.4353
2SPL	29	PHE	6.129536	PHE	109.5760
1B5M	35	PHE	5.848448	PHE	126.8820
1ICC	35	PHE	6.276818	PHE	121.2740
1U9U	35	PHE	6.094672	PHE	120.9680
2SPL	43	PHE	5.815167	PHE	96.0910
5CN5	43	PHE	5.981197	PHE	99.8337
4B8N	44	PHE	6.120000	PHE	119.7920
4JET	50	PHE	6.875792	PHE	101.1990
4Y1Q	50	PHE	6.555816	PHE	113.8000
4UZV	53	PHE	6.941930	PHE	134.2300
2CJ0	57	PHE	6.484645	PHE	126.1650
2CPO	57	PHE	6.473913	PHE	125.6230
2J18	57	PHE	6.534471	PHE	126.3090
1B5M	58	PHE	6.096500	PHE	85.0021
1ICC	58	PHE	6.182239	PHE	70.5320
4B8N	67	PHE	6.248829	PHE	78.7253
4UZV	67	PHE	5.984317	PHE	105.7360
1SY2	68	PHE	6.098374	PHE	105.5040
3MVF	68	PHE	6.146303	PHE	102.8610
3TGC	68	PHE	6.152796	PHE	103.4820
2VEB	74	PHE	6.405384	PHE	96.7886
3QZZ	74	PHE	6.218919	PHE	94.8642

Table B.17: HEM: All CA-CB-Fe Angles *(continued)*

PDB_ID	Residue_Number	Residue_Code.x	Mean_Distance	Residue_Code.y	Angle
3ZJS	74	PHE	6.270262	PHE	95.7239
3VP5	76	PHE	6.844578	PHE	108.6770
4JET	77	PHE	6.310922	PHE	57.4300
4XZD	77	PHE	6.275751	PHE	57.5972
4Y1Q	77	PHE	6.412846	PHE	49.1641
2VEB	93	PHE	5.810118	PHE	112.4610
3QZZ	93	PHE	6.033470	PHE	111.4380
3ZJS	93	PHE	5.922481	PHE	109.4020
2CJ0	103	PHE	6.182880	PHE	112.2600
2CPO	103	PHE	6.396792	PHE	112.7860
2J18	103	PHE	6.235843	PHE	111.5310
3VP5	112	PHE	6.509162	PHE	98.9329
4UZV	119	PHE	5.820671	PHE	139.8230
1SI8	132	PHE	6.553242	PHE	138.1490
1SI8	140	PHE	5.575451	PHE	139.2170
2VEB	145	PHE	6.211153	PHE	170.3740
3QZZ	145	PHE	6.192963	PHE	171.6250
3ZJS	145	PHE	6.059949	PHE	169.5920
1P3T	181	PHE	5.974488	PHE	104.9100
2CJ0	186	PHE	5.833496	PHE	170.8360
2CPO	186	PHE	5.891089	PHE	173.0070
2J18	186	PHE	5.882819	PHE	174.2510
2J0P	199	PHE	6.468406	PHE	116.5200
1IPH	206	PHE	6.665963	PHE	134.5530
1N45	207	PHE	5.975984	PHE	104.6170
1VGI	207	PHE	6.238995	PHE	106.2160
1IPH	214	PHE	5.767678	PHE	138.4550
2FC2	231	PHE	6.129726	PHE	115.0550
4CDP	243	PHE	5.994465	PHE	125.6670
2J0P	246	PHE	6.155004	PHE	127.9200
2IIZ	257	PHE	5.749045	PHE	119.3170
4MF9	259	PHE	5.680334	PHE	124.8600
7C74	347	PHE	6.478230	PHE	83.5884
7DMR	347	PHE	6.671472	PHE	87.2067
2BHJ	363	PHE	5.980185	PHE	116.4950

Table B.17: HEM: All CA-CB-Fe Angles *(continued)*

PDB_ID	Residue_Number	Residue_Code.x	Mean_Distance	Residue_Code.y	Angle
2Q6N	429	PHE	6.192258	PHE	80.7723
5VEU	434	PHE	6.084164	PHE	82.5712
4I3Q	435	PHE	6.161681	PHE	83.4925
1ZVI	584	PHE	6.009975	PHE	116.6380
2CJ0	28	PRO	6.127671	PRO	76.4322
2CPO	28	PRO	6.018197	PRO	69.8826
2J18	28	PRO	6.103023	PRO	75.1381
2CJ0	30	PRO	5.960531	PRO	65.8824
2CPO	30	PRO	6.017188	PRO	65.4937
2J18	30	PRO	5.936382	PRO	66.0535
1B5M	40	PRO	6.032548	PRO	84.9302
1ICC	40	PRO	6.016737	PRO	84.5709
1U9U	40	PRO	6.149502	PRO	87.3619
4B8N	49	PRO	6.182011	PRO	79.7519
1SI8	315	PRO	6.539721	PRO	121.9570
1IPH	393	PRO	6.703993	PRO	126.7810
2Q6N	428	PRO	6.945175	PRO	74.9040
5VEU	433	PRO	6.574196	PRO	65.9573
4I3Q	434	PRO	6.893037	PRO	69.3456
1B2V	42	SER	6.443386	SER	82.8367
1DK0	42	SER	6.540219	SER	80.4760
1DKH	42	SER	6.070312	SER	32.8371
2FC2	59	SER	6.581787	SER	146.0560
2E2Y	92	SER	6.454585	SER	115.2050
2SPL	92	SER	6.650791	SER	113.0460
5CN5	92	SER	6.529632	SER	111.5180
1P3T	117	SER	5.531584	SER	57.1608
1N45	142	SER	6.525024	SER	110.0660
1VGI	142	SER	5.700272	SER	125.4790
4MYP	205	SER	6.655356	SER	154.8290
6A2J	261	SER	6.949581	SER	84.4336
1QHU	266	SER	6.680148	SER	59.3970
1QJS	267	SER	6.730283	SER	71.5751
1IPH	414	SER	6.728176	SER	141.7910
1DK0	33	THR	6.991008	THR	13.7171

Table B.17: HEM: All CA-CB-Fe Angles *(continued)*

PDB_ID	Residue_Number	Residue_Code.x	Mean_Distance	Residue_Code.y	Angle
2R7A	52	THR	5.945515	THR	116.2990
2E2Y	67	THR	6.891096	THR	106.0790
3VP5	68	THR	6.164947	THR	105.7800
4XZD	82	THR	6.830323	THR	18.2203
1B2V	84	THR	6.798527	THR	18.8827
1DK0	84	THR	6.799510	THR	19.3165
1DKH	84	THR	6.267175	THR	31.3703
2CN4	84	THR	6.804573	THR	19.9645
1SY2	121	THR	6.333312	THR	142.1010
3MVF	121	THR	6.595150	THR	151.0630
3TGC	121	THR	6.343084	THR	149.1780
3VP5	130	THR	5.980868	THR	115.4180
1N45	135	THR	6.713859	THR	60.4070
1VGI	135	THR	6.883314	THR	58.3823
5O1M	168	THR	6.373467	THR	85.9567
6A2J	178	THR	6.772182	THR	86.8748
5O1L	194	THR	6.305648	THR	104.6020
5O1M	194	THR	6.409916	THR	101.5220
4MF9	208	THR	6.202558	THR	107.1870
5O1L	230	THR	6.574103	THR	168.0670
5O1M	230	THR	6.603918	THR	174.9180
2Q6N	302	THR	5.748396	THR	151.7240
4I3Q	309	THR	6.214341	THR	172.7070
5VEU	309	THR	5.895842	THR	174.8590
2E2Y	43	TRP	5.845537	TRP	95.5213
2FC2	56	TRP	5.737975	TRP	91.6643
3QZZ	60	TRP	6.491833	TRP	126.4880
3ZJS	60	TRP	6.366999	TRP	127.6490
4NL5	66	TRP	6.235302	TRP	112.7010
2R7A	68	TRP	6.192116	TRP	91.3335
1QHU	171	TRP	6.147194	TRP	135.3190
1QJS	171	TRP	6.211700	TRP	138.2760
2VEB	185	TRP	5.717992	TRP	165.6030
3QZZ	185	TRP	6.111800	TRP	156.0610
3ZJS	185	TRP	5.960798	TRP	163.3900

Table B.17: HEM: All CA-CB-Fe Angles *(continued)*

PDB_ID	Residue_Number	Residue_Code.x	Mean_Distance	Residue_Code.y	Angle
2BHJ	188	TRP	6.049049	TRP	95.4808
2CJ0	213	TRP	6.764355	TRP	116.4780
2J18	213	TRP	6.782850	TRP	117.0960
2FC2	234	TRP	6.837576	TRP	40.3488
1QHU	267	TRP	5.987630	TRP	70.5501
1QJS	268	TRP	6.230710	TRP	64.5387
2BHJ	366	TRP	6.764735	TRP	39.6654
1ZVI	409	TRP	5.660275	TRP	90.9270
1ZVI	587	TRP	6.843603	TRP	40.2585
1SY2	40	TYR	5.887937	TYR	145.2220
3MVF	40	TYR	6.759408	TYR	155.4560
3TGC	40	TYR	5.967215	TYR	142.7160
2O6P	52	TYR	6.682161	TYR	136.9010
2CN4	55	TYR	6.806239	TYR	136.9090
4JET	55	TYR	6.877273	TYR	128.1770
4XZD	55	TYR	6.821652	TYR	129.5380
4Y1Q	55	TYR	6.699820	TYR	130.2460
1SY2	58	TYR	6.964531	TYR	29.9485
1U9U	58	TYR	6.232812	TYR	75.1903
3ZJS	61	TYR	6.548411	TYR	78.2808
2R7A	67	TYR	4.159993	TYR	116.4820
1B2V	75	TYR	4.251885	TYR	132.4540
1DK0	75	TYR	4.346840	TYR	131.4420
1DKH	75	TYR	4.792830	TYR	125.4210
2CN4	75	TYR	4.345054	TYR	126.9230
4JET	75	TYR	4.420106	TYR	129.0130
4XZD	75	TYR	4.329954	TYR	127.5350
3VP5	91	TYR	6.574739	TYR	135.6840
2O6P	132	TYR	4.055037	TYR	132.9670
2O6P	136	TYR	5.148558	TYR	145.4090
3SIK	136	TYR	4.260470	TYR	131.7390
1B2V	137	TYR	6.232518	TYR	107.0750
1DK0	137	TYR	6.186950	TYR	107.9930
1DKH	137	TYR	6.409147	TYR	103.9420
2CN4	137	TYR	6.142879	TYR	102.8860

Table B.17: HEM: All CA-CB-Fe Angles *(continued)*

PDB_ID	Residue_Number	Residue_Code.x	Mean_Distance	Residue_Code.y	Angle
3SIK	140	TYR	5.120136	TYR	140.8870
1QHU	204	TYR	6.239544	TYR	82.8848
1QJS	204	TYR	6.225721	TYR	82.0806
4MYP	280	TYR	4.465249	TYR	129.7640
4MYP	289	TYR	5.900895	TYR	133.7170
1SI8	337	TYR	3.976560	TYR	101.8400
1IPH	415	TYR	4.218561	TYR	114.2710
1P3T	26	VAL	6.716946	VAL	118.5490
1SY2	36	VAL	6.479806	VAL	130.3660
3TGC	36	VAL	6.135653	VAL	128.7560
1B2V	37	VAL	5.425221	VAL	150.5390
1DK0	37	VAL	5.400636	VAL	154.2260
1DKH	37	VAL	5.642973	VAL	149.8520
1B5M	45	VAL	5.846522	VAL	132.2220
1ICC	45	VAL	5.992035	VAL	128.6010
1U9U	45	VAL	6.500194	VAL	133.1230
1SI8	53	VAL	6.238869	VAL	132.7600
4NL5	53	VAL	5.909472	VAL	175.0330
1B5M	61	VAL	6.074911	VAL	142.4900
1ICC	61	VAL	5.726742	VAL	157.5600
1U9U	61	VAL	6.163696	VAL	152.2510
2SPL	68	VAL	5.598014	VAL	111.2660
5CN5	68	VAL	5.556498	VAL	104.0070
4B8N	75	VAL	6.033658	VAL	149.8530
2VEB	89	VAL	5.917494	VAL	126.3020
3QZZ	89	VAL	5.927268	VAL	128.6650
3ZJS	89	VAL	5.790982	VAL	125.8290
2O6P	119	VAL	6.176593	VAL	171.6540
1SI8	125	VAL	6.016899	VAL	127.3950
1IPH	127	VAL	6.256166	VAL	129.5510
3VP5	131	VAL	5.568423	VAL	118.6510
3VP5	148	VAL	6.888565	VAL	110.6600
5O1L	152	VAL	6.293389	VAL	97.5310
5O1M	152	VAL	6.250877	VAL	96.3132
6A2J	175	VAL	6.202413	VAL	96.8786

Table B.17: HEM: All CA-CB-Fe Angles *(continued)*

PDB_ID	Residue_Number	Residue_Code.x	Mean_Distance	Residue_Code.y	Angle
6A2J	182	VAL	6.679490	VAL	146.8970
4CDP	192	VAL	5.600764	VAL	109.6320
2J0P	195	VAL	6.307524	VAL	111.4460
5O1L	197	VAL	6.648164	VAL	117.0650
5O1M	197	VAL	6.631076	VAL	113.6940
1IPH	199	VAL	6.294207	VAL	124.0950
2IIZ	228	VAL	5.315815	VAL	165.2710
2BHJ	346	VAL	6.643571	VAL	125.1020
2IPS	354	VAL	6.655642	VAL	133.4880
5VEU	369	VAL	6.886497	VAL	120.7080
1ZVI	416	VAL	5.960795	VAL	55.0798

Table B.18: HEC: All CA-CB-Fe Angles

PDB_ID	Residue_Number	Residue_Code.x	Mean_Distance	Residue_Code.y	Angle
5KPF	81	ALA	6.517051	ALA	45.2733
5LFT	81	ALA	6.400723	ALA	49.6961
5T8W	81	ALA	6.484127	ALA	46.8814
3EAH	147	ALA	6.240842	ALA	152.0380
2BC5	106	ARG	5.961420	ARG	119.2950
6WZA	106	ARG	6.631682	ARG	132.5260
1BBH	129	ARG	5.790808	ARG	148.1750
3EAH	149	ARG	5.803314	ARG	75.1674
3EAH	153	ARG	6.514542	ARG	70.9288
2BC5	99	ASN	6.936196	ASN	26.5703
3X15	12	CYS	6.451594	CYS	87.5164
5KPF	14	CYS	6.631432	CYS	91.6899
5LFT	14	CYS	6.598389	CYS	89.7859
5T8W	14	CYS	6.647516	CYS	89.3990
6XNK	14	CYS	6.275930	CYS	94.7801
2BH5	15	CYS	6.513509	CYS	93.4388

Table B.18: HEC: All CA-CB-Fe Angles *(continued)*

PDB_ID	Residue_Number	Residue_Code.x	Mean_Distance	Residue_Code.y	Angle
3X15	15	CYS	6.178945	CYS	124.5130
5KPF	17	CYS	6.098545	CYS	128.9880
5LFT	17	CYS	6.056595	CYS	131.2330
5T8W	17	CYS	6.188739	CYS	130.6870
6XNK	17	CYS	5.903640	CYS	129.1390
1W2L	18	CYS	6.554906	CYS	83.0319
2BH5	18	CYS	6.369197	CYS	129.9250
1W2L	21	CYS	6.223591	CYS	129.4480
2BC5	98	CYS	5.957326	CYS	83.1994
6WZA	98	CYS	5.774303	CYS	89.2313
2BC5	101	CYS	6.394766	CYS	122.7380
6WZA	101	CYS	6.455707	CYS	120.0850
1BBH	121	CYS	5.737156	CYS	88.6062
1BBH	124	CYS	6.272059	CYS	118.4660
3EAH	150	CYS	4.247423	CYS	109.9070
6VDQ	317	CYS	6.231170	CYS	153.4870
1S56	58	GLN	6.005777	GLN	114.9080
1BBH	17	GLU	6.940695	GLU	46.8470
3X15	16	HIS	4.360557	HIS	123.2520
5KPF	18	HIS	4.310334	HIS	121.8690
5LFT	18	HIS	4.342999	HIS	122.5120
5T8W	18	HIS	4.334295	HIS	122.3910
6XNK	18	HIS	4.599701	HIS	122.1970
2BH5	19	HIS	4.283790	HIS	122.4230
1W2L	22	HIS	4.350769	HIS	122.1140
1S56	81	HIS	4.475028	HIS	112.6780
2BC5	102	HIS	4.186908	HIS	96.2948
6WZA	102	HIS	4.440577	HIS	93.6577
1BBH	125	HIS	4.218890	HIS	95.2502
6VDQ	274	HIS	4.500421	HIS	121.1700
6VDQ	313	HIS	4.120545	HIS	123.2950
3X15	30	ILE	6.412845	ILE	143.9220
1W2L	61	ILE	6.839545	ILE	64.6202
6XNK	75	ILE	6.412701	ILE	119.2950
1S56	86	ILE	5.878780	ILE	163.7880

Table B.18: HEC: All CA-CB-Fe Angles *(continued)*

PDB_ID	Residue_Number	Residue_Code.x	Mean_Distance	Residue_Code.y	Angle
6VDQ	278	ILE	5.358791	ILE	112.0200
2BC5	3	LEU	6.742954	LEU	93.4646
6WZA	3	LEU	6.697674	LEU	97.4908
2BC5	10	LEU	6.154091	LEU	145.5220
6WZA	10	LEU	6.067786	LEU	145.9270
5KPF	32	LEU	6.145036	LEU	120.1710
5LFT	32	LEU	6.106815	LEU	122.2640
5T8W	32	LEU	5.994375	LEU	121.4370
6XNK	32	LEU	6.085909	LEU	119.5620
2BH5	39	LEU	5.728784	LEU	123.5750
1S56	54	LEU	5.947501	LEU	117.0640
5KPF	68	LEU	6.268124	LEU	84.1501
5LFT	68	LEU	6.315525	LEU	85.1852
5T8W	68	LEU	6.123569	LEU	85.5580
6VDQ	238	LEU	6.409586	LEU	130.4750
6VDQ	277	LEU	6.506868	LEU	130.8480
6XNK	79	LYS	3.938274	LYS	132.9060
2BH5	100	LYS	4.313747	LYS	174.4600
2BC5	7	MET	4.661903	MET	112.0730
6WZA	7	MET	4.611608	MET	112.1700
1BBH	19	MET	6.049470	MET	132.1620
1W2L	76	MET	4.403618	MET	95.5351
1S56	77	MET	6.187616	MET	79.9304
5KPF	80	MET	4.692154	MET	126.7040
5LFT	80	MET	4.757864	MET	124.0680
5T8W	80	MET	4.693021	MET	126.3770
1W2L	34	PHE	5.935685	PHE	94.2433
3X15	44	PHE	6.024333	PHE	118.7300
1S56	46	PHE	5.938368	PHE	100.7840
2BC5	65	PHE	6.201901	PHE	87.4034
6WZA	65	PHE	6.184290	PHE	90.1118
5KPF	82	PHE	6.311357	PHE	145.9170
5LFT	82	PHE	6.466458	PHE	143.5030
5T8W	82	PHE	6.527249	PHE	141.0090
2BH5	102	PHE	6.736126	PHE	125.9060

Table B.18: HEC: All CA-CB-Fe Angles *(continued)*

PDB_ID	Residue_Number	Residue_Code.x	Mean_Distance	Residue_Code.y	Angle
3EAH	319	PHE	6.137327	PHE	117.8130
6VDQ	320	PHE	6.121894	PHE	123.1650
3X15	25	PRO	6.252857	PRO	84.9462
5KPF	30	PRO	6.184028	PRO	77.6163
5LFT	30	PRO	6.179273	PRO	78.6390
5T8W	30	PRO	6.138272	PRO	79.9221
6XNK	30	PRO	5.900245	PRO	78.3181
1W2L	32	PRO	6.457693	PRO	80.5165
2BH5	37	PRO	6.202537	PRO	77.9642
5KPF	71	PRO	6.976183	PRO	151.2390
5LFT	71	PRO	6.983064	PRO	154.1260
5T8W	71	PRO	6.909375	PRO	148.7700
1W2L	77	PRO	6.071845	PRO	84.7339
2BH5	83	PRO	6.953188	PRO	141.6410
1W2L	60	SER	6.470812	SER	107.3410
6XNK	28	THR	6.983672	THR	95.9136
6VDQ	309	THR	6.443589	THR	99.5431
3EAH	144	TRP	5.647844	TRP	91.6868
6VDQ	271	TRP	5.880644	TRP	138.8540
3EAH	322	TRP	6.529256	TRP	42.5273
1BBH	16	TYR	4.795494	TYR	126.0380
1S56	33	TYR	6.252015	TYR	98.2768
1BBH	58	TYR	6.554347	TYR	118.4030
5KPF	67	TYR	5.922923	TYR	117.3570
5LFT	67	TYR	5.919346	TYR	117.9010
5T8W	67	TYR	5.858639	TYR	116.3210
6XNK	67	TYR	5.613420	TYR	126.9700
2BH5	79	TYR	5.535216	TYR	107.5970
1W2L	80	TYR	6.249808	TYR	159.9880
6VDQ	310	TYR	6.768220	TYR	57.7313
1W2L	75	VAL	6.753821	VAL	68.5700
1S56	80	VAL	6.205932	VAL	122.1110
2BH5	80	VAL	6.887770	VAL	86.0062
6XNK	83	VAL	6.004096	VAL	114.6820
1S56	94	VAL	6.626107	VAL	156.6730

Table B.18: HEC: All CA-CB-Fe Angles *(continued)*

PDB_ID	Residue_Number	Residue_Code.x	Mean_Distance	Residue_Code.y	Angle
1S56	126	VAL	6.029592	VAL	116.6120
3EAH	151	VAL	6.103944	VAL	58.7518

Table B.19: SRM: All CA-CB-Fe Angles

PDB_ID	Residue_Number	Residue_Code.x	Mean_Distance	Residue_Code.y	Angle
1ZJ8	468	ALA	6.774896	ALA	54.3434
3B0G	486	ALA	6.469408	ALA	52.3271
3VKP	486	ALA	6.471195	ALA	52.9419
3VLX	486	ALA	6.481752	ALA	51.8739
3VLY	486	ALA	6.503895	ALA	51.7331
3VLZ	486	ALA	6.507235	ALA	53.7924
5H8V	545	ALA	6.528336	ALA	49.2614
2AOP	83	ARG	5.905472	ARG	162.1930
1ZJ8	97	ARG	5.632921	ARG	148.8370
2AKJ	109	ARG	5.624044	ARG	148.4620
3B0G	109	ARG	5.714505	ARG	157.7590
3VKP	109	ARG	5.727950	ARG	159.0060
3VLX	109	ARG	5.657293	ARG	157.8390
3VLY	109	ARG	5.670401	ARG	156.2520
3VLZ	109	ARG	5.666461	ARG	159.7330
5H8V	124	ARG	5.731236	ARG	158.1950
2AOP	153	ARG	6.898322	ARG	144.7120
1ZJ8	166	ARG	6.411696	ARG	157.1260
2AKJ	179	ARG	6.270969	ARG	150.8160
3B0G	179	ARG	6.332302	ARG	150.2730
3VKP	179	ARG	6.261289	ARG	149.5410
3VLX	179	ARG	6.332845	ARG	148.5140
3VLY	179	ARG	6.349458	ARG	149.9780
3VLZ	179	ARG	6.432708	ARG	147.1060
5H8V	193	ARG	6.748373	ARG	152.0550

Table B.19: SRM: All CA-CB-Fe Angles *(continued)*

PDB_ID	Residue_Number	Residue_Code.x	Mean_Distance	Residue_Code.y	Angle
2AOP	116	ASN	6.627004	ASN	95.1407
1ZJ8	465	ASN	6.589731	ASN	126.9150
2AOP	481	ASN	6.568014	ASN	121.7600
3B0G	483	ASN	6.105308	ASN	124.8060
3VKP	483	ASN	6.093849	ASN	125.9350
3VLX	483	ASN	6.149563	ASN	124.5220
3VLY	483	ASN	6.199685	ASN	124.0840
3VLZ	483	ASN	6.172324	ASN	122.9020
2AKJ	484	ASN	6.180565	ASN	125.4620
5H8V	542	ASN	6.517505	ASN	120.9920
1ZJ8	129	ASP	6.873987	ASP	96.5485
1ZJ8	467	CYS	4.642760	CYS	106.8380
2AOP	483	CYS	4.593058	CYS	115.6650
3B0G	485	CYS	4.334547	CYS	114.2180
3VKP	485	CYS	4.338921	CYS	113.1560
3VLX	485	CYS	4.333556	CYS	112.7580
3VLY	485	CYS	4.349260	CYS	114.5360
3VLZ	485	CYS	4.361247	CYS	115.6310
2AKJ	486	CYS	4.400598	CYS	106.3630
5H8V	494	CYS	6.918908	CYS	129.0520
5H8V	544	CYS	4.294361	CYS	112.4810
2AOP	121	GLN	6.832109	GLN	146.9480
1ZJ8	134	GLN	6.870508	GLN	147.3840
5H8V	161	GLN	6.725078	GLN	141.5670
1ZJ8	207	LYS	5.279599	LYS	172.2200
1ZJ8	209	LYS	5.254105	LYS	132.2160
2AOP	215	LYS	5.521547	LYS	157.3800
2AOP	217	LYS	5.485034	LYS	135.7480
2AKJ	224	LYS	5.292960	LYS	179.3020
3B0G	224	LYS	5.579947	LYS	175.7930
3VKP	224	LYS	5.500133	LYS	175.8260
3VLX	224	LYS	5.605021	LYS	177.4260
3VLY	224	LYS	5.637976	LYS	177.5250
3VLZ	224	LYS	5.601385	LYS	175.4720
3VLY	226	LYS	5.485627	LYS	132.6280

Table B.19: SRM: All CA-CB-Fe Angles *(continued)*

PDB_ID	Residue_Number	Residue_Code.x	Mean_Distance	Residue_Code.y	Angle
3VLZ	226	LYS	5.641233	LYS	129.8350
5H8V	276	LYS	5.805329	LYS	174.1460
5H8V	278	LYS	5.495851	LYS	140.5820
1ZJ8	466	SER	6.539429	SER	46.1914
2AKJ	485	SER	6.504302	SER	45.1203
2AKJ	142	THR	6.814343	THR	112.5850
3B0G	142	THR	6.442796	THR	114.5110
3VKP	142	THR	6.428882	THR	114.3200
3VLX	142	THR	6.455248	THR	113.9840
3VLY	142	THR	6.452740	THR	113.0910
3VLZ	142	THR	6.394057	THR	112.9370
5H8V	156	THR	6.490994	THR	114.0040
3B0G	484	THR	6.402854	THR	31.8530
3VKP	484	THR	6.412766	THR	32.2678
3VLX	484	THR	6.401875	THR	31.6972
3VLY	484	THR	6.414362	THR	32.6034
3VLZ	484	THR	6.437540	THR	35.4494
1ZJ8	69	TYR	6.963349	TYR	168.2380
5H8V	106	TYR	6.992106	TYR	153.7720

Table B.20: VERDOHEME: All CA-CB-Fe Angles

PDB_ID	Residue_Number	Residue_Code.x	Mean_Distance	Residue_Code.y	Angle
2ZVU	28	ALA	6.962159	ALA	120.0970
3MOO	136	ASP	6.778611	ASP	23.6316
2ZVU	140	ASP	6.674210	ASP	26.6732
3MOO	24	GLU	6.275511	GLU	110.6430
2ZVU	29	GLU	6.221641	GLU	117.2590
3MOO	20	HIS	4.614778	HIS	111.0890
2ZVU	25	HIS	4.603252	HIS	110.7510
3MOO	134	LEU	6.100073	LEU	77.1733

Table B.20: VERDOHEME: All CA-CB-Fe Angles *(continued)*

PDB_ID	Residue_Number	Residue_Code.x	Mean_Distance	Residue_Code.y	Angle
2ZVU	138	LEU	6.249768	LEU	76.7687
3MOO	201	PHE	5.958999	PHE	104.2170
2ZVU	207	PHE	6.037412	PHE	105.4400
3MOO	138	SER	5.886820	SER	125.3120
2ZVU	142	SER	6.048311	SER	126.2110
2ZVU	135	THR	6.765195	THR	58.6713
3MOO	131	VAL	6.796515	VAL	60.1702
1TWN	140	ASP	6.273979	ASP	27.4847
1TWR	140	ASP	6.553790	ASP	27.4184
1TWN	29	GLU	6.123574	GLU	100.1730
1TWR	29	GLU	6.517157	GLU	103.1100
1TWN	25	HIS	4.673370	HIS	113.5160
1TWR	25	HIS	4.786588	HIS	108.8640
1TWN	138	LEU	6.399559	LEU	75.1317
1TWR	138	LEU	6.579770	LEU	75.0669
1TWN	207	PHE	6.263716	PHE	105.9700
1TWR	207	PHE	6.447849	PHE	107.0750
1TWN	142	SER	6.035867	SER	114.7150
1TWR	142	SER	6.195017	SER	129.2760
1TWN	135	THR	6.865192	THR	60.8151

B.6 CA-CB-Fe Angles of Closest Residues

Table B.21: HEM: CA-CB-Fe Angles of Closest Residues

PDB_ID	Residue_Number	Residue_Code.x	Mean_Distance	Residue_Code.y	Angle
1B2V	75	TYR	4.251885	TYR	132.4540
1B2V	32	HIS	4.667618	HIS	116.3150
1B2V	83	HIS	5.366599	HIS	102.9160
1B5M	63	HIS	4.211990	HIS	125.8380
1B5M	39	HIS	4.456809	HIS	101.8130

Table B.21: HEM: CA-CB-Fe Angles of Closest Residues *(continued)*

PDB_ID	Residue_Number	Residue_Code.x	Mean_Distance	Residue_Code.y	Angle
1DK0	75	TYR	4.346840	TYR	131.4420
1DK0	32	HIS	4.556145	HIS	116.4470
1DK0	83	HIS	5.314133	HIS	102.7520
1DKH	75	TYR	4.792830	TYR	125.4210
1DKH	32	HIS	5.099382	HIS	121.3750
1DKH	83	HIS	5.223800	HIS	122.9600
1ICC	63	HIS	4.451283	HIS	114.1290
1ICC	39	HIS	4.542187	HIS	101.5070
1IPH	415	TYR	4.218561	TYR	114.2710
1IPH	411	ARG	5.321024	ARG	108.2630
1IPH	128	HIS	5.713777	HIS	129.2180
1N45	25	HIS	4.545004	HIS	112.7600
1P3T	23	HIS	4.573926	HIS	111.7580
1P3T	117	SER	5.531584	SER	57.1608
1QHU	265	HIS	4.200094	HIS	121.1810
1QHU	213	HIS	4.734866	HIS	114.5350
1QHU	267	TRP	5.987630	TRP	70.5501
1QJS	266	HIS	4.484379	HIS	120.9930
1QJS	213	HIS	4.696712	HIS	122.0930
1QJS	171	TRP	6.211700	TRP	138.2760
1SI8	337	TYR	3.976560	TYR	101.8400
1SI8	333	ARG	5.247624	ARG	116.1170
1SI8	140	PHE	5.575451	PHE	139.2170
1SY2	59	HIS	4.045387	HIS	126.3700
1SY2	40	TYR	5.887937	TYR	145.2220
1SY2	123	LEU	5.902915	LEU	147.6300
1U9U	63	HIS	4.417873	HIS	116.0130
1U9U	39	HIS	4.589294	HIS	102.2750
1VGI	25	HIS	4.646180	HIS	113.1630
1ZVI	415	CYS	4.181834	CYS	112.7440
1ZVI	409	TRP	5.660275	TRP	90.9270
2BHJ	194	CYS	4.487497	CYS	118.0500
2BHJ	193	ARG	5.745098	ARG	61.6429
2CJ0	29	CYS	4.390905	CYS	117.5660
2CJ0	31	ALA	5.440871	ALA	114.8710

Table B.21: HEM: CA-CB-Fe Angles of Closest Residues *(continued)*

PDB_ID	Residue_Number	Residue_Code.x	Mean_Distance	Residue_Code.y	Angle
2CJ0	183	GLU	5.716050	GLU	106.0810
2CN4	75	TYR	4.345054	TYR	126.9230
2CN4	83	HIS	5.251875	HIS	107.5140
2CN4	140	MET	5.816277	MET	172.2930
2CPO	29	CYS	4.443549	CYS	118.1890
2CPO	31	ALA	5.505123	ALA	115.0400
2CPO	183	GLU	5.799506	GLU	105.9460
2E2Y	93	HIS	4.514535	HIS	114.4980
2E2Y	68	ILE	5.517060	ILE	97.7283
2E2Y	43	TRP	5.845537	TRP	95.5213
2FC2	62	CYS	4.482879	CYS	112.5820
2FC2	56	TRP	5.737975	TRP	91.6643
2IIZ	224	HIS	4.533607	HIS	124.3380
2IIZ	242	ARG	5.236889	ARG	162.0190
2IIZ	228	VAL	5.315815	VAL	165.2710
2IPS	351	HIS	4.125792	HIS	94.9759
2IPS	433	LEU	5.458537	LEU	130.0630
2IPS	108	ASP	5.870986	ASP	152.6010
2J0P	196	HIS	4.310325	HIS	111.1620
2J0P	102	ARG	5.002395	ARG	139.6090
2J0P	246	PHE	6.155004	PHE	127.9200
2J18	29	CYS	4.359887	CYS	118.4250
2J18	31	ALA	5.457126	ALA	114.2550
2J18	183	GLU	5.722472	GLU	107.1960
2O6P	132	TYR	4.055037	TYR	132.9670
2O6P	136	TYR	5.148558	TYR	145.4090
2O6P	48	ILE	5.365972	ILE	141.3220
2Q6N	436	CYS	4.305637	CYS	109.8240
2Q6N	298	ALA	5.672036	ALA	129.8410
2R7A	67	TYR	4.159993	TYR	116.4820
2R7A	169	ALA	5.223004	ALA	132.6020
2R7A	257	LEU	5.559331	LEU	156.1720
2SPL	93	HIS	4.578545	HIS	112.4730
2SPL	68	VAL	5.598014	VAL	111.2660
2SPL	43	PHE	5.815167	PHE	96.0910

Table B.21: HEM: CA-CB-Fe Angles of Closest Residues *(continued)*

PDB_ID	Residue_Number	Residue_Code.x	Mean_Distance	Residue_Code.y	Angle
2VEB	120	HIS	4.471709	HIS	110.4880
2VEB	185	TRP	5.717992	TRP	165.6030
2VEB	93	PHE	5.810118	PHE	112.4610
3MVF	59	HIS	4.066882	HIS	126.0770
3MVF	42	ALA	5.827660	ALA	147.3790
3MVF	123	LEU	5.891492	LEU	147.9850
3QZZ	120	HIS	4.599066	HIS	109.3460
3QZZ	89	VAL	5.927268	VAL	128.6650
3QZZ	93	PHE	6.033470	PHE	111.4380
3SIK	136	TYR	4.260470	TYR	131.7390
3SIK	140	TYR	5.120136	TYR	140.8870
3SIK	54	ARG	6.090293	ARG	163.0460
3TGC	59	HIS	4.100823	HIS	124.3700
3TGC	123	LEU	5.908675	LEU	148.3100
3TGC	40	TYR	5.967215	TYR	142.7160
3VP5	149	HIS	4.350835	HIS	100.8200
3VP5	72	HIS	4.371971	HIS	101.6570
3VP5	131	VAL	5.568423	VAL	118.6510
3ZJS	120	HIS	4.427156	HIS	110.7000
3ZJS	89	VAL	5.790982	VAL	125.8290
3ZJS	93	PHE	5.922481	PHE	109.4020
4B8N	71	HIS	4.416116	HIS	119.3920
4B8N	48	HIS	4.479396	HIS	104.9040
4CDP	193	HIS	4.417630	HIS	109.7720
4CDP	100	ARG	5.360373	ARG	139.0430
4CDP	192	VAL	5.600764	VAL	109.6320
4I3Q	442	CYS	4.085782	CYS	103.9950
4I3Q	305	ALA	5.305272	ALA	115.6050
4JET	75	TYR	4.420106	TYR	129.0130
4JET	81	HIS	5.381133	HIS	121.2740
4JET	40	ARG	5.660400	ARG	117.6700
4MF9	209	HIS	4.606487	HIS	108.6490
4MF9	112	ARG	5.056393	ARG	134.9890
4MF9	259	PHE	5.680334	PHE	124.8600
4MYP	280	TYR	4.465249	TYR	129.7640

Table B.21: HEM: CA-CB-Fe Angles of Closest Residues *(continued)*

PDB_ID	Residue_Number	Residue_Code.x	Mean_Distance	Residue_Code.y	Angle
4MYP	289	TYR	5.900895	TYR	133.7170
4MYP	293	ALA	6.207799	ALA	133.2580
4NL5	75	HIS	4.473936	HIS	117.7090
4NL5	7	ASN	5.402231	ASN	170.5520
4NL5	23	PHE	5.580423	PHE	91.4353
4UZV	106	HIS	4.502311	HIS	110.2430
4UZV	119	PHE	5.820671	PHE	139.8230
4UZV	111	ILE	5.897899	ILE	140.3930
4XZD	75	TYR	4.329954	TYR	127.5350
4XZD	81	HIS	5.263108	HIS	114.4420
4XZD	40	ARG	5.892195	ARG	118.8830
4Y1Q	81	HIS	5.294289	HIS	126.8310
4Y1Q	40	ARG	5.725205	ARG	121.1480
4Y1Q	147	MET	6.115760	MET	164.0570
5CN5	93	HIS	4.575365	HIS	113.1870
5CN5	68	VAL	5.556498	VAL	104.0070
5CN5	64	HIS	5.804727	HIS	107.1420
5O1L	198	HIS	4.305405	HIS	102.4410
5O1L	171	LEU	5.743071	LEU	140.5170
5O1L	222	ILE	6.024951	ILE	133.4090
5O1M	198	HIS	4.392715	HIS	100.3070
5O1M	167	LYS	5.125712	LYS	134.4970
5O1M	222	ILE	6.241067	ILE	136.2240
5VEU	441	CYS	4.349464	CYS	106.7690
5VEU	309	THR	5.895842	THR	174.8590
6A2J	216	HIS	4.601722	HIS	122.2890
6A2J	278	HIS	4.655598	HIS	124.6210
7C74	351	HIS	4.494179	HIS	92.7950
7C74	433	LEU	5.275537	LEU	124.6650
7C74	105	GLN	5.667218	GLN	97.8161
7DMR	351	HIS	4.201640	HIS	96.7615
7DMR	433	LEU	5.225161	LEU	132.7140
7DMR	105	GLN	5.517249	GLN	100.6130

Table B.22: HEC: CA-CB-Fe Angles of Closest Residues

PDB_ID	Residue_Number	Residue_Code.x	Mean_Distance	Residue_Code.y	Angle
1BBH	125	HIS	4.218890	HIS	95.2502
1BBH	16	TYR	4.795494	TYR	126.0380
1BBH	121	CYS	5.737156	CYS	88.6062
1S56	81	HIS	4.475028	HIS	112.6780
1S56	86	ILE	5.878780	ILE	163.7880
1S56	46	PHE	5.938368	PHE	100.7840
1W2L	22	HIS	4.350769	HIS	122.1140
1W2L	76	MET	4.403618	MET	95.5351
1W2L	34	PHE	5.935685	PHE	94.2433
2BC5	102	HIS	4.186908	HIS	96.2948
2BC5	7	MET	4.661903	MET	112.0730
2BC5	98	CYS	5.957326	CYS	83.1994
2BH5	19	HIS	4.283790	HIS	122.4230
2BH5	100	LYS	4.313747	LYS	174.4600
2BH5	79	TYR	5.535216	TYR	107.5970
3EAH	150	CYS	4.247423	CYS	109.9070
3EAH	144	TRP	5.647844	TRP	91.6868
3X15	16	HIS	4.360557	HIS	123.2520
3X15	44	PHE	6.024333	PHE	118.7300
3X15	15	CYS	6.178945	CYS	124.5130
5KPF	18	HIS	4.310334	HIS	121.8690
5KPF	80	MET	4.692154	MET	126.7040
5KPF	67	TYR	5.922923	TYR	117.3570
5LFT	18	HIS	4.342999	HIS	122.5120
5LFT	80	MET	4.757864	MET	124.0680
5LFT	67	TYR	5.919346	TYR	117.9010
5T8W	18	HIS	4.334295	HIS	122.3910
5T8W	80	MET	4.693021	MET	126.3770
5T8W	67	TYR	5.858639	TYR	116.3210
6VDQ	313	HIS	4.120545	HIS	123.2950
6VDQ	274	HIS	4.500421	HIS	121.1700
6VDQ	278	ILE	5.358791	ILE	112.0200
6WZA	102	HIS	4.440577	HIS	93.6577
6WZA	7	MET	4.611608	MET	112.1700
6WZA	98	CYS	5.774303	CYS	89.2313

Table B.22: HEC: CA-CB-Fe Angles of Closest Residues *(continued)*

PDB_ID	Residue_Number	Residue_Code.x	Mean_Distance	Residue_Code.y	Angle
6XNK	79	LYS	3.938274	LYS	132.9060
6XNK	18	HIS	4.599701	HIS	122.1970
6XNK	67	TYR	5.613420	TYR	126.9700

Table B.23: SRM: CA-CB-Fe Angles of Closest Residues

PDB_ID	Residue_Number	Residue_Code.x	Mean_Distance	Residue_Code.y	Angle
1ZJ8	467	CYS	4.642760	CYS	106.838
1ZJ8	209	LYS	5.254105	LYS	132.216
1ZJ8	207	LYS	5.279599	LYS	172.220
2AKJ	486	CYS	4.400598	CYS	106.363
2AKJ	224	LYS	5.292960	LYS	179.302
2AKJ	109	ARG	5.624044	ARG	148.462
2AOP	483	CYS	4.593058	CYS	115.665
2AOP	217	LYS	5.485034	LYS	135.748
2AOP	215	LYS	5.521547	LYS	157.380
3B0G	485	CYS	4.334547	CYS	114.218
3B0G	224	LYS	5.579947	LYS	175.793
3B0G	109	ARG	5.714505	ARG	157.759
3VKP	485	CYS	4.338921	CYS	113.156
3VKP	224	LYS	5.500133	LYS	175.826
3VKP	109	ARG	5.727950	ARG	159.006
3VLX	485	CYS	4.333556	CYS	112.758
3VLX	224	LYS	5.605021	LYS	177.426
3VLX	109	ARG	5.657293	ARG	157.839
3VLY	485	CYS	4.349260	CYS	114.536
3VLY	226	LYS	5.485627	LYS	132.628
3VLY	224	LYS	5.637976	LYS	177.525
3VLZ	485	CYS	4.361247	CYS	115.631
3VLZ	224	LYS	5.601385	LYS	175.472
3VLZ	226	LYS	5.641233	LYS	129.835

Table B.23: SRM: CA-CB-Fe Angles of Closest Residues *(continued)*

PDB_ID	Residue_Number	Residue_Code.x	Mean_Distance	Residue_Code.y	Angle
5H8V	544	CYS	4.294361	CYS	112.481
5H8V	278	LYS	5.495851	LYS	140.582
5H8V	124	ARG	5.731236	ARG	158.195

Table B.24: VERDOHEME: CA-CB-Fe Angles of Closest Residues

PDB_ID	Residue_Number	Residue_Code.x	Mean_Distance	Residue_Code.y	Angle
2ZVU	25	HIS	4.603252	HIS	110.751
3MOO	20	HIS	4.614778	HIS	111.089
1TWN	25	HIS	4.673370	HIS	113.516
1TWR	25	HIS	4.786588	HIS	108.864

Works Cited

[1] Thomas L. Poulos. "Heme enzyme structure and function". In: *Chemical Reviews* 114.7 (2014), pp. 3919–3962. DOI: 10.1021/cr400415k.

[2] Jesus A. Araujo, Min Zhang, and Fen Yin. "Heme oxygenase-1, oxidation, inflammation, and atherosclerosis". In: *Frontiers in Pharmacology* 3 JUL.July (2012), pp. 1–17. DOI: 10.3389/fphar.2012.00119.

[3] Lei Du et al. "Selective oxidation of aliphatic C-H bonds in alkylphenols by a chemomimetic biocatalytic system". In: *Proceedings of the National Academy of Sciences of the United States of America* 114.26 (2017), E5129–E5137. DOI: 10.1073/pnas.1702317114.

[4] Jim Lalonde. "Highly engineered biocatalysts for efficient small molecule pharmaceutical synthesis". In: *Current Opinion in Biotechnology* 42 (2016), pp. 152–158. DOI: 10.1016/j.copbio.2016.04.023. URL: http://dx.doi.org/10.1016/j.copbio.2016.04.023.

[5] Hazel M. Girvan and Andrew W. Munro. "Applications of microbial cytochrome P450 enzymes in biotechnology and synthetic biology". In: *Current Opinion in Chemical Biology* 31 (2016), pp. 136–145. DOI: 10.1016/j.cbpa.2016.02.018. URL: http://dx.doi.org/10.1016/j.cbpa.2016.02.018.

[6] Zhong Li et al. "Engineering cytochrome P450 enzyme systems for biomedical and biotechnological applications". In: *Journal of Biological Chemistry* 295.3 (2020), pp. 833–849. DOI: 10.1016/s0021-9258(17)49939-x.

[7] Sarah E.J. Bowman and Kara L. Bren. "The chemistry and biochemistry of heme c: Functional bases for covalent attachment". In: *Natural Product Reports* 25.6 (2008), pp. 1118–1130. DOI: 10.1039/b717196j.

[8] Jesse G. Kleingardner and Kara L. Bren. "Biological Significance and Applications of Heme c Proteins and Peptides". In: *Accounts of Chemical Research* 48.7 (2015), pp. 1845–1852. DOI: 10.1021/acs.accounts.5b00106.

[9] Baishnab C. Tripathy, Irena Sherameti, and Ralf Oelmüller. "Siroheme: An essential component for life on earth". In: *Plant Signaling and Behavior* 5.1 (2010), pp. 14–20. DOI: 10.4161/psb.5.1.10173.

[10] Adrian M.V. Brânzanic, Ulf Ryde, and Radu Silaghi-Dumitrescu. "Why does sulfite reductase employ siroheme?" In: *Chemical Communications* 55.93 (2019), pp. 14047–14049. DOI: 10.1039/c9cc05271b.

[11] Wenzhen Lai et al. "Enzymatic ring-opening mechanism of verdoheme by the heme oxygenase: A combined X-ray crystallography and QM/MM study". In: *Journal of the American Chemical Society* 132.37 (2010), pp. 12960–12970. DOI: 10.1021/ja104674q.

[12] Hideaki Sato et al. "Electrochemical reduction of ferrous α-verdoheme in complex with heme oxygenase-1". In: *Journal of Inorganic Biochemistry* 101.10 (2007), pp. 1394–1399. DOI: 10.1016/j.jinorgbio.2007.05.016.

[13] Latesh Lad, Paul R. Ortiz De Montellano, and Thomas L. Poulos. "Crystal structures of ferrous and ferrous-NO forms of verdoheme in a complex with human heme oxygenase-1: Catalytic implications for heme cleavage". In: *Journal of Inorganic Biochemistry* 98.11 (2004), pp. 1686–1695. DOI: 10.1016/j.jinorgbio.2004.07.004.

[14] Manabu Ishida et al. "Design and synthesis of de Novo cytochromes c". In: *Biochemistry* 43.30 (2004), pp. 9823–9833. DOI: 10.1021/bi049546e.

[15] Ting Li, Herbert L Bonkovsky, and Jun Tao Guo. "Structural analysis of heme proteins: Implications for design and prediction". In: *BMC Structural Biology* 11 (2011). DOI: 10.1186/1472-6807-11-13.